



UNIVERSITÀ
DEGLI STUDI
DI PADOVA

Sede Amministrativa: Università degli Studi di Padova

Dipartimento di Geoscienze

SCUOLA DI DOTTORATO DI RICERCA IN : SCIENZE DELLA TERRA

CICLO XXVII

- 1.1 **TECTONOTHERMAL EVOLUTION OF THE CENTRAL-WESTERN
CARPATHIANS AND**
- 1.2 **THEIR FORELAND**

Direttore della Scuola : Ch.mo Prof. Massimiliano Zattin

Supervisore :Ch.mo Prof. Massimiliano Zattin

Co-supervisore: Ch.mo Prof. Stefano Mazzoli

Dottorando : Ada Castelluccio

SUMMARY

ABSTRACT	3
INTRODUCTION.....	7
1 CHAPTER I.....	9
GEOLOGICAL SETTING	9
1.1 OVERVIEW OF THE OUTER CARPATHIAN TECTONO-STRATIGRAPHIC UNITS.....	12
1.1.1 <i>The Polish Outer Carpathians</i>	12
1.1.2 <i>The Ukrainian Outer Carpathians</i>	14
1.2 OVERVIEW OF THE INNER CARPATHIAN TECTONO-STRATIGRAPHIC UNITS.....	20
1.2.1 <i>The Slovakian and Polish Inner Carpathians</i>	20
1.2.2 <i>The Ukrainian Inner Carpathians</i>	21
1.3 THE PIENINY KLIPPEN BELT	22
2 CHAPTER II.....	25
METHODS	25
2.1 BALANCED CROSS-SECTIONS AND 2D KINEMATIC MODEL.....	25
2.1.1 <i>Principles of section balancing</i>	25
2.1.2 <i>Workflow</i>	27
2.2 LOW-T THERMOCHRONOMETRY	28
2.2.1 <i>Apatite Fission Track thermochronometry</i>	28
2.2.2 <i>Apatite (U-Th)/He thermochronometry</i>	31
2.3 APPLICATION OF THERMOCHRONOLOGY IN VALIDATING A TECTONIC SCENARIO: THE THERMO-KINEMATIC MODEL	33
2.3.1 <i>Topography</i>	33
2.3.2 <i>Tectonics</i>	34
3 CHAPTER III.....	39
BUILDING AND EXHUMATION OF THE WESTERN CARPATHIANS: NEW CONSTRAINTS FROM SEQUENTIALLY RESTORED, BALANCED CROSS- SECTIONS INTEGRATED WITH LOW-TEMPERATURE THERMOCHRONOMETRY	39
3.1 <i>ABSTRACT</i>	40
3.2 INTRODUCTION.....	41
3.3 GEOLOGICAL SETTING	43
3.4 MAIN TECTONO-STRATIGRAPHIC UNITS OF THE WESTERN CARPATHIANS	45
3.4.1 <i>Outer Carpathians</i>	45
3.4.2 <i>Pieniny “Klippen Belt”</i>	49
3.4.3 <i>Inner Carpathians</i>	50
3.5 STRUCTURAL MODELING.....	53
3.5.1 <i>Sequential restoration and 2D forward modeling</i>	56

3.6	LOW-TEMPERATURE THERMOCHRONOMETRIC DATA	57
3.6.1	<i>New thermochronometric data from the PKB</i>	59
3.6.2	<i>Thermal Modeling</i>	63
3.7	BALANCED CROSS SECTIONS.....	66
3.7.1	<i>Profile I</i>	66
3.7.2	<i>Profile II</i>	71
3.7.3	<i>Profile III</i>	74
3.8	FORWARD MODELING.....	80
3.9	DISCUSSION.....	84
3.10	CONCLUSIONS.....	88
3.11	ACKNOWLEDGMENTS.....	90
4	CHAPTER IV	92
	COUPLING SEQUENTIAL RESTORATION OF BALANCED CROSS-	
	SECTIONS AND LOW-TEMPERATURE THERMOCHRONOMETRY: THE CASE	
	STUDY OF THE WESTERN CARPATHIANS	92
4.1	<i>ABSTRACT</i>	93
4.2	INTRODUCTION.....	93
4.3	GEOLOGICAL SETTING	95
4.4	METHODS	100
4.5	MODELLING TOPOGRAPHY EVOLUTION: CONSTRAINTS AND ASSUMPTIONS	103
4.6	TESTING TWO DIFFERENT CASE HISTORIES	105
4.7	DISCUSSION.....	107
4.8	CONCLUSIONS.....	110
4.9	ACKNOWLEDGEMENTS	111
5	CHAPTER V	112
	BALANCED AND SEQUENTIALLY RESTORED SECTIONS ACROSS THE	
	UKRAINIAN CARPATHIAN THRUST AND FOLD BELT.....	112
5.1	<i>ABSTRACT</i>	113
5.2	INTRODUCTION.....	114
5.3	GEOLOGICAL SETTING	115
5.3.1	<i>The main tectono-stratigraphic units</i>	117
5.4	METHODS	122
5.5	BALANCED CROSS-SECTIONS	122
5.5.1	<i>Profile I</i>	123
5.5.2	<i>Profile II</i>	128
5.6	DISCUSSION.....	132
5.7	CONCLUSIONS.....	133
6	DISCUSSION	136
7	CONCLUSIONS	141
8	REFERENCES	144

Abstract

In Italian

Lo studio dell'evoluzione tettonica e termica dei Carpazi è stato da sempre un argomento di grande interesse sia per la presenza di giacimenti ad olio e gas potenzialmente sfruttabili sia per questioni scientifiche. Il quadro geologico e geodinamico dell'area è caratterizzato da aspetti ancora enigmatici che potrebbero essere spiegati con modelli alternativi a quelli comunemente accettati in letteratura. In particolare, questo lavoro è incentrato sullo studio dell'area comprendente la Polonia Meridionale, la Slovacchia e l' Ucraina occidentale e si basa sullo studio di sezioni geologiche bilanciate e retrodeformate integrate con dati termocronometrici di bassa temperatura. Combinando opportunamente questi dati è possibile definire un modello termo-cinematico strettamente connesso con il modello strutturale adottato e che, allo stesso tempo, ne consente la validazione.

In questo lavoro verranno presentate cinque sezioni geologiche che dall'avampaese polacco e ucraino si estendono fino alla regione dei Carpazi Interni. Queste sezioni sono state bilanciate e retrodeformate grazie all'utilizzo di Move, programma dedicato alla modellizzazione strutturale e successivamente integrate con dati di tracce di fissione e (U-Th)/He su apatite per vincolarne l'ultima fase esumativa. Sebbene l'età di esumazione dei Carpazi Interni ad Esterni sia ben documentata in letteratura, non si può dire lo stesso per la Pieniny Klippen Belt compresa fra i sopracitati domini tettonici. Sono stati prelevati ed analizzati cinque campioni di arenarie silicoclastiche lungo la Pieniny Klippen Belt sui quali sono state fatte analisi di tracce di fissione ed (U-Th)/He su apatite. Questi dati, insieme alle sezioni retrodeformate, sono stati processati con FETKIN, software sviluppato presso l'University of Texas in Austin in collaborazione con Ecopetrol e dedicato al calcolo delle età di raffreddamento lungo una sezione bilanciata. In questo modo è stato possibile anche definire l'evoluzione del campo termico nel tempo.

Sulla base della revisione dei lavori sedimentologici e stratigrafici fatti in quest'area, i Carpazi Esterni and Interni sono qui interpretati come appartenenti allo stesso dominio sedimentario pre-orogenico e la Pieniny Klippen Belt come un'unità sedimentaria depositatasi in una zona prossimale dell'avampaese dei Carpazi Interni.

Durante l'Eocene Superiore questa unità è sovrascorsa sui depositi dei Carpazi Esterni. Gli olistoliti e olistostromi Mesozoici, che rappresentano una delle componenti principali del cosiddetto Pieniny wildflysch, sono qui interpretate come parte della successione Mesozoica dei Carpazi Interni, erosa durante l'Eocene e sedimentatasi nel relativo avampaese. L'età di esumazione di questi depositi risale al Miocene Medio-Superiore e risulta essere coeva all'esumazione registrata per i Carpazi Interni. Diverse età e processi esumativi sono stati invece riconosciuti nei Carpazi Esterni. In Polonia occidentale, nonostante la presenza di faglie normali ad alto angolo, l'esumazione è controllata principalmente dal thrusting. Un'ulteriore conferma viene dal modello termo-cinematico prodotto con FETKIN. Il settore orientale della Polonia, invece, risulta essere interessato da faglie normali a basso angolo successive al thrusting che ne controllano l'esumazione del blocco di letto. In Ucraina non ci sono evidenze di faglie normali. Qui l'esumazione è controllata da un sollevamento isostatico che ha interessato la regione successivamente al thrusting. La costruzione di sezioni geologiche bilanciate ha permesso inoltre di calcolare il raccorciamento che risulta essere crescente verso est. (dal 60% dei Carpazi Polacchi al 64% in quelli Ucraini).

Va sottolineata inoltre l'applicazione di FETKIN in regime compressivo. Questo software è stato testato con successo e ha permesso di valutare l'effetto che le variazioni topografiche, la tettonica e la subsidenza hanno sulla modellizzazione delle isoterme e quindi sul calcolo delle età di raffreddamento.

In English

The tectonic and thermal evolution of the Carpathian thrust and fold belt-foreland system is a topic of great interest both for the occurrence of potential oil and gas fields and for the presence of any enigmatic features that needs an alternative interpretation to the commonly accepted models proposed so far. This study is focussed on the area including the southern Poland, the western Ukraine and the crystalline complex and its sedimentary cover cropping out in the Western Slovakia. The analysis of such a complex tectonic scenario is carried out by the construction of new balanced and sequentially restored cross-sections integrated with low-Temperature (low-T) thermochronometry. Coupling these data it is possible to provide a thermo-kinematic model honouring both the presented structural model and the thermochronometric data and, at the same time, validate the proposed tectonic scenario.

Five balanced cross-sections were constructed from the foreland to the Inner Carpathian domain. Cross-section building and balancing are performed using Move, software dedicated to the kinematic restoration. These sections were then integrated with new apatite fission track and apatite (U-Th)/He data to constrain the last cooling event. Although the cooling of the Inner and the Outer Carpathians are well documented in literature, no low-T thermochronometric data are present from the Pieniny Klippen Belt located between them. Apatite fission track and apatite (U-Th)/He analysis were performed on five samples made of siliciclastic sandstones coming from this narrow belt .Both the balanced sections and low-T thermochronometric data were processed with FETKIN, software developed at The University of Texas in Austin in collaboration with Ecopetrol and dedicated to low-T thermochronometric age prediction and forward modelling. This processing allows to define the evolution of the thermal field through time.

Basing on a review of the sedimentological and stratigraphic works, the Outer and the Inner Carpathian successions are interpreted as deposited in the same sedimentary domain and the Pieniny Klippen Belt as a sedimentary unit deposited in the proximal part of the Inner Carpathian foreland basin, overthrust on the Outer Carpathian deposits during the Late Eocene. The Mesozoic olistoliths and olistostromes forming the Pieniny wildflysh are here interpreted as coming from the

eroded Mesozoic cover of the IC range. New apatite fission track and apatite (U-Th)/He data coming from the Pieniny Klippen Belt constrained its last cooling event to the Middle-Late Miocene, coeval with the cooling of the Inner Carpathian region. The balanced cross-sections show a progressive increasing of the Outer Carpathian shortening moving to the east (from 60% in the Polish region to 64% in the Ukrainian Carpathians). Furthermore, the cross-sections constructed in the central part of our study area highlight the relevant role of the post-thrusting low-angle normal faults in the exhumation process of this area. On the other side, no evidences of post thrusting normal faults occur in the Ukrainian region, where published low-T thermochronometric data suggest an exhumation triggered mainly by regional uplift. In this work the suggested tectonic scenario is successfully tested with FETKIN, to demonstrate that thrusting is the principal mechanism controlling the exhumation ages of the Western Polish Carpathians and to evaluate the effects of subsidence, topography and tectonics on the thermochronometric age prediction.

Introduction

The Carpathians are an arcuate belt extending for more than 1300 km. It represents the Northern prolongation of the Eastern Alps, formed after the movement of the ALCAPA and Tisza-Dacia micro-plates, belonging to the Africa domain, towards the European Platform. The formation of this belt is related to lateral eastward escape of material from Alpine collision zone and slab-pull of the European plate due to subduction of oceanic or thinned continental crust [e.g. *Krzywiec & Jochym*, 1997; *Nemcok*, 1993; *Ratschbacher, Frisch, Linzer, & Merle*, 1991; *Ratschbacher, Merley, Davy, & Cobbold*, 1991; *Royden & Burchfiel*, 1989; *Royden & Karner*, 1984; *Zoetemeijer, Tomek, & Cloetingh*, 1999]. The Carpathians are made by two tectonic domains (Inner and Outer Carpathians) [*Książkiewicz*, 1977] separated by the Pieniny Klippen belt (PKB). The Inner Carpathians (IC) are the oldest range made of a Variscan substratum covered by Miocene successions, while the Outer Carpathians (OC) consists in several nappes made of Cretaceous to Middle Miocene successions. The PKB is 600 km suture zone bordered by a high-angle strike-slip contact [*Birkenmajer*, 1986] along which the movement of the far-traveler ALCAPA and Tisza-Dacia microplates was transferred. The PKB together with the Magura Unit (the innermost units of the Western Carpathians) has been interpreted as the remnants of oceanic basins opening during the Jurassic. There are still some open issues regarding the existence of these oceanic embayments. The lack of any in situ ophiolitic rocks and the absence of continuous oceanic slab under the Western Carpathians doubt the presence of such a wide oceans between the IC and OC. In addition, the northern boundary of the PKB shows an overprinting of opposite senses of movement [i.e. *Birkenmajer*, 1984; *Ratschbacher et al.*, 1993] and its sedimentological features are not in line with the interpretation made by some authors [e.g. *Tomek and Hall*, 1993; *Froitzheim et al*, 2008] considering it as the fossil plate boundary. In this work an alternative scenario is proposed in which the tectonic evolution of the Carpathian thrust and fold belt is integrated with thermal parameters. In spite of the occurrence of numerous low-T thermochronometric data, they are not yet used to validate a structural model. One of

the main problems of this technique is the variation of the thermal field at the surface with the tectonic deformation.

This work is aimed to model the deformation of the thermal field in order to reconstruct the tectonic evolution of the Carpathians. This is possible thanks to FETKIN, software dedicated to the thermochronometric age prediction and the definition of a thermo-kinematic model.

In this work the reconstruction of the main stages of the evolution of this orogenic belt, using forward kinematic modelling, is provided. Particular attention is given to the timing and processes of the last exhumation phase. The shortening rate is also calculated by comparing the balanced with the restored cross-sections. A new interpretation is provided for the Pieniny Klippen Belt for which the timing of exhumation is also constrained.

1 Chapter I

Geological setting

The Carpathians are a curved thrust and fold belt extending from the Vienna Basin to the southern Romania for more than 1300 km (Fig. 1.1).

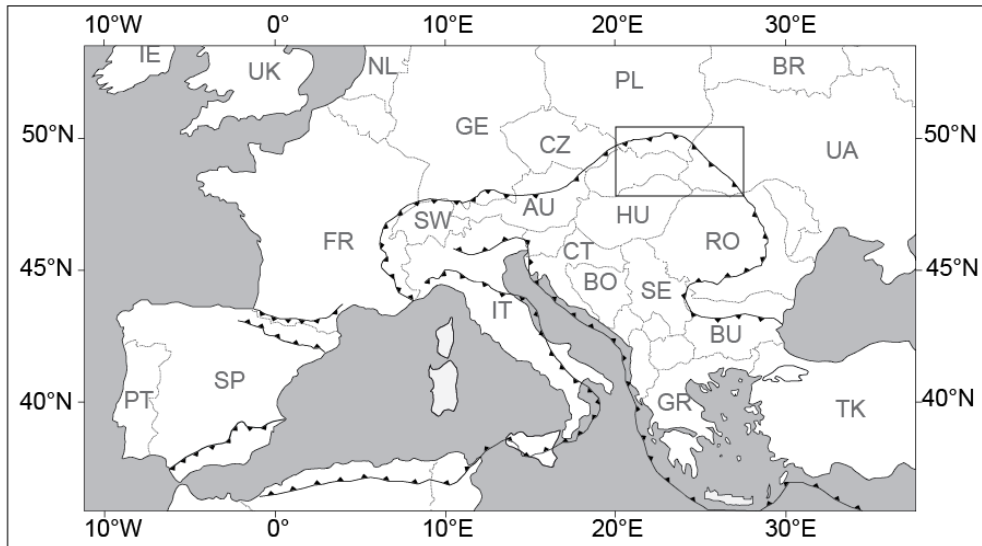


Figure 1.1: Geographic map of the Europe showing the main orogenic front. The black box indicates the study represented in detail in Fig. 1.3.

This orogenic belt formed after the collision between the ALCAPA and Tisza-Dacia Plates and the European Platform and the subsequent subduction of the oceanic domains interposed between them. According to the widely accepted lateral extrusion model [e.g. Royden, 1988; Ratchbacher et al., 1989, 1990] the N-S compression affecting the Eastern Alpine region produced the lateral movement of material toward the east (Fig. 1.2), where the foreland buttress was located more to the north and the oceanic or thin continental crust was subducted. The Pieniny and Magura basins are the main oceanic domains resulting from the Lower Cretaceous palinspastic reconstruction [Csontos and Vörös, 2004]. Several other pre-orogenic sedimentary basins separated by horsts are recognized [e.g. Golonka et al., 2006; Picha et al., 2006; Oszczypko et al., 2006]. Their sediments were detached from their own substratum and stacked in the different tectonic units building the Outer

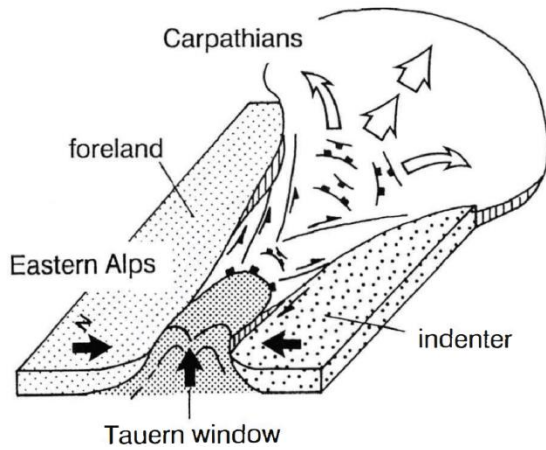


Figure 1.2: Block diagram representing the lateral extrusion model [from Ratschbacher et al., 1991]

Carpathian accretionary wedge (OC). The main detachment corresponds to the Lower and Upper Cretaceous shaly deposits. Every pre-orogenic sedimentary basin takes the name from the associated tectonic units (Magura, Rakhiv, Dukla, Silesian-Čhorna-Hora, Subsilesian, Skole and Borislav-Pokuttya) (Fig. 1.3). The OC are bordered to the south by the Pieniny Klippen Belt (PKB), a curved

belt made of Mesozoic olistoliths and olistostromes bounded by Upper Cretaceous-Paleocene shales and marls.

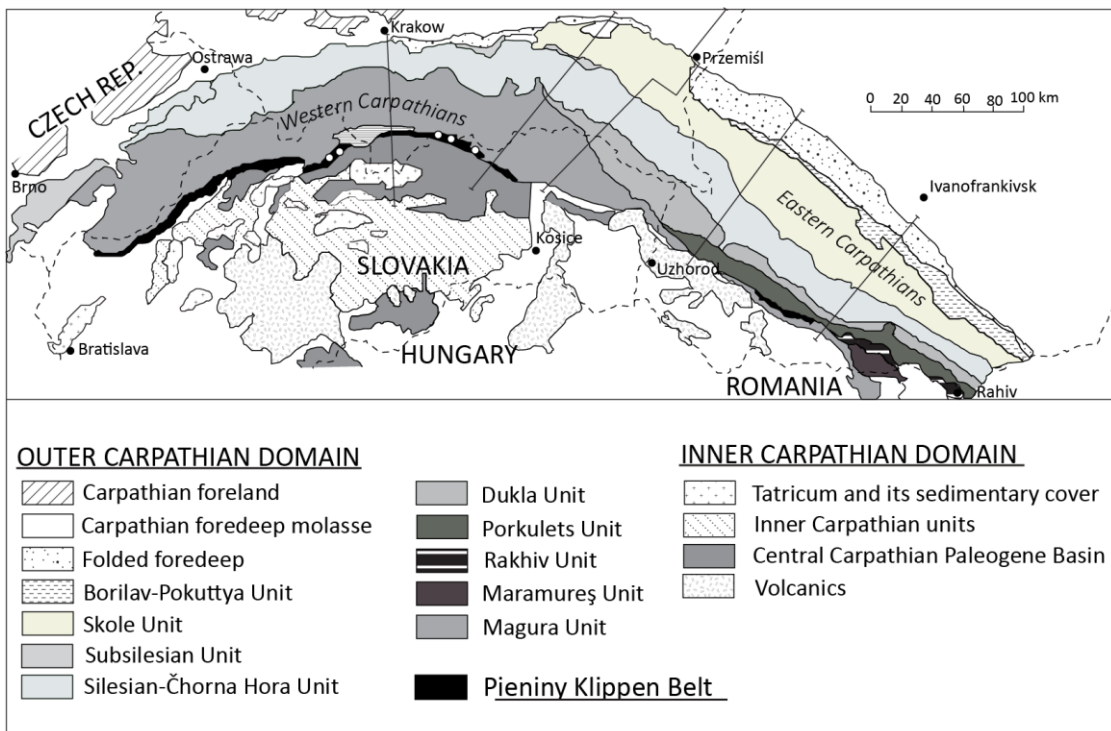


Figure 1.3: Tectonic map of the study area with the location of the samples (white spots) and the location of the section traces.

This belt is interpreted to be the remnant of the Pieniny Ocean although there are not in situ ophiolites or evidences of continuous oceanic slab under the OC belt.

The inner part of this belt, the so-called Inner Carpathians (IC), represents the ancient part of this orogen, where the thick-skinned thrusting produced the imbrication and uplift of the Variscan basement together with the Palaeozoic deposits and the Mesozoic sedimentary cover. These successions are in turn unconformably overlain by the Paleogene deposits of the Central Carpathian Paleogene Basin (CCPB) and the Miocene deposits belonging to the Pannonian Basin (PB).

According to the commonly accepted model of the paleogeographic evolution of the Western Carpathians, thrusting involved the IC domain during the Upper Cretaceous [Golonka *et al.*, 2004; Oszczypko *et al.*, 2006, Picha *et al.*, 2006] (Fig. 1.4).

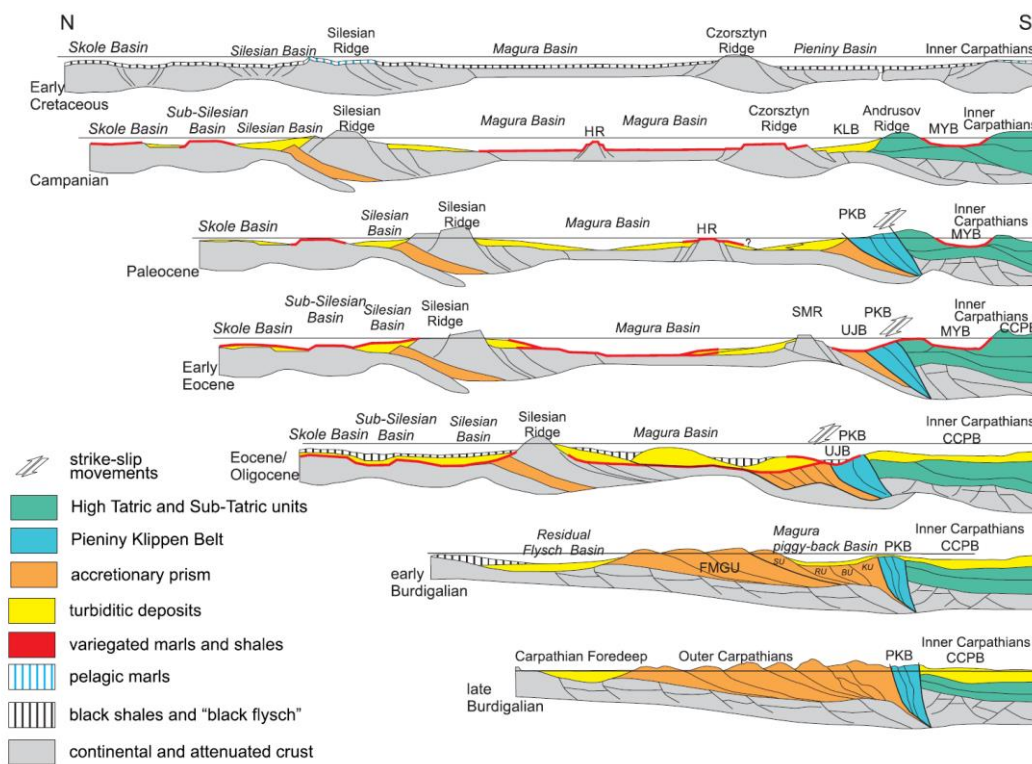


Figure 1.4: Palinspastic evolution of the Western Carpathians [from Oszczypko *et al.*, 2006]

During the Paleocene the subduction of the Pieniny oceanic crust led to the formation of its suture zone (PKB). Then thrusting propagated northward, involving the oceanic/deep water Magura Basin and the other adjacent basins farther to the north. In the Polish region, stratigraphic and sedimentological evidences suggest that thrusting ended 18 Ma ago while was still active to the east [Nemčok *et al.*, 2006].

The change in the thrusting direction from N to NE and the subsequent younging of the end of thrusting eastward (from 18 Ma to 11Ma) [Nemčok *et al.*, 2006] around the arc are explained by the eastward migration of the slab detachment below the OC belt [Wortel, 2000]. The maximum curvature of the orogenic belt corresponds to the area where the slab is still continuous (Vrancea region- Romania). According to this model we should expect a slab at intermediate depth below the Eastern Carpathians and progressively deeper moving to the Western Carpathians; but seismic tomography shows a cold lithosphere at depth ranging between 410 and 660 km along the whole Western and Eastern Carpathians except in its southernmost part where a narrow slab is still preserved.

1.3 Overview of the Outer Carpathian tectono-stratigraphic units

The Carpathian thrust and fold belt are formed by several tectono-stratigraphic units. Some of them are almost continuous in the study area, some others crop out in correspondence of the main tectonic windows. The prevalent tectonic transport is north- oriented. The most external unit is thrust on top of the Miocene molassic deposits laying on the North European Platform. They are made of Lower Miocene marine pelitic deposits overlain by middle Miocene conglomerates passing upwards into sandstones intercalated with tuffite and evaporitic layers [Oszczypko *et al.*, 2006].

1.3.1 The Polish Outer Carpathians

The Outer Carpathians are formed by several thrust sheets detached from their original substratum. From the foreland to the hinterland five main tectonic units can be recognized: Skole, Subsilesian, Silesian, Dukla and Magura units (Fig. 1.5).

The **Skole Unit** crops out in the eastern part of the Polish region. It is detached in correspondence of the Lower Cretaceous anoxic black shales (Spas shales). The Upper Cretaceous-Paleocene deposits show very different facies. Here the shales are replaced by thick-bedded siliciclastic turbiditic deposits. Another abrupt change of sedimentation is recorded during the Eocene and Oligocene, when the sedimentation becomes more shaly and the thin beds of sandstones are intercalated with thick bedded shales. During this time interval two important layers for the stratigraphic correlations deposited: The *Globigerina marls* (Late Eocene) and the dark

bituminous shales of the Menilite Fm. (Oligocene). The youngest deposits are made of calcareous sandstones interbedded with grey marls belonging to the Krosno Fm. (early Miocene) [Ślączka *et al.*, 2006].

The **Subsilesian Unit** gets exposed in narrow zones in front of the Silesian Unit and in some tectonic windows. This nappe is detached along the Lower Cretaceous dark shales. These black shales start to be interbedded with thick layers of sandstones during the Upper Cretaceous (Lgota Beds). The sedimentation of conglomerates and then green marls marks the beginning of the Paleogene. Also in this nappe the Eocene and Oligocene sequences are characterized by the deposition of *Globigerina marls* and Menilite Fm. The succession ends with the medium-bedded calcareous sandstone and marly shales of the Miocene Krosno Fm.

The **Silesian Unit** is a continuous nappe overthrusting the Subsilesian Unit. The oldest deposits are Tithonian mudstones but they rarely crop out. They are interbedded with turbiditic deposits during the Upper Jurassic- Lower Cretaceous. Thick bedded sandstones intercalated with green shales sedimented during the Upper Cretaceous-Paleocene, becoming more shaly in the upper part of the succession. The Eocene deposits are characterized by lenses of conglomerate included in red shale beds. The conglomerates are replaced by thick beds of sandstones during the Upper Eocene (Hieroglyphic Beds) and covered by *Globigerina marls*, Menilite Beds and the younger Krosno Beds whose lithology is the same described for the other units. The Upper Miocene deposits are made of olistoliths coming from the unit directly above it [Ślączka and Oszczytko, 1987].

The **Dukla Unit** starts with Lower Cretaceous black shales intercalated with cherts and siderites. Dark shales intercalated with sandstones also characterized the Upper Cretaceous-Paleocene sedimentation. During the Eocene the sedimentation changes, passing into red and green shales only locally intercalated with sandstones. This sedimentary sequence is closed by the Hieroglyphic Fm., the *Globigerina Marls*, the dark bituminous shales of the Menilite Fm. and the uppermost thick-bedded calcareous sandstones (Cergowa ss.) [Ślączka and Unrug, 1976].

The **Magura Unit** is the innermost nappe of the OC flysch belt detached along the Upper Cretaceous shales. From the Upper Cretaceous to the Oligocene the sedimentation is characterized by the deposition of three turbiditic cycles

[Oszczypko et al., 1992] starting with pelitic basinal deposits passing into thin to thick bedded sandstones and variegated shales. The youngest deposits are characterised by the Oligocene Krosno Beds [Ślaczka et al., 2006].

1.3.2 The Ukrainian Outer Carpathians

In Ukraine the deposits building the OC flysch belt are grouped into several formations NW-SE oriented. Some of them can be easily recognized all over the study area. For some others the correlation with the Polish units remains uncertain because of the lack of homogeneous nomenclature applied to several formations. The first attempt to tie the Ukrainian OC stratigraphy has been made by *Jankowski et al.*, [2012] recognizing the main stratigraphic units and simplifying their formational names. The following description is made analyzing the most external one, at first, and then the more internal (e.i. Maramureş Unit) (Fig. 1.6).

The **Borislav-Pokuttya Unit** oldest deposits consist in a thick siliciclastic turbidite followed by thick-bedded turbidites intercalated with conglomerates of the Yamne Beds (Paleocene). Higher up they become more shaly and then covered by gray marls, slump deposits and exotic material (Popeli Beds) during the Late Eocene. The Oligocene sequence starts with the dark bituminous shales of the Menilite Fm. passing upward into more sandy deposits intercalated with lenses of conglomerates. The youngest deposits are made of medium to thick-bedded sandstones intercalated with shales belonging to the Stebnik and Balychi Fms.

The **Skole Unit** detaches in correspondence of the Lower Cretaceous anoxic black shales of the Spas Beds [Kotlarczyk, 1985; Kruglov, 2001]. During the Upper Cretaceous a thin layer of green radiolaritic shales passed upward to the red shales and whitish, siliceous turbiditic marls till the Paleocene. Then they were covered by thick-bedded calcareous sandstones intercalated with shales. This sedimentation is

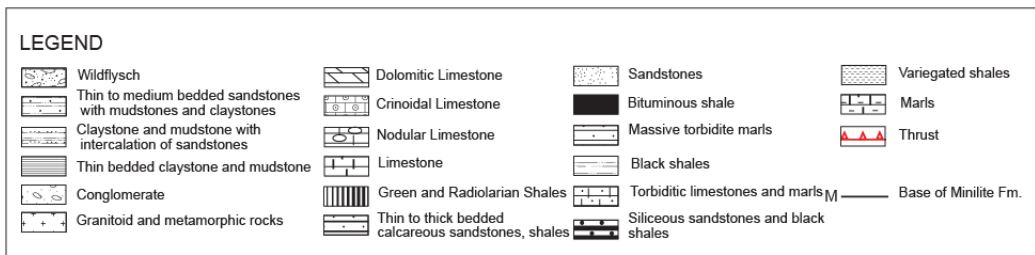
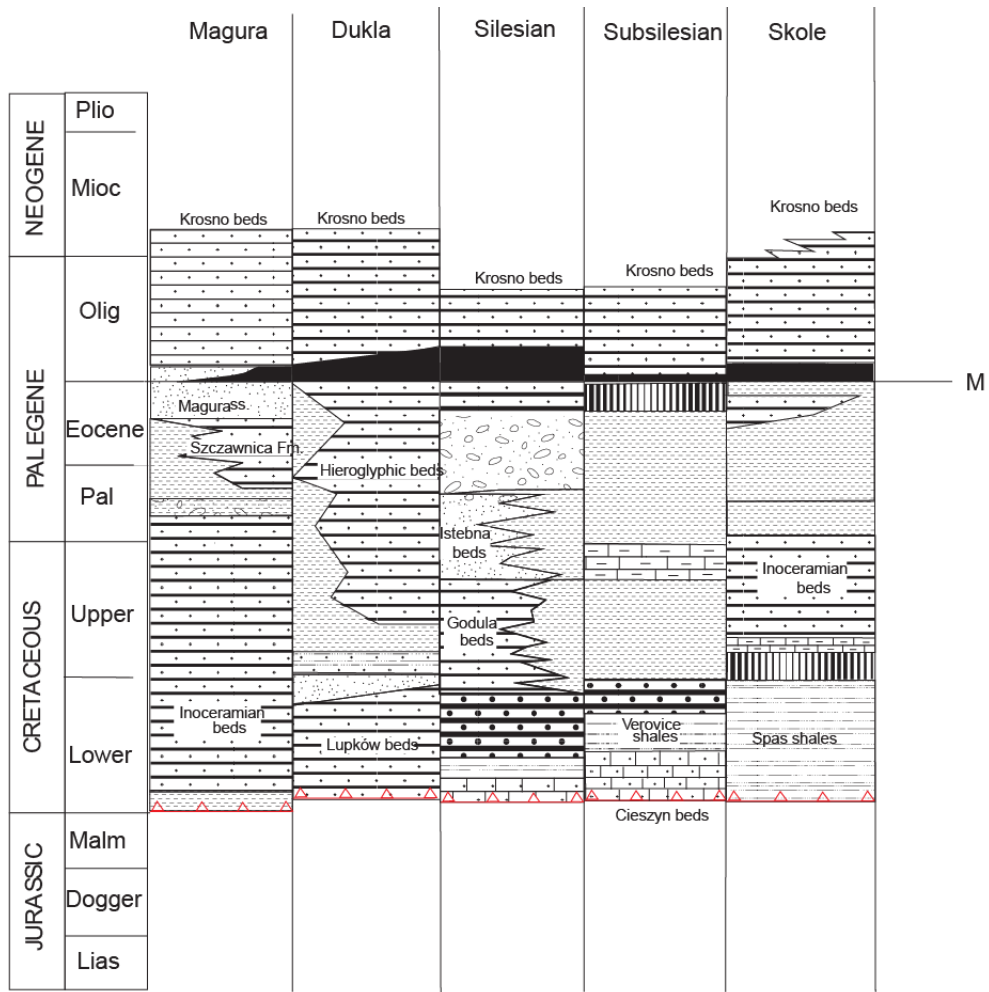


Figure 1.5: Correlation chart for the main tectono-stratigraphic units of the Polish Outer Carpathians. The successions are not represented with true thickness

continuous up to the Eocene, when it is replaced by green shales intercalated with thin-bedded sandstones (Bystrytsia Formation) and gray marls (*Globigerina Marls*) Locally slump deposits with exotic material (Popiele beds) interrupts the continuous sedimentation. During the Oligocene the sedimentation is characterized by an anoxic facies (Menilite Fm.). The Early Miocene Krosno Beds close the stratigraphic sequence with an intercalation of marls and thin bedded sandstones (Polanitsia Beds).

The **Silesian Unit (Svydovets Unit)** starts with the Lower Cretaceous-Turonian dark mudstones. The stratigraphy of these formations is the same as the adjacent Dukla Unit. The Upper Cretaceous-Paleocene deposits consist of thick-bedded sandstones intercalated with grey shales (Lolyn Beds) higher up increasing the sandy component. The Eocene deposits are mainly characterized by thick variegated shales passing into dark bituminous shales during the Oligocene.

The **Dukla Unit** has its dècollement surface along the Lower Cretaceous black shales of the Shypit Fm. Higher up the shaly deposits remain prevailing till the Cenomanian with the deposition of the Yalovets shales. From the Upper Cretaceous to the Paleocene the sedimentation is characterized by dark shales and medium bedded, fine-grained, calcareous sandstones increasing its sandy component in the upper part (Luta ss.). The Eocene deposits developed as a complex of medium to thin-bedded green shales, passing upwards into the more marly deposits. The thick-bedded calcareous Cergova sandstones [*Ślącka and Unrug, 1976*] and the upper Menilite Fm., close the stratigraphic sequence together with the youngest calcareous sandstones and shales belonging to the Maly Vyszn Fm.

The **Čorna Hora Unit** is located in the southeastern part of the Ukrainian Carpathians. According to some authors [e.g. *Ślącka 1959*] it represents the inner part of the Silesian Unit. The Skypit Beds are the oldest sediments (Barremian–Aptian) of this unit, made by black, calcareous shales with siderites, fucoid marls, and thin-bedded sandstones. Thick bedded sandstones intercalated with shales and marls characterized the Upper Cretaceous sedimentation (Yalovets beds and Skupiv Beds). From the Paleocene to the early Eocene an increase of the sandy component is recorded. Higher up this succession gets more shaly with the Batonian-Priabonian

Parodsyn Beds. This unit is closed by the Oligocene deposits of the Menilite Fm. and the Transitional Beds, composed by dark brown shale.

The **Krasnoshora Unit** is detached in correspondence of the Lower Cretaceous black shales and marls locally interbedded with thin beds of sandstones. The sedimentation gets more sandy in the upper part of the succession. The younger deposits are represented by the Upper Cretaceous-Paleocene Krasnoshora Fm., consisting of thick- to thin-bedded sandstones and gray shales.

The **Burkut Unit** starts with Lower Cretaceous black, calcareous shales with siderites, fucoid marls, and thin-bedded sandstones passing into the upper dark, quartzitic sandstones with black shales series. These deposits are unconformably overlain by the thick to medium-bedded sandstones and conglomerates of the Burkut Fm. reaching more than 500m of thickness [*Ślęcka et al., 2006*].

The Suhiv Unit are made of Lower Cretaceous gray marly shales and thin- to thick-bedded laminated sandstones at the bottom, intercalated with lenses of conglomerates. This succession passes upwards into the gray shales, marls, and sandstones of the Upper Cretaceous Sukhiv Beds. Thick to thin-bedded Paleocene sandstones and gray shales [*Jankowski et al., 2012*] represent the youngest deposits of this unit.

The **Rachiv Unit** starts with the Upper Jurassic-Hauterivian deposits of the Vovchyi Beds and terminates with the 1000 m thick Barremian deposits belonging to the Rahiv Beds. The oldest deposits consist of black shales, calcareous thin- and medium-bedded turbiditic sandstones, and limestones passing upward into a more sandy complex, intercalated with conglomerates. Exotic blocks of Mesozoic limestones and diabases are also present. The youngest deposits are represented by black shales and thin bedded calcareous sandstones [*Ślęcka et al., 2006*].

The **Maramureş Unit** is located in the innermost part of the OC flysch belt. This unit, in particular the more internal Maramureş Klippen Zone, consists in two parts differing in the sedimentological characters. The lower part is formed by Mesozoic olistoliths and olistostromes (Soimul olistostromes) covered by the flysch deposits of the Monastyles subzone. These mega-blocks are made of Paleozoic and Proterozoic schists and gneisses, Paleozoic, Triassic, Jurassic, and Barremian–Aptian dolomites and limestones, and Permian–Triassic quartzitic sandstones and conglomerates

[*Ślęcza et al.*, 2006]. Blocks of serpentinites, diabases, gabbro-diabases, pebbles and boulders of granites, quartz porphyries, and granitoids also occur. Higher up the Soimul formation is overlain by the Upper Cretaceous red marls of Pukhiv beds and thin-bedded sandstones with green-gray and sparse red shales of the Jarmuta beds [*Kruglov*, 1965, 1969]. The Paleocene succession begins with the Motova conglomerates covered by Eocene marls. During the Oligocene the sedimentation is characterized by marly deposits intercalated with black shales and sandstones. These deposits, better-known as Menilite and Malcov formations, unconformably overlay the above-described Eocene deposits. After the Miocene sedimentation gap, the Eocene succession is in turn covered by the Upper Miocene deposits belonging to the Terebla Beds.

The sedimentological features of the Maramureş Unit change radically to the SW where it is built by metamorphosed Riphean-Vendian rocks and by sedimentary, volcanic, and epizonally metamorphosed Carboniferous, Triassic, and Jurassic formations. The Cretaceous conglomerates, organogenic limestones, and marls discordantly overlie older rocks [see *Kropotkin*, 1991 for more details].

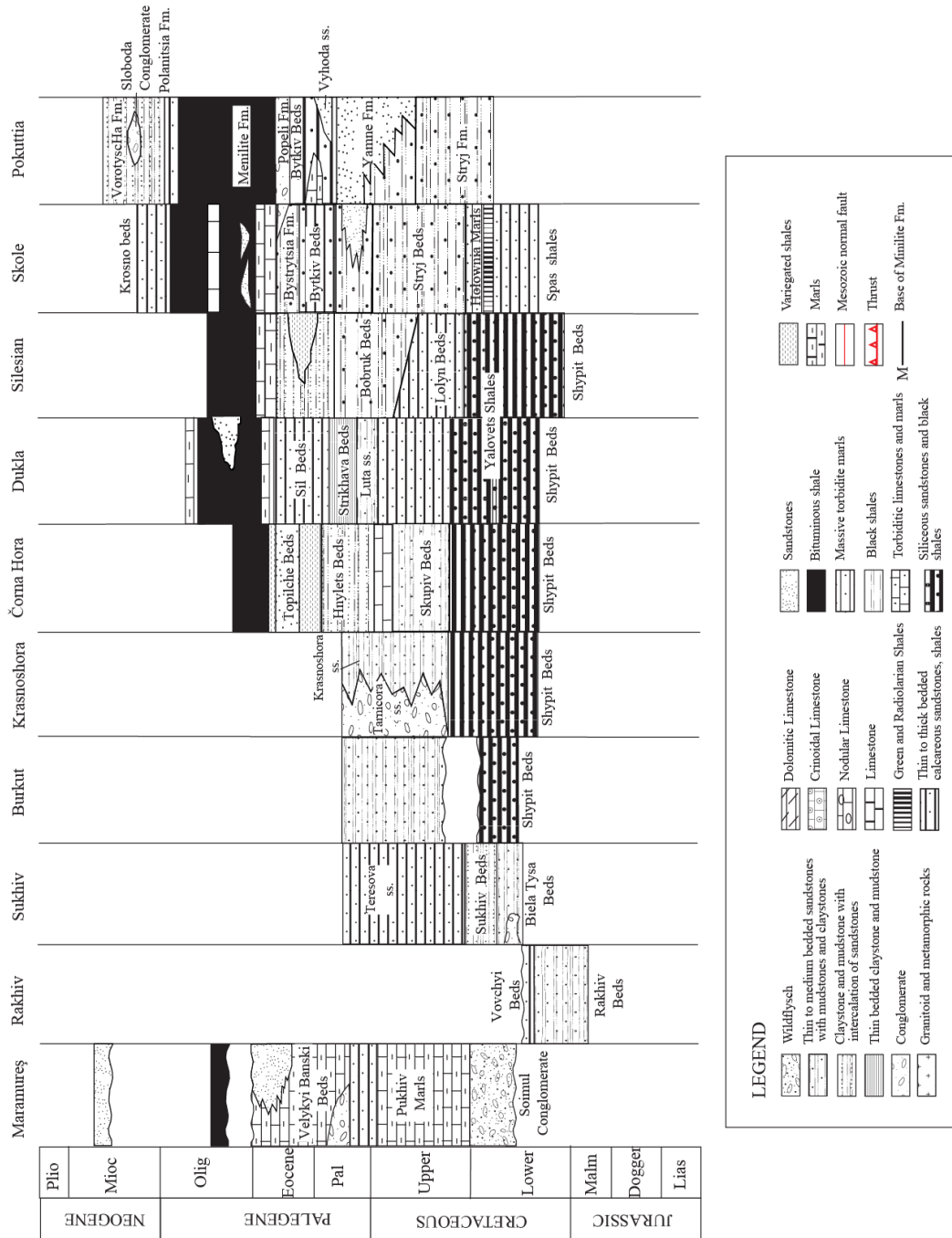


Figure 1.6: Correlation chart for the main tectono-stratigraphic units of the Ukrainian Outer Carpathians. The successions are not represented with true thickness.

1.4 Overview of the Inner Carpathian tectono-stratigraphic units

The Inner Carpathian region represents a retro-wedge extensional basin where the Oligo-Miocene deposits lay unconformably on top of a deformed substratum made of crystalline rocks with its sedimentary cover. The Paleogene to Neogene deposits are the sedimentary infilling of the Central Carpathian Paleogene Basin (CCPB) and the Pannonian Basin (PB). Their morphology is characterized by localized depressions forming minor basins. The architecture of their substratum consists of several nappes emplaced one on top of the others during the early Alpine orogeny.

1.4.1 The Slovakian and Polish Inner Carpathians

In the following paragraph the description of the main tectono-stratigraphic units of the Slovakian Inner Carpathians is presented starting from the youngest deposits of the CCPB to the oldest north verging nappes constituting its substratum (Fig. 1.7)

The **Central Carpathian Paleogene Basin** is formed by a sequence of mainly marine deposits. They are locally interrupted by isolated reliefs made of crystalline massifs. The Paleogene flysch deposits sedimented on top of an Eocene erosional surface. At the bottom they are made of breccias, conglomerates, polymictic sandstones to siltstones [Chmelik, 1957] covered by sandstones interbedded with the Menilite-type shales and coarse clastic fans constituting the youngest deposits (Upper Oligocene).

The **Variscan crystalline nappes and their Mesozoic sedimentary cover** represent the substratum of the CCPB. The Variscan basement is composed of metamorphic and granitoid rocks, overlain by Cambrian to Carboniferous volcano-sedimentary deposits [Hovorka *et al.*, 1994]. They are subdivided into three different crustal units: Tatricum, Veporicum and Gemericum [e.g., Mahel, 1986; Plasienka, 1997]. The Mesozoic cover consists of carbonatic rocks stacked in several north-verging thrust sheets. They are detached in correspondence of the Triassic evaporitic layers. These latter are overlain by shallow water limestones intercalated with dolomitised layers [Jaglarz & Szulc, 2003]. The Triassic succession ends with variegated shales and evaporites intercalated with dolomite and sandy beds of the Keuper Fm. [Prokešová *et al.*, 2012]. Sandy crinoidal limestone and silicified radiolarian limestone and radiolarian cherts characterized the Jurassic sedimentation. Lower Cretaceous marls

and cherty limestones overlain by Upper Cretaceous sandstones and claystones close the Mesozoic stratigraphy [Janočko *et al.*, 2006]. These allochthonous successions differ from the autochthonous cover and represent in general more basinal facies.

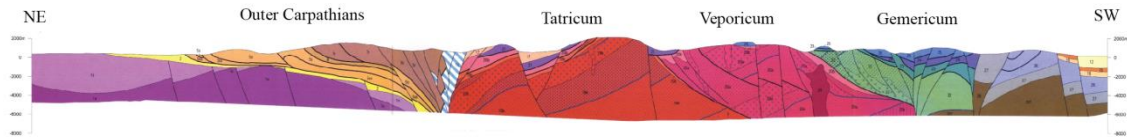


Figure 1.7: Geological section across the Polish and Slovakian Carpathians showing the structural position of the Inner Carpathian tectonic units [from Lexa *et al.*, 2000]

1.4.2 The Ukrainian Inner Carpathians

The **Pannonian Basin** is a Neogene extensional basin formed while thrusting was still active at the Carpathian front. It comprises many minor basins bordered by strike-slip fault (e.i. the Transcarpathian Depression). The basin fill starts with the Eocene and Oligocene flysch deposits. Synrift sediments, although dominantly terrigenous, included marls, algal limestones, evaporites, nonmarine clastics, and coals. Tuffs and pyroclastics are also present. The post-rift sequence is marked by a suite of undeformed nonmarine, lacustrine, deltaic, and fluvial clastic facies [Royden and Horváth, 1988; Kázmér, 1990; Müller and others, 1999] and represents the youngest deposits (Fig. 1.8).

The **pre-Neogene substratum** is made by structural units differing in origin and age [e.g. Tözsér and Rudinec, 1975; Sviridenko, 1976; Soták *et al.*, 1993]. The northernmost Mesozoic successions are interpreted as belonging to the Križna Nappe [Mahel, 1986]. The orientation of the tectonic units buried under the Neogene deposits is NW-SE and consists of thick-skinned nappes involving deposits from the Precambrian anchimetamorphic basement to the Eocene. The inner units are known as Inatchevo-Kritchevo nappe, made of Permian to Eocene deposits overthrust by the Tatric and Veporic crystalline basement [Tomek, 1993]. Their characteristics are the same as the one building the IC range buried under the CCPB.

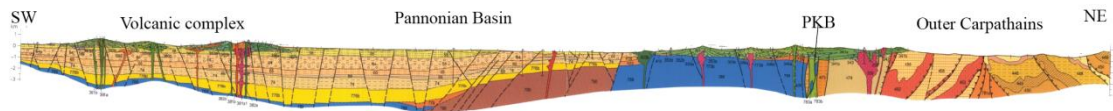


Figure 1.8: Geological section across the Pannonian Basin [from Kaličiak et al., 2008]

1.5 The Pieniny Klippen Belt

The Pieniny “Klippen Belt” (PKB) is a 600 km belt separating the OC and the IC tectonic domains (Fig. 1.9). It represents one of the enigmatic features characterizing the Carpathian orogeny. Several descriptions have been provided: first described as a tectonic *mélange* [e.g. *Roca et al.*, 1995] and then as a “wildflysch” [*Plašienka and Mikuš*, 2010], the PKB includes rocks from the Triassic to the Lower Eocene. Triassic deposits, although not very common within the PKB, have been found as mega-blocks in northern and western part of Slovakian PKB [*Andrusov*, 1950]. They consist mainly of dolomites and dolomitic limestones. Jurassic sediments include clastic (partly conglomeratic) deposits, passing upward to a more deep-water facies. Crinoidal limestones followed by red radiolarian cherts and nodular limestones characterized the depositional environment from the Middle to the Upper Jurassic [*Birkenmajer*, 1960]. Triassic and Jurassic deposits together with Lower Cretaceous marls, flyschoid sediments and, locally, cherty limestones, occur in the PKB as mega-blocks [*Plašienka and Mikuš*, 2010]. These Mesozoic successions are found as olistoliths surrounded by an intensely deformed matrix consisting of Upper Cretaceous-Paleogene shales, sandstones and marls (also known as Klippen mantle [*Birkenmajer*, 1960]). The occurrence of different tectonic units within the PKB has been correlated with distinct pre-shortening palaeogeographic domains. Simplifying, the shallow-water deposits have been associated to two distinct ridges: the Czorsztyn Ridge, originally separating the Magura basin from the Pieniny basin, and the Andrusov Ridge, originally located between the Pieniny basin and the innermost Manín basin [*Birkenmajer*, 1986].

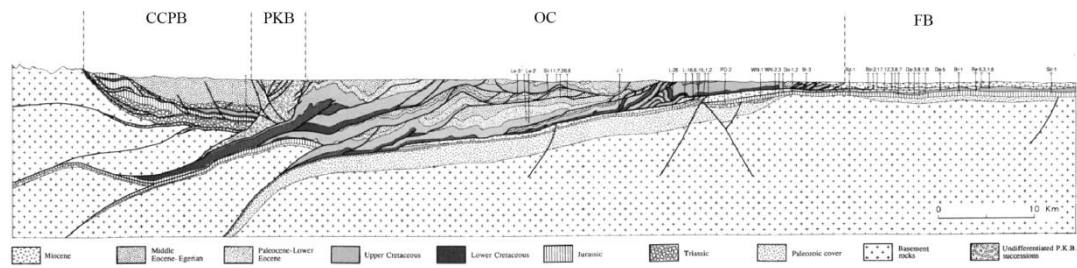


Figure 1.9: Geological cross-section showing the structural position of the PKB [modified after Roca et al., 2005]

2 Chapter II

Methods

This work is the result of the combination of two different methods: the kinematic modelling and low-T thermochronometry. Their integration allows the definition of a thermo-kinematic model that simulates the evolution of the thermal field through time and validates the chosen structural model. Five balanced and sequentially restored cross-sections were constructed across our study area from the Carpathian foreland to the IC domain. For one of them the thermo-kinematic model was performed. In the following paragraphs the principles of cross-section balancing and low-T thermochronometry are summarized.

2.1 Balanced cross-sections and 2D kinematic model

2.1.1 Principles of section balancing

Cross-section balancing is a technique present in literature from the early 1900s. *Chamberlain* [1910, 1919] was the first introducing the concept of area conservation during deformation to calculate the depth of the décollement. This technique was then developed by geologists of oil companies that understand the importance of timing and deformation of the rocks on the fluid migration. Section balancing consists in deforming a geological cross-section back in time to provide the undeformed (or less deformed) depositional setting.

This methods was then applied to calculate the shortening assuming that if the area of cross-section remains constant, the bed lengths measured along the section must remain constant [*Dahlstrom* 1969a]. The most important point in section balancing is that the end of the section must be fixed at points where no interbed slip occurs (pin line) and the section plane must be normal to the main tectonic transport direction in order to avoid “out of plane” movement that cannot be restored.

At first, cross section balancing was used to restore simple tectonic structures as the whole process was made by hand. Now, several software have been developed allowing also the restoration of complex tectonic settings. In this work, the restoration is performed using Move, software developed by Midland Valley Exploration Ltd. It allows the construction of horizon automatically using the dip

domains and to apply different algorithms in order to restore folds and the displacement along the faults.

Flexural slip, *simple shear* and *fault parallel flow* are the main algorithms applied in this work.

The *flexural slip* algorithm assumes that deformation occurs by slip along bedding planes. It allows the preservation of the area, length and thickness in a vertical plane. If the thickness is not constant along the section the application of this method implies changes of areas (Fig. 2.1).

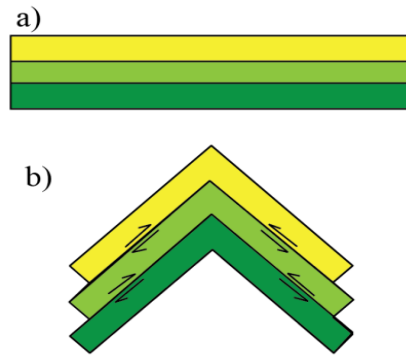


Figure 2.1: Schematic representation of the flexural slip deformation mechanism in a multi-layer.

With the *simple shear* the distance in the shear direction is preserved. This technique were first used in extensional regime by Verral [1981] and Gibbs [1983] who assume that hanging-wall moves laterally by a constant amount and slides vertically. In this case the variation of thickness and bed length can be introduced and area is not preserved (Fig. 2.2).

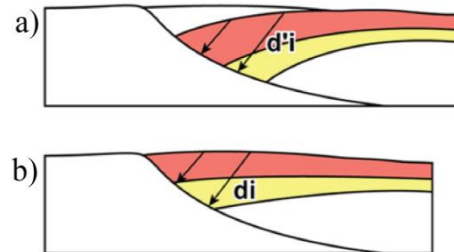


Figure 2.2: Schematic representation of the simple shear mechanism deforming the hangingwall of a listric normal fault [from Moretti, 2008]

The *fault parallel flow*, which rules were first applied by Sanderson, [1982] and Keetley and Hill, [2000] are suitable for reverse restoration. All points in the hanging-wall move parallel to the fault surface. In this

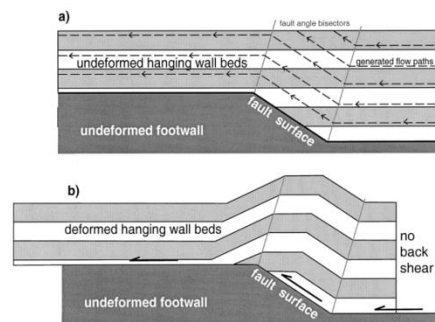


Figure 2.3: Schematic representation of the fault parallel flow mechanism deforming the hangingwall of an inverse fault [from Savage and Cooke, 2003]

case bed area is conserved (Fig. 2.3).

Restoration generates the undeformed or less deformed state that can be validated applying the inverse approach, called

forward kinematic model [Suppe, 1983; Endignaux and Mugnier, 1990]. Starting

from the initial state the deformed cross-section is generated. The forward modelling does not take into account the rheology of the material, thus it is formally admissible but physically impossible. Anyway if a geological solution honouring all data can be restored it can be considered a valid model [Elliot, 1983]. In this way, the obtained solution is not the unique possible scenario but the one better representing our field data.

2.1.2 Workflow

During the construction of a geological cross-section, all the lithostratigraphic units deposited during the same time interval were grouped together in the same horizon. Equal area calculation [Chamberlin, 1910, 1919] is applied to calculate the depth of the décollement surface where not constrained (Fig. 2.4) and the upper

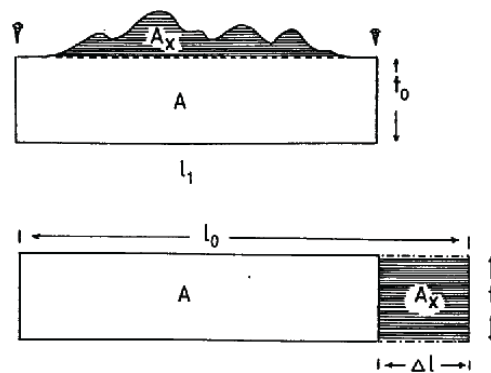


Figure 2.4: Equal area balancing principle

Cretaceous-Paleocene horizon as regional datum for the restoration. Flexural slip restoration has been first performed. This is based on the minimum shortening and area conservation assumptions. Each thrust sheet has been unfolded individually tracing a pin line parallel to the axial plane of the folds. Once unfolded all the thrust sheets and minimized the gaps and/or the overlaps between them, they have been re-folded back to their original position using the Upper Cretaceous-Paleocene horizon as a template to fix any geometric problems in the balanced cross-sections. The structures have been restored taking into account the timing of deformation provided by stratigraphic studies of syn-tectonic deposits and the relationships among the tectonic structures. Vertical simple shear algorithm was applied for listric normal

faults, fault parallel flow algorithm for reverse restoration and the flexural slip algorithm to simulate the flexure of the downgoing plate. The undeformed section resulting from the sequential restoration has then been deformed forward in time in order to validate our structural interpretation and define the geometry of the eroded successions.

2.2 Low-T thermochronometry

Low-T thermochronometry has been here used to validate the kinematic restoration. Several low-T thermochronometric data are available for the study area and we integrated them with five new samples coming from the Pieniny wildflysch. Apatite fission track (AFT) and apatite (U-Th)/He (AHe) analysis were performed on these samples made of siliciclastic sandstones and siltstones belonging to Upper Cretaceous-Eocene successions.

2.2.1 Apatite Fission Track thermochronometry

This technique is based on the characterization of the damage tracks produced in the crystal lattice after the emission of a neutrons and gamma radiations subsequent to the fission of heavy nucleus into two daughter isotopes. This fission could be spontaneous or inducted by a neutron irradiation from an external source. In apatites these damages are produced by the breakdown of ^{238}U [Wagner, 1968] and appear in the crystal as linear trails (Fig. 2.5).

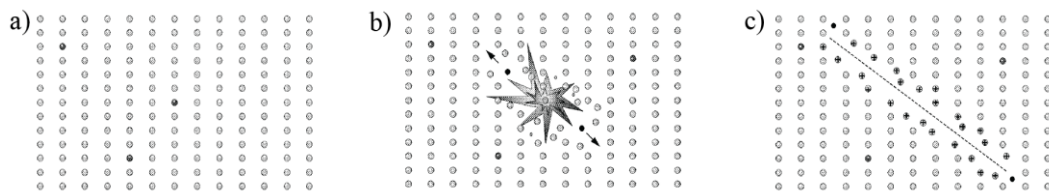


Figure 2.5: Schematic cartoon showing the formation of the fission tracks in a mineral. a) dark spots are the radioactive ^{238}U ; b) Spontaneous fission of ^{238}U producing two highly charged daughter isotopes; c) damage trail left in the crystalline lattice.

These linear tracks start to be preserved in the crystal lattice below 110°C . This temperature is known as the closure temperature, it means that below it the system can be considered close [Dodson, 1973]. Above this temperature all tracks disappear

(anneal) whereas at temperature between 80°C and 110°C, known as Partial Annealing Zone (PAZ) [Gleadow and Fitzgerald, 1987] the fission tracks are partially preserved and their length decreases (annealing) [Green et al., 1986; Laslett et al., 1987; Duddy et al., 1988; Green et al., 1989; Gallagher, 1995]. All the formed tracks are preserved at temperature lower than 80°C with their original length. Length and width of these tracks depend on the temperature and time of permanence at certain temperatures. They commonly are ca. 10-20 µm long and 10 nm wide.

AFT ages is calculated by counting the spontaneous and the induced fission tracks. The former are produced by the spontaneous decay of the ^{238}U , the latter after the nuclear irradiation of the grain mount and the muscovite mica sheet attached on it (Fig. 2.6). The mica records the fission tracks produced by the ^{235}U decay, thus knowing the $^{238}\text{U}/^{235}\text{U}$ that has the constant value of 137.88 [Steiger and Jäger, 1977], is possible to establish with good precision the concentration of the former even for small crystal [Donelick, 2004]. This method is known as “External Detector Method” [Gleadow, 1981; Hurford and Green, 1982; 1983; Green, 1985; Gleadow et al., 1986; Hurford, 1990a].

The AFT age is calculated applying the following formula:

$$AFT\ age = 1/\lambda_D * \ln [1 + \lambda_D * \zeta * (\rho_s/\rho_i) * \rho_d]$$

where

λ_D = total decay constant;

ζ = calibration factor different for each person [Hurford and Green, 1982; 1983];

ρ_s = spontaneous track density in the sample;

ρ_i = induced track density in the sample;

ρ_d = induced track density in the ^{235}U doped glass.

The calculated ages is approximately the ages of the last cooling event through the PAZ, and in order to be used as constrain for thermal histories additional information must be considered (e.g. the tracks lengths and the age as function of the populations).

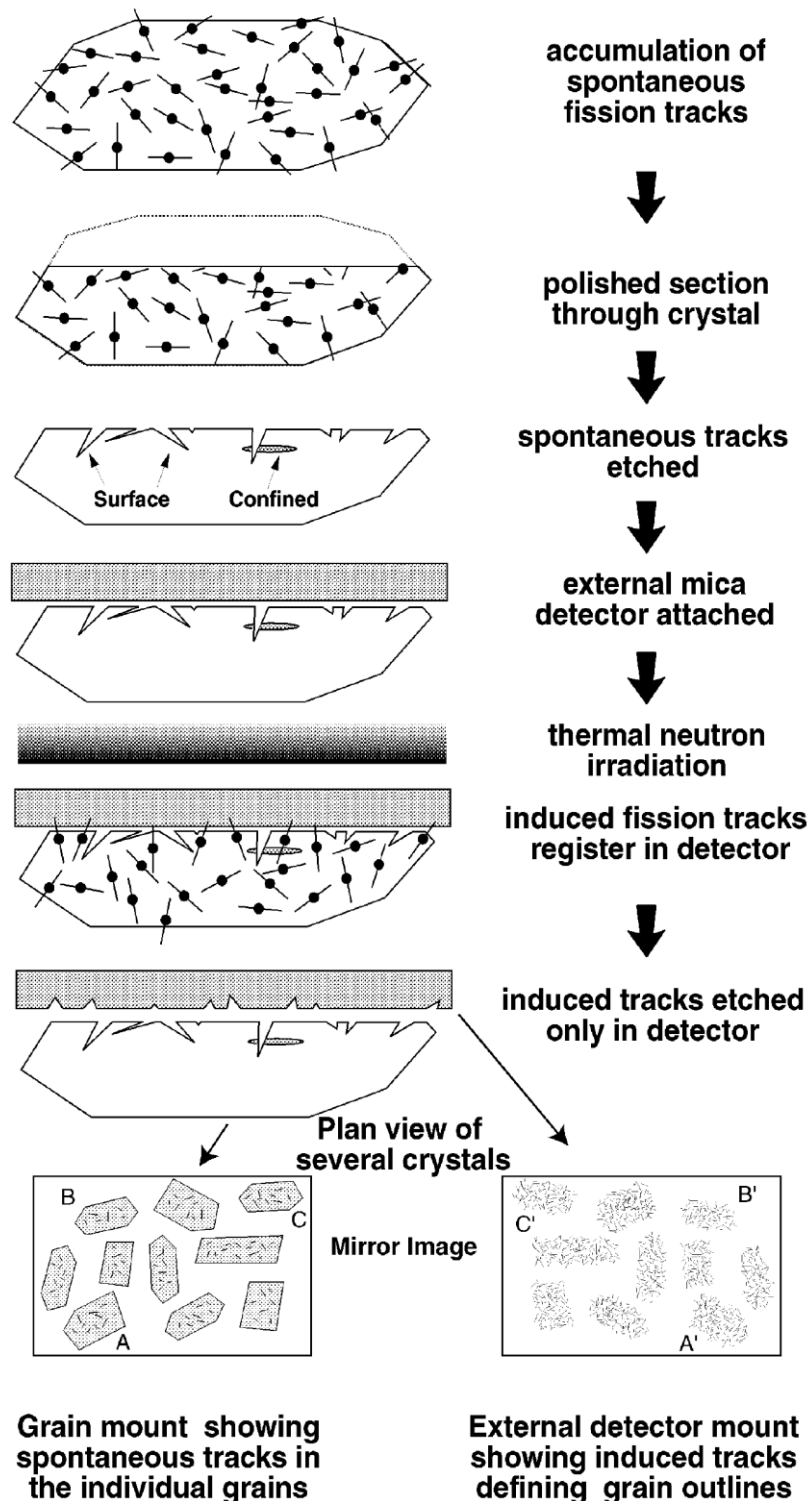


Figure 2.6: Representation of the procedures applied in the external detector method. By counting the tracks in the mineral, the concentration of U can be estimated: By counting the tracks on the mica sheet the concentration of daughter isotopes can be inferred.

2.2.2 Apatite (U-Th)/He thermochronometry

Among the low-T thermochronometers the apatite (U-Th)/He is the one sensitive to the lowest temperature (Fig. 2.7).

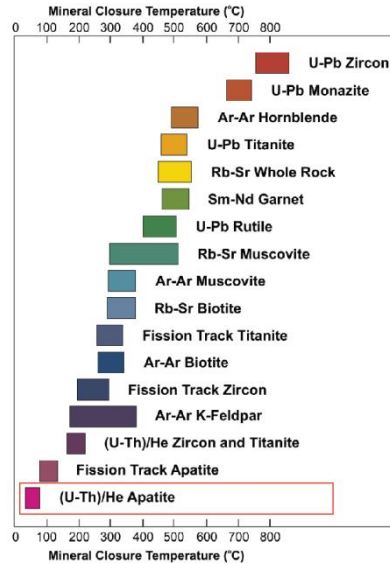


Figure 2.7: Closure temperatures of geochronometers and thermochronometers [from Gwilym, 2005]. The red box highlight the (U-Th)/He system sensitive to the lowest temperature.

It is based on the production of ^4He by the radioactive decay of the ^{238}U , ^{235}U and ^{232}Th [Farley, 2002] in the stable ^{206}Pb , ^{207}Pb and ^{208}Pb . By measuring the concentration of uranium and helium within a crystal, the cooling age of the sample can be calculated [e.g. Rutherford, 1905; Strutt, 1905]. This is possible when no parent or daughter isotopes are gained or lost, that is when the system is closed. The (U-Th)/He dating system, passes from an open to a closed system gradually, in a temperature interval ranging between 45°C and 65°C (so-called Partial Retention Zone (PRZ) [Wolf et al., 1998; Farley, 2000]

The amount of ^4He can be obtained by the following equation:

$$^4\text{He} = 8^{238}\text{U}(e^{\lambda_{238}t} - 1) + 7^{235}\text{U}(e^{\lambda_{235}t} - 1) + ^{232}\text{Th}(e^{\lambda_{232}t} - 1) + ^{147}\text{Sm}(e^{\lambda_{147}t} - 1)$$

where

He , U , Th , Sm = present-day amounts;

λ = decay constant ($\lambda^{238} = 1.551 \times 10^{-10} \text{ yr}^{-1}$; $\lambda^{235} = 9.849 \times 10^{-10} \text{ yr}^{-1}$; $\lambda^{232} = 4.948 \times 10^{-11} \text{ yr}^{-1}$; $\lambda^{147} = 0.654 \times 10^{-11} \text{ yr}^{-1}$).

The ^4He concentration can be calculated as a function of U, Th and Sm taking into account the $^{238}\text{U}/^{235}\text{U}$ constant ratio. This equation also assumes the total absence of initial ^4He in the sample. It means that no apatite hosting fluid or mineral inclusions must be picked for this analysis.

In this study, five apatites for each sample were handpicked using an optical microscope at magnification up to ca. 150 x. The crystals are selected on the base of good morphology and the absence of inclusion and coating. The minimum dimension must be $\geq 60 \mu\text{m}$. Every crystal has to be measured to apply the α -ejection correction using the method applied by *Farley* [2002]. These crystals are then photographed and loaded into a 0.8 Nb tubes before sending to the laboratory to be analysed (Fig. 2.8).

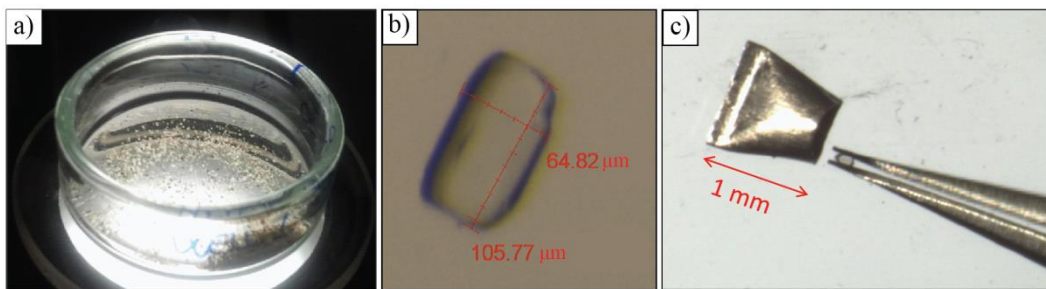


Figure 2.8: Procedure to prepare samples for (U-Th)/He analysis. a) crystal picking was made under optical microscope then b) measured and c) inserted in the Nb tube.

In calculating and correcting the cooling ages several factors must be considered: the α -ejection, that takes into account the distance travelled by the α particles in the solid crystal before stopping; the zonation, the distribution of U and Th within the crystal [*Meesters and Dunai, 2002b*]; the inclusions, that can make the age older increasing the concentration of parent isotopes.

This paragraph wants to be a summary of the main principles at the base of these two low-T thermochronometers. For more details on the methods, application and factors affecting the age calculation see [*Reiners 2005; Reiners and Brandon 2006*].

2.3 Application of thermochronology in validating a tectonic scenario: the thermo-kinematic model

Interpretation of thermochronologic data coming from multiple dating, especially in obtaining the exhumation rate, is often made ignoring the role of topography, tectonics and heat advection on the isotherm deformation. One of the assumption is on the paleogeothermal gradient that is thought to be constant during the cooling phase [Mancktelow and Grasemann, 1997; Safran, 2003], neglecting the role of heat advection. Another assumption is on the closure temperature of a thermochronometric system, considered flat respect to the topography [Parrish, 1983; Stüwe et al., 1994; Brown and Summerfield, 1997]. The last important assumption is made on the topography often considered not changed by tectonics through time.

2.3.1 Topography

Focussing on the role of topography on the deformation of the isotherms, shallower are the isotherm more influence has the topography on it. At depth higher than 20 km, isotherms are considered almost flat, whereas at shallow depth they follow approximately the topography. Between these two end members some intermediate deformation must exists and it depends on the wavelength of the relief, exhumation rate and heat advection. The larger is the wavelength the deeper is the perturbation [Stüwe et al., 1994]. Furthermore the higher is the exhumation rate the more accentuated is the curvature of the isotherms [Mancktelow and Grasemann, 1997]. A relevant effect is recorded after **increasing** or **decreasing the relief**. In the first case the erosion is localized in correspondence of the valley where the isotherms are advected closer to the surface than the high. Thus in the valley the youngest ages are observed [Braun, 2002].

In case of decreasing relief, the erosion is localized in correspondence of the morphologic high. Closure temperature isotherms are advected to the surface more rapidly than in the valley, causing the younging of the cooling ages. On the contrary,

in the valley, where the isotherm become deeper, the cooling ages become older compared to a constant topography scenario [Safran, 2003].

2.3.2 Tectonics

Tectonics plays an important role in controlling the cooling ages across the faults. The lateral heat flow produced by the relative movement of the blocks has relevant effect on the deformation of the closure temperature isotherms.

In **normal fault** setting the uplift of the isotherms at the footwall are produced by many factors such as the uplift and erosion of the footwall, the sedimentation and tilting at the hanging-wall and the topography [Ehlers and Farley, 2003].

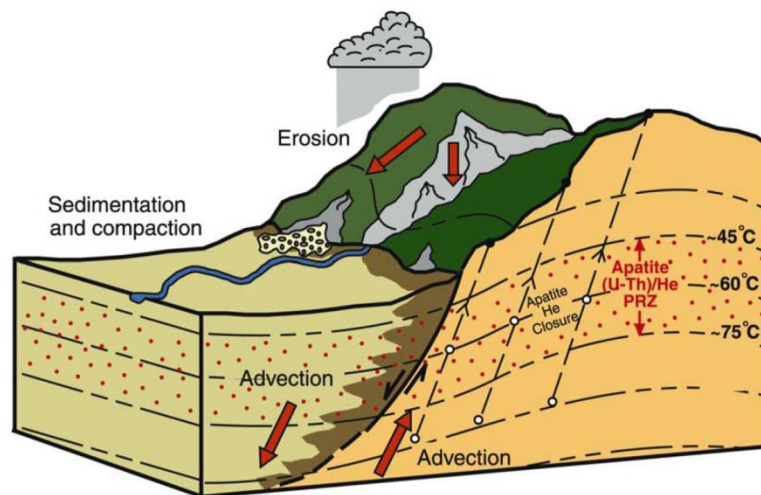


Figure 2.9: Thermal processes in a normal fault setting. Red arrows represent the advection of heat and mass influencing the isotherm deformation [from Ehlers and Farley, 2003].

The lateral variation in exhumation rate and thermal gradient affect the cooling age path across the fault. A 2D numerical model was carried out by Ehlers and Farley [2003], showing the youngest cooling ages close to the fault zone at the footwall.

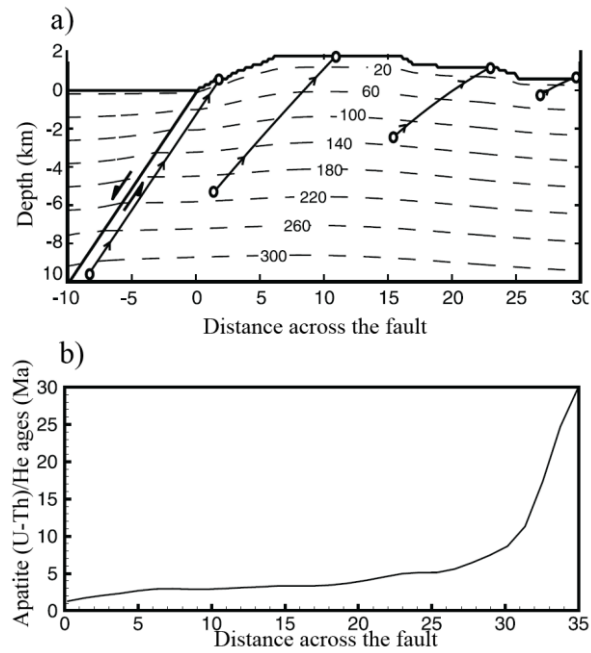


Figure 2.10: a) Thermal field at the footwall of a normal fault; b) predicted apatite (U-Th)/He age profile along the footwall.

More detailed studies [e.g. *Brewer, 1981; Rahn and Grasemann, 1999; Lock and Willet, 2008*] were carried out on the thermal processes in **thrust belt setting**. The factors affecting the thermal field in a contractional regime are approximately the same as the extensional one. The movement of the warm hanging wall on the cool footwall causes later heat flow. Furthermore the uplift and erosion of the hanging wall, the sedimentation at the footwall, the thickening of radiogenic deposits, topography and frictional heating along the fault plane are additional factors influencing the thermal field and subsequently the cooling ages across an inverse tectonic structure. In this case, the cooling of the hanging wall is due to the heat advection from the warmer hanging wall to the cooler footwall.

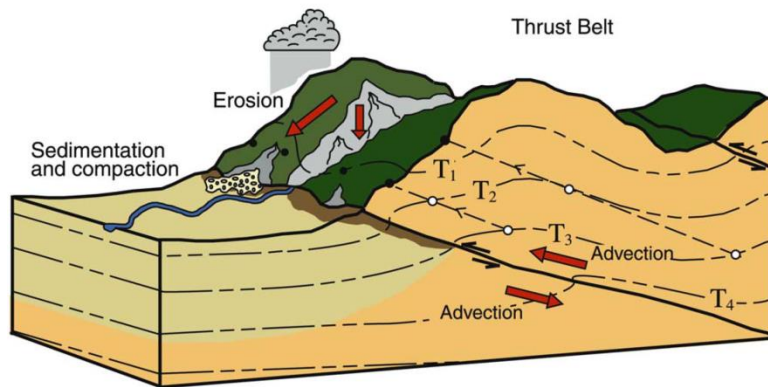


Figure 2.11: Thermal processes in an inverse fault setting. Red arrows represent the advection of heat and mass influencing the isotherm deformation [from Ehlers and Farley, 2003]

Here the exhumation is controlled by the erosion of the uplifted rocks. Physical erosion model and thermo-kinematic model has been elaborated in order to consider the erosion but also the structural cooling due to the emplacement of several thrust sheets over a short distance in a thin-skinned tectonic system. This allows also to predict the cooling ages along inverse structures. The younger ages are recorded in correspondence of the ramp (so-called Ramp Reset Zone) [Lock and Willet, 2008] whereas moving out of this zone the ages become older, preserving the inherited cooling regime.

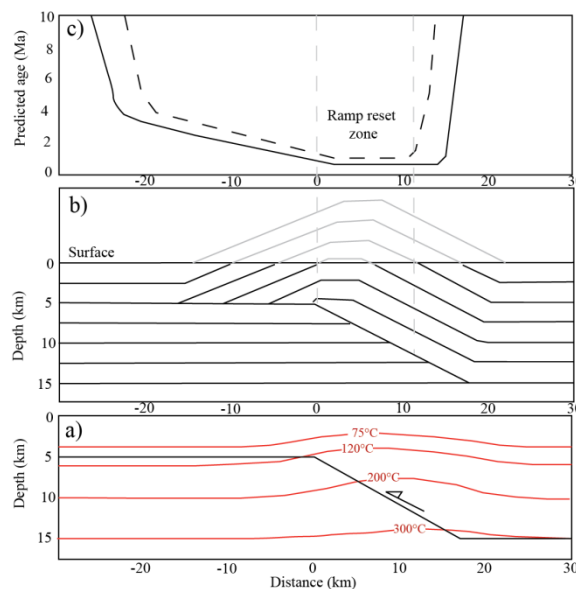


Figure 2.12: Thermal field in compressional setting; a) isotherms bending in correspondence of the thrust ramp; b) layer cake deformed by fault bend fold mechanism; c) predicted AFT (dashed line) and AHe (solid line) age profile across the fault. The ramp reset zone correspond to the area where the ages are reset, corresponding to the ramp.

These are the main factor taken into account for the elaboration of the thermo-kinematic model presented in the Chapter 4. FETKIN [Almendral *et al.*, 2014] was used to model the isotherms and the low-T thermochronometric ages in the complex compressional regime of the Carpathian thrust and fault belt. FETKIN solves numerically in time and space the transient advection-diffusion heat flow equation in two dimension [Carslaw and Jaeger, 1986]:

$$\rho c (\delta T/\delta t - v_x * (\delta T/\delta x) - v_y * (\delta T/\delta y)) = (\delta/\delta x) * k_1 * (\delta T/\delta x) + (\delta/\delta y) * k_2 * (\delta T/\delta y) + \rho H$$

where

$T(x,y,T)$ = temperature at location (x,y) and time t;

$P(x,y)$ = (space-dependent) rock density;

k_1 and k_2 = rock thermal conductivity tensor;

$c(x,y)$ = specific heat

$v(x,y)$ = velocity of the moving grid;

H = radioactive heat production.

All these parameters can be inserted in FETKIN using an .xml file whereas the velocity field was generated directly from the kinematic restoration. All the geological sections must be exported as ASCII files and then processed with FETKIN that provides the modelling of the isotherms through time and the prediction of the cooling ages along the present-day topographic profile. In order to validate a geological scenario, the predicted ages have to equal the measured themrochronometric data.

In addition, FETKIN calculates the t-T path for each point of the present-day topography. These paths can be compared with thermal histories obtained from the Hefty inverse modelling [Ketcham *et al.*, 2005] to further verify the validity of the predicted ages.

3 Chapter III

This work is a paper in preparation for the submission to *Tectonics*. It is mainly focused on the western part of the study area and deals with the analysis of three balanced sections across the Polish and Slovakian Carpathians integrated with some low-T thermochronometric data (AFT and AHe ages) located in the PKB.

Building and exhumation of the Western Carpathians: new constraints from sequentially restored, balanced cross-sections integrated with low-temperature thermochronometry

Ada Castelluccio*^a, Benedetta Andreucci^a, Leszek Jankowski^b, Stefano Mazzoli^c,
Rafał Szaniawski^d & Massimiliano Zattin^a

^a *Department of Geosciences, University of Padua, Via G. Gradenigo, 6, Padova 35131 Italy;*

^b *Polish Geological Institute-Carpathian Branch, ul. Skrzatów 1, Cracow, 31-560, Poland;*

^c *Department of Earth Sciences, University of Naples "Federico II", Largo San Marcellino 10, Napoli, 80138 Italy;*

^d *Institute of Geophysics, Polish Academy of Science, Ks. Janusza 64, Warsaw, 01-452, Poland*

*Corresponding author: ada.castelluccio@studenti.unipd.it; +393209734857

3.1 *Abstract*

Extensive subduction of various oceanic domains is generally invoked to explain the development of the Western Carpathian thrust belt. However, this belt is characterized by the lack of in situ ophiolite, and of any geophysical evidence indicating the occurrence of an oceanic slab at depth. In this paper, a new interpretation for the tectonic evolution of the Western Carpathians is provided based on: (i) an analysis of the stratigraphy of the Mesozoic-Tertiary successions across the thrust belt domains; (ii) a reappraisal of the stratigraphy and sedimentology of the envisaged subduction mélangé (i.e. the so-called Pieniny “Klippen Belt”) marking the ‘suture’ between the Inner and Outer Carpathians; and (iii) the construction of a series of balanced and restored cross-sections then validated by 2D forward modeling. Our analysis provides a robust correlation of the stratigraphy from the Outer to the Inner Carpathians, independently of the occurrence of oceanic lithosphere in the area, and allows for the reinterpretation of the Pieniny “Klippen Belt” as a sedimentary unit (wildflysch) characterized by a block-in-matrix texture and representing the deformed infill of a foredeep developed in front of the Inner Carpathian orogen. To constrain the evolution during the last 20 Ma, our model also integrates previously published and new apatite fission track and apatite (U-Th-Sm)/He data. These latter indicate a Middle-Late Miocene exhumation of the Pieniny “Klippen Belt”. In this study, the recent regional uplift of the Pieniny wildflysch is described for the first time using the forward model for the tectonic evolution of the Western Carpathians.

Keywords: fold and thrust belts; foreland basins; subduction; extension, Pieniny Klippen Belt.

Key points:

- Inner and Outer Carpathian domains have been balanced and restored;
- Interplay between thick and thin-skinned thrusting;
- The Pieniny wildflysch was deposited in the Inner Carpathian foredeep basin.

3.2 Introduction

The development of arcuate mountain belts and associated back-arc basins in the Mediterranean-Carpathian area is generally associated with the process of rollback of subducting oceanic lithosphere and trench retreat [e.g. *Malinverno and Ryan, 1986; Faccenna et al., 2004*]. This process has led to seafloor spreading in (e.g.) the Tyrrhenian back-arc basin, which developed since the Late Miocene in the hinterland of the coevally forming Apennines-Calabria-Sicily orogen [*Kastens et al., 1988; Sartori, 2003*], and resulted in significant arching of a formerly rectilinear belt [e.g. *Faccenna et al., 2001, 2004; Johnston and Mazzoli, 2009*]. Ophiolite suites - including blueschist facies metabasites and metasediments - are well exposed along the Apennine belt and Calabria, thus providing a clear record of the subduction of oceanic lithosphere predating continent-continent collision [e.g. *Rossetti et al., 2004; Ciarcia et al., 2009, 2012; Vitale et al., 2011, 2013*]. Similar features characterize the Alboran domain in the Western Mediterranean, where back-arc extension occurred in the hinterland of the ophiolite-bearing Betic Cordillera and Rif chains [e.g. *Faccenna et al., 1997; Mazzoli and Algarra, 2011* and references therein]. However, the rollback of subducting oceanic lithosphere has also been invoked in areas where high-pressure metamorphic rocks and ophiolitic nappes are completely lacking as any geophysical evidence for a continuous oceanic slab. For instance, the widely accepted interpretation for the geodynamic evolution of the Western Carpathians is based on the subduction of oceanic lithosphere, representing the eastern continuation of the Piemont-Liguria Ocean, during the Late Jurassic-Early Cretaceous [e.g. *Birkenmajer, 1986; Oszczypko, 2006; Picha et al., 2006*] and the later imbrication of the passive margin deposits belonging to the European Platform. The remnants of the former ocean are generally interpreted as being preserved in the so-called Pieniny “Klippen Belt” (PKB), a narrow, arcuate zone consisting of intensely sheared Mesozoic to Paleogene rocks. Traditionally, this belt is interpreted as a suture between the so-called Inner and Outer Carpathians, marking the original locus of the completely subducted eastern segment of the Piemont-Liguria Ocean (also known as the Vahic Ocean in the Western Carpathian region [*Mahel', 1981; Plašienka, 1995 a, 2003*]). Several stratigraphic [e.g. *Birkenmajer, 1960; 1986*] and tectonic studies

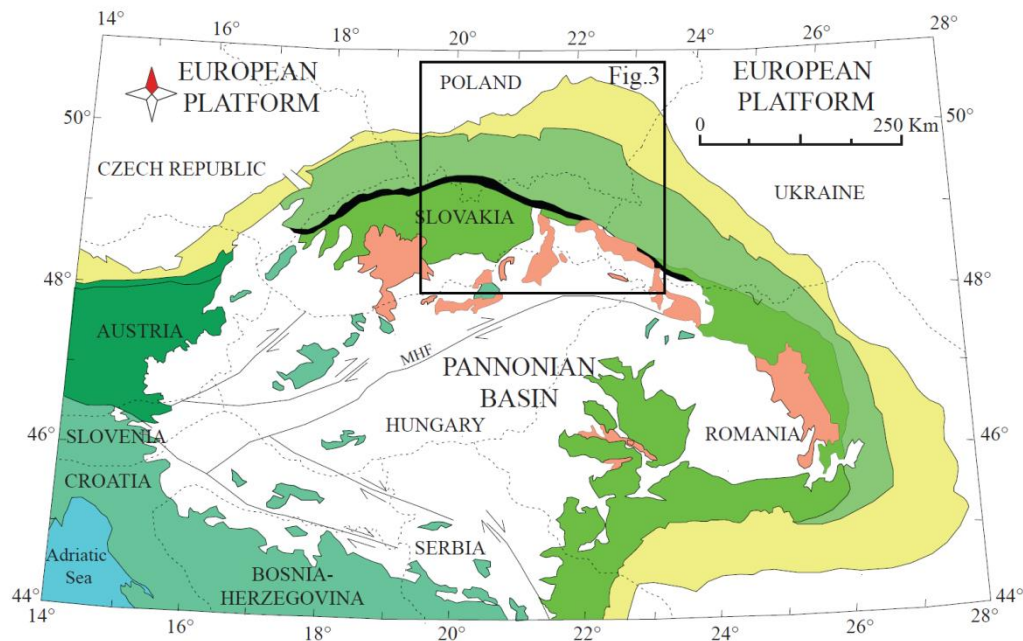
[*Plašienka*, 2012 and references therein] have been carried out supporting this hypothesis, leading to the definition of a “Pieniny Ocean”. However, this interpretation is in contrast with the absence of detritus coming from oceanic basement [e.g. *Săndulescu*, 1988] and the lack of evidence for oceanic lithosphere beneath the overriding Inner Carpathian Plate [*Malinowski et al.*, 2013]. The lack of geophysical evidence for a subducting slab beneath the Western Carpathians has been interpreted as a result of partial break off of a previously continuous slab extending to the Eastern Carpathians of Romania [*Sperner et al.*, 2002]. *Jurewicz* [2005] first put into doubt the original presence of oceanic lithosphere beneath the Pieniny Basin, suggesting instead the occurrence of thinned continental crust between the Outer and the Inner Carpathian domains. Such a scenario would imply that the Piemonte-Liguria Ocean originally closed west of our study area, which in this case would have represented a wide rifted area floored by thinned continental crust during the Mesozoic, giving way to a further oceanic segment to the south (i.e. in the Eastern Carpathian area). On the other hand, an ‘Alpine’ perspective, emphasizing the eastward continuity of the Austroalpine Nappes into the Inner Carpathian Nappes [*Schmid et al.*, 2008], would imply continuity of the Piemonte-Liguria into the Vahic Ocean and therefore the occurrence of a cryptic oceanic suture between the Outer and the Inner Carpathian domains.

Independent of the undeterminable original occurrence and extent of oceanic lithosphere in the study area, a reappraisal of the stratigraphy and sedimentology of the PKB is integrated in this paper with the analysis of the tectonic and stratigraphic relationships between the Inner and Outer Carpathian successions using a series of balanced and restored cross-sections. The proposed tectonic evolution, validated by applying suitable algorithms to a 2D forward kinematic model, reproduces thick- and thin-skinned thrusting in the Western Carpathians from the Early Cretaceous to the present-day. The restoration is carried out independently for the Inner and the Outer Carpathian domains, thereby taking into account the possibility of the original occurrence and later subduction of oceanic lithosphere between the two domains. To constrain the tectonic and thermal evolution during the last 20 Ma, our model also integrates new and previously published apatite fission track and apatite (U-Th-Sm)/He ages. In this way, the progressive evolution of topography as a result of

erosion and crustal deformation is effectively taken into account in the sequential restoration of balanced cross-sections and related forward modeling, thus providing for the first time a comprehensive picture of the tectonic evolution of the area extending from the Inner Carpathians of Slovakia to the Outer Carpathian front in Poland.

3.3 Geological setting

The Central-Western Carpathians are part of a curved orogenic system extending from the Danube Valley in Austria to southern Romania (Fig. 3.1). The origin of this chain is related to the collision between the European Platform and the Alps-Carpathians-Pannonia (ALCAPA) and Tisza-Dacia Mega-Units belonging to the Adriatic palaeogeographic domain. The northeastward and eastward movement of these microplates is generally interpreted as being triggered by the interplay between lateral extrusion [*Ratschbacher et al.*, 1991 a, b] and rollback of the subducting slab [*Sperner et al.*, 2002]. The closure of the southern branch of the Alpine Tethys [sensu *Schmid et al.*, 2008] started in the Jurassic-Early Cretaceous. It involved the Dacia Mega-Unit, whereas the Tisza Plate started being affected by shortening during the Late Cretaceous [*Schmid et al.*, 2008]. The movement of the ALCAPA unit, which shape the Western Carpathians, started during the Late Cretaceous and lasted until the Neogene [*Sandulescu*, 1988; *Földvary*, 1988]. It led to the emplacement of the Western Carpathian accretionary wedge on top of the southern margin of the European Platform. The tectonic transport direction changed progressively from NW to NE [*Csontos and Vörös*, 2004 and references therein]. This was associated with a diachronous end of thrusting, from ca. 15.5 Ma in the Western Polish sector, to 11.5 Ma in the Ukrainian region [*Nemčok et al.*, 2006]. Basing on structural and stratigraphic evidences, the Carpathians are subdivided into two different tectonic domains [*Książkiewicz*, 1977]: the Inner Carpathians (IC) and the Outer Carpathians (OC). The former are made up of Variscan crystalline basement,



LEGEND


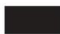


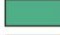




	Foredeep		Pieniny Klippen Belt		Eastern Alps
	Outer Carpathian Flysch Belt		Dinarides		Major strike-slip faults
	Inner Carpathians		Neovolcanics		State Borders

Figure 3.1: General tectonic map of the Carpathian-Pannonian region. Major tectonic domains include: Foredeep, Outer Carpathians, Pieniny Klippen Belt, Inner Carpathians, Dinarides, Eastern Alps and areas of volcanic rocks. The Mid-Hungarian fault zone (MHF) separates the ALCAPA and Tiza-Dacia Mega Units of the Inner Carpathian domain.

including Paleozoic metamorphic rocks, and its Mesozoic sedimentary cover, that was incorporated into a series of thick-skinned thrust sheets (in this paper, the so-called Western Central Carpathian domain [e.g. *Froitzheim et al.*, 2008] is included in the Inner Carpathians for the sake of simplicity). These thrust sheets are unconformably overlain by clastic deposits belonging to the Central Carpathian Paleogene Basin (CCPB). Early Alpine shortening involved the Inner Carpathian zone during the Late Cretaceous [*Maluski et al.*, 1993]. Thrusting caused the uplift of the Variscan crystalline basement and the imbrication and subsequent erosion of its Mesozoic cover [e.g. *Anczkiewicz et al.*, 2013 and references therein; *Janočko et al.*, 2006; *Roca et al.*, 1995]. The movement of the Inner Carpathian range toward the N and NE produced a flexure of the European Platform and the progressive migration of thrusting towards the north, thereby involving the successions deposited in the Outer Carpathian sedimentary basin. The Outer Carpathians consist of a fold and

thrust belt formed mainly in siliciclastic turbiditic deposits of Upper Jurassic to Lower Miocene age [Książkiewicz, 1962, 1977; Bieda *et al.*, 1963; Mahel' *et al.*, 1968; Koszarski and Ślaczka, 1976], which were deformed since Oligocene times. Stratigraphic investigations suggest a diachronous end of thrusting, which is younging to the east, although generally ceasing within the Middle Miocene [Nemčok *et al.*, 2006]. The Outer and Inner Carpathian realms are separated by a few hundreds of meters to twenty kilometres wide zone called the Pieniny “Klippen Belt” [Andrusov, 1931, 1938, 1950, 1974; Birkenmajer, 1956 b, 1957c, 1958d, 1960; 1986; Birkenmajer and Dudziak, 1988; Plašienka 1995a, b; Plašienka and Mikuš, 2010; Roca *et al.*, 1995; Uhlig, 1890]. This belt runs from the Vienna Basin to northern Romania and consists of Mesozoic blocks of shallow to deep-water facies embedded in a less competent Upper Cretaceous to Paleocene matrix. Some papers suggest the occurrence of even younger deposits, such as the Oligocene Myjava succession [Oszczypko *et al.*, 2005].

3.4 Main tectono-stratigraphic units of the Western Carpathians

3.4.1 Outer Carpathians

The Outer Carpathian accretionary wedge is built by a series of thrust sheets whose stratigraphy is well described in term of thickness, lithology, sedimentary features and provenance analysis. The thrust sheets are traditionally grouped, based on their stratigraphy (see below), into larger tectonic units. These groups of thrust sheets - loosely defined as “nappes” in the older literature – include from the innermost to the outermost: (i) the Magura, (ii) the Dukla, (iii) the Silesian, (iv) the Subsilesian and (v) the Skole units (Fig. 3.2). The usage of these traditional names, essentially referring to tectonostratigraphic units, is maintained in this study as they are well established in the regional geological literature. In the following, the thrust ramps separating these tectonostratigraphic units are indicated with the name of the hanging-wall unit (e.g. the Magura Unit thrust is the fault carrying the Magura on top of the Dukla and further units, etc.).

The Outer Carpathian thrust sheets are completely detached from their original substratum and involved in Oligocene-Early Miocene thin-skinned thrusting. The

Skole Unit, together with the laterally equivalent narrow belt of the Borislav-Pokuttia Unit cropping out in the eastern region (Ukraine), is the outermost unit that thrusts on top of the Middle Miocene foredeep deposits. These latter deposits are made of shallow to deep-water siliciclastic sediments coming from Carpathian chain erosion, intercalated with Lower to Middle Miocene evaporitic layers. A general thickening (up to 2500 m) of the basin succession towards the south and southwest is recorded, mainly due to the flexure of the European Platform during the emplacement of the Carpathian accretionary wedge [Krzywiec, 2001 and references therein].

Skole Unit

The Skole Unit extends from the Eastern Polish Carpathians along the whole western Ukraine. This succession starts with the Spas Shales, a Lower Cretaceous anoxic black shale formation interbedded with thin, laminated siltstones [Kotlarczyk, 1985; Kruglov, 2001] that represents the main decollement level for this unit. These deposits are followed by a thin layer of red radiolaritic shales, that pass upward to a more competent formation (Inoceramian beds) [Kotlarczyk, 1978]. The overlying unit is a 1500 m thick siliciclastic turbiditic formation, characterized by abundant marly layers in the lower part (Siliceous marls-Biancone type facies), which become more calcareous in the central and upper parts of the succession. The oldest deposits of this formation are Upper Cretaceous-Paleocene in age and are overlain by green clayey shales intercalated with the thin-bedded sandstones of the Hieroglyphic beds (Late Paleocene-Middle Eocene). The Eocene sequence terminates with the Globigerina marls and is overlain by the ca. 250 m thick Oligocene bituminous shales belonging to the Menilite Fm. The youngest formation of the Skole Unit is the Krosno Fm., which consists of thick-bedded calcareous sandstones that become more marly and very thin-bedded in the upper part. Its youngest deposits, the so-called Upper Krosno beds, are Lower Miocene in age and, together with the Lower Krosno deposits, reach 2400 m in thickness [Ślaczka *et al.*, 2006].

Subsilesian Unit

The Subsilesian Unit is not continuous across the region, being exposed only in a series of tectonic windows. In the western sector of the Polish Carpathians, its external part is formed by a sort of mélangé, in which Miocene rocks are mixed

together with other units (such as the Subsilesian Unit). In the eastern sector this unit is known as Węglówka unit, which is placed between the Silesian and Skole Units. The oldest deposits consist of Lower Cretaceous euxinic shales intercalated, in the upper part, with turbiditic limestones and marls (Cieszyn beds). The Upper Cretaceous-Paleocene succession starts with a thin layer of green radiolarian shales and radiolarites and become more marly and sandy in the upper part. The occurrence of about 700 m of green marls and variegate shales characterizes the Eocene succession. The uppermost deposits, as for the adjacent unit, consist of the Oligocene bituminous shales of the Menillite Fm. passing upward to the more calcareous sandstones and marly shales of the Krosno Fm.

Silesian Unit

The oldest deposits belonging to this unit are the Cieszyn Limestones (Tithonian-Berriasian) [Matyszkiewicz and Słomka, 1994], which only crop out in a few small areas of the Western Carpathians. This 250 m thick calcareous flysch [Książkiewicz, 1960; Peszat, 1967] passes upwards to Lower Cretaceous sandy deposits (Grodziszczce ss.) and, higher up, to more shaly ones (Verovice shales, followed by Lgota beds). During the Upper Cretaceous to Paleocene, the deposition of up to 2000 m thick flysch deposits of Godula beds in the inner part of the Silesian Unit is intercalated with the deposition of variegate shales. The youngest deposits of the Paleocene succession consist in thick-bedded sandstones (Istebna beds) alternated with layers of grey shales. The Eocene sediments are very heterogeneous and are characterized by several facies variations: thick variegate shale sequence is intercalated with sandstones belonging to the Ciężkowice Fm. Eocene sedimentation ends with the calcareous sandstones and shales constituting the so-called Hieroglyphic beds. The whole sequence is closed by the Globigerina marls and the Oligocene Menillite Fm., as it occurs in the neighbor unit. For this reason, both formations represent a useful marker for lithostratigraphic correlations. Younger deposits also occur in the Silesian unit and belong to the Oligocene-Lower Miocene Krosno beds, whose lithology is quite similar to the outer units (calcareous sandstones intercalated with shales, increasing its marly content in the upper part [Ślączka et al., 2006]).

Dukla Unit

In the Polish region, the base of the succession consists of Upper Cretaceous deposits (although older deposits can be found in the Ukrainian region) known as Lupków beds [Leško and Samuel, 1968; Ślącza, 1971; Korab and Durkovic, 1978]. These beds are made up of dark shales intercalated with thin to thick-bedded calcareous sandstones. The Upper Cretaceous sequence is followed by calcareous and/or micaceous sandstones belonging to the Cisna beds deposited during the Paleocene. A 1000 m sequence of thick-bedded sandstones (Hieroglyphic beds), locally intercalated with variegated shales, characterizes the Eocene sedimentation. As for the previously described units, the Globigerina marls are the uppermost deposits of the Eocene sequence, followed by dark bituminous shales belonging to the Menilite Fm. and the Cergowa sandstones. This succession passes gradually upward to Lower Oligocene calcareous shales intercalated with calcareous sandstones of the Krosno Fm., whose maximum thickness reaches ca. 1000 m [Ślącza et al., 2006].

Magura Unit

The Magura Unit is the uppermost thrust sheet of the OC, being bounded by a continuous thrust running from the Western to the Eastern Carpathians, across the Czech Republic, Slovakia, Poland, Ukraine and Romania. The Magura Unit is detached along Aptian-Cenomanian black and green radiolarian shales, which are the oldest deposits of the unit. Higher up, Upper Cretaceous variegated shales pass to the Inoceranian beds, a thin to massive sandstones and turbiditic succession, that is interbedded with dark shales containing submarine slumping and intensely deformed layers [Cieszkowski et al., 1987]. The sandy component of this turbiditic succession increases laterally in the so-called Szczawnica Fm. [Oszczypko et al., 1990]. These deposits become rich of exotic carbonate blocks in their upper part (Jarmuta Fm.; Paleocene) [Burtan et al., 1984]. Sedimentation during Middle and Upper Eocene changes gradually to shale-rich deposits (Łabowa Fm.). That are interpreted by some authors [e. g. Oszczypko 1991] as deposited below the calcite compensation depth. These deposits are overlain by sandy units of the Beloveža beds, marly deposits belonging to the Łącko Fm. [Jankowski et al., 2012] and, higher up, by the Maszkovice Fm. These deposits are partially covered by the Globigerina marls (Oligocene) and then by the Menilite and Malcov Fm., consisting of black

bituminous shales and thick calcareous sandstone and shales, respectively [Jankowski *et al.*, 2012].

3.4.2 Pieniny “Klippen Belt”

The Pieniny “Klippen Belt” (PKB) is a fanlike structure separating the OC and the IC tectonic domains. Several publications on the geology of the PKB come out in the past fifty years, which described the belt as either a tectonic *mélange* [e.g. Roca *et al.*, 1995] or as a “wildflysch” [Plašienka and Mikuš, 2010]. The PKB includes rocks from the Triassic to the Lower Eocene. Triassic deposits, although not very common within the PKB, have been found as mega-blocks in the Pieniny Mts. (Haligowce Series) and in the western part of Slovakian PKB [Andrusov, 1950]. They consist mainly of dolomites and dolomitic limestones. Jurassic sediments include clastic (partly conglomeratic) deposits, passing upward to a more deep-water facies. Crinodal limestones followed by red radiolarian cherts and nodular limestones characterized the depositional environment from the Middle to the Upper Jurassic [Birkenmajer, 1960]. Triassic and Jurassic deposits together with Lower Cretaceous marls, flyschoid sediments and, locally, cherty limestones, occur in the PKB as mega-blocks (Milpoš Breccia) [Plašienka and Mikuš, 2010]. Birkenmajer, [1956 b] documented for the first time the southern provenance of these blocks, later confirmed by Roca *et al.* [1995]. This latter study also point out their similarity with the facies outcropping in the Inner Carpathian domain (although the uncommon occurrence of Triassic rocks within the PKB must be emphasized). The above-described Mesozoic olistoliths are surrounded by an intensely deformed matrix consisting of Upper Cretaceous-Paleogene shales, sandstones and marls (also known as Klippen mantle [Birkenmajer, 1960]). Basalt olistoliths and metamorphic pebbles of Jurassic blueschists have also been found in the PKB successions [Dal Piaz *et al.*, 1995] and are interpreted to come from the Meliata-Maliac oceanic suture located south of the Inner Western Carpathians [Schmid *et al.*, 2008]. This interpretation is in contrast with the hypothesis of an oceanic domain originally interposed between the Inner and the Outer Carpathians (i.e. an eastern prolongation of the Piemonte-Liguria Ocean). Sedimentological investigations highlight the occurrence of syn-tectonic submarine slumping in the less competent matrix, which is intercalated with

fragment of Jurassic and Lower Cretaceous deposits [Birkenmajer, 1960; Plašienka, 2012]. The occurrence of different tectonic units within the PKB has been postulated and correlated with distinct pre-shortening palaeogeographic domains. Simplifying, the shallow-water deposits have been associated to two distinct ridges: the Czorsztyn Ridge, originally separating the Magura basin from the Pieniny basin, and the Andrusov Ridge, originally located between the Pieniny basin and the innermost Manín basin [Birkenmajer, 1986]. A progressive change of facies occurs from the shallow-water to the Middle-Upper Jurassic deep-water deposits belonging to the basins originally interposed between the above-mentioned ridges. The Jurassic sequence is conformably overlain by Lower Cretaceous marls and Upper Cretaceous flysch deposits [see Birkenmajer, 1986 for details]. The youngest deposits are represented by the clastic sediments of the Jarmuta Fm.

3.4.3 Inner Carpathians

South of the PKB, the IC (here including the Central Western Carpathians) represent the inner part of the study area. Shortening in this IC started during the Early Cretaceous [Voigt and Wagneich *et al.*, 2008], involving the IC s. s. (Tatra Mts and Podhale regions) during the Late Cretaceous [Sandulescu, 1988; Rakús *et al.*, 1990]. This early-alpine phase led to the imbrication of several nappes made up of Variscan basement rocks and Permian to Turonian deposits [Roca *et al.*, 1995]. These nappes are unconformably overlain by the Paleogene deposits of the Central Carpathian Paleogene Basin (CCPB), later affected by the Late Miocene extensional tectonics.

Central Carpathian Paleogene Basin

This basin extends throughout the Inner Western Carpathians realm, being filled by Paleogene flysch-like deposits. It is composed of several minor basins, such as the Orava Basin, Podhale and Liptov Basins, and the Poprad Depression, all of them characterized by a similar sedimentary infill. The regional unconformity defining the bottom of this basin is overlain by Eocene to Oligocene [Gross *et al.*, 1993; Samuel & Fusan, 1992] or even Early Miocene deposits [Olszewska & Wiczorek, 1998; Sotak, 1998a,b; Spisiak *et al.*, 1996]. The lowermost succession consists in conglomerates, poorly sorted sandstones and boulder-bearing breccias [Filo & Siranova, 1998] that are overlain by the Szaflary beds (representing the equivalent to

the “Nummulite Eocene” transgression). The hemipelagic *Globigerina* marls lie on top of this transgressive sequence which is covered by the lower member of the Zakopane beds (Huty Formation sensu *Gross et al.*, [1984]). These beds are predominantly characterized by thin-bedded claystones and mudstones intercalated with thin-bedded sandstones and “Menilite-type” shales. The sandy component increases upward into the Lower Oligocene Chochołów beds and becomes relevant in the upper part of this formation, where it is also intercalated with thin tuff layers. The Upper Oligocene-Lower Miocene Ostrysz beds are the youngest deposits of the CCPB and are made up of thick-bedded sandstones intercalated with mudstones and claystones.

The Variscan basement and its cover

Pre-Paleogene successions crop out in the northern Inner Carpathian domain as isolated mountain massifs within the widespread Paleogene succession belonging to the CCPB. Several boreholes and seismic lines reveal the occurrence of both sedimentary cover and basement-cored nappes below the CCPB deposits. The Variscan basement is composed of metamorphic and granitoid rocks, overlain by Cambrian to Carboniferous volcano-sedimentary deposits [*Hovorka et al.*, 1994]. In the Tatra region, the Mesozoic cover consists of Lower Triassic clastic continental deposits [*Roniewicz*, 1959; *Dzuleński & Gradziński*, 1960] followed by Middle Triassic sabkha and shallow water limestones intercalated with dolomitised layers [*Jaglarz & Szulc*, 2003]. The Triassic succession ends with variegated shales and evaporites intercalated with dolomite and sandstone beds of the Keuper Fm. [*Prokešová et al.*, 2012], which has similar facies to those outcropping as megablocks in the PKB [*Andrusov*, 1931, 1938]. Higher up, the Jurassic sequence starts with sandy crinoidal limestone that passes upward into silicified radiolarian limestone and radiolarian cherts of Middle Jurassic age. A thin layer of limestone and gray marls closes the Upper Jurassic sequence, which is overlain by Lower Cretaceous marls and cherty limestones. The clastic supply increases during the Upper Cretaceous, where formations are characterized by sandstones and claystones [*Janočko et al.*, 2006]. The above-described (so-called “High-Tatric”) Mesozoic autochthonous sedimentary cover of the Tatra basement is tectonically overlain by

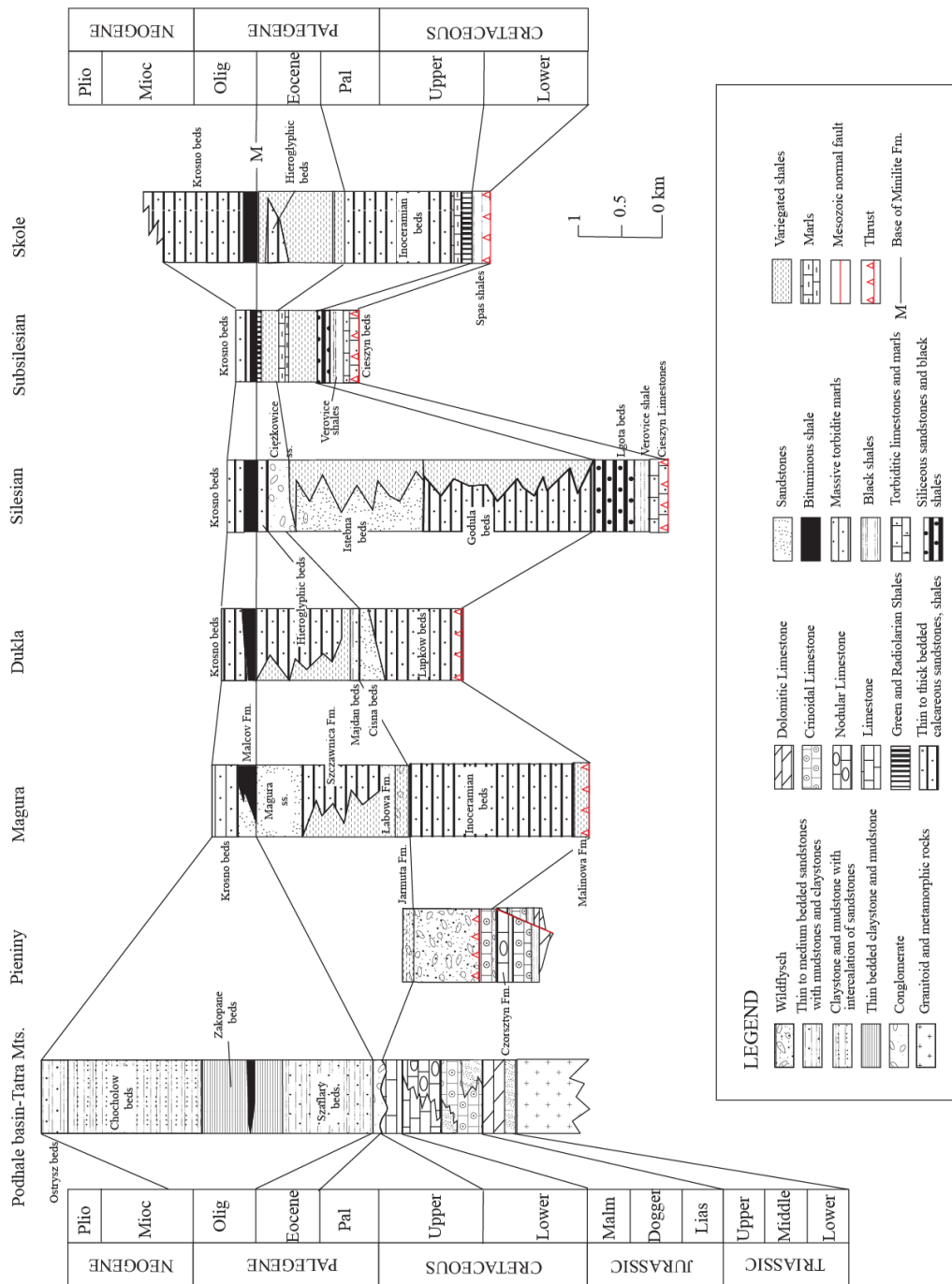


Figure 3.2: Chrono-stratigraphic chart of the main tectonic units of the Polish-Slovakian Carpathians. All stratigraphic columns are aligned to the same isochronous horizon, the Menilite Fm. ('M'). Lithological description and average thickness of each formation are based on published data (see text for details). The Tatra stratigraphic column represents a simplification of the autochthonous succession [Uchman, 2004]. The Pieniny column is made accordingly to the Czorsztyn Unit description by Voigt and Wagreich et al., [2008]. All formations are grouped into horizons of similar age. This subdivision has been used in the construction of the geological cross-sections.

the Sub-Tatric nappes (Križna and Choč nappes) [Kotáňski, 1963a]. The sedimentary succession of the Sub-Tatric nappes, which were thrust northward during the LateCretaceous orogenic event, differs from the autochthonous cover and represents in general more basinal facies.

3.5 Structural modeling

Several balanced and restored cross-sections have been constructed across the Western Carpathians [Behrmann *et al.*, 2000; Gagala *et al.*, 2012; Morley, 1996; Nemčok *et al.*, 1999, 2000, 2001, 2006a; Roca *et al.*, 1995; Roure *et al.*, 1993] in order to provide a geometrically valid interpretation for the structures building the mountain belt. Most of them [Behrmann *et al.*, 2000; Gagala *et al.*, 2012; Morley, 1996; Nemčok *et al.*, 1999, 2000, 2001, 2006a] only include the Outer Carpathians in the restoration and, except for Gagala *et al.* [2012], do not include a 2D kinematic model validating the balanced cross-sections and explaining their structural evolution.

In this study, three balanced and sequentially restored geological sections are constructed across the Western Carpathians (Fig. 3.3) using Move, a software developed by Midland Valley Exploration Ltd. and dedicated to cross-section building and restoration.

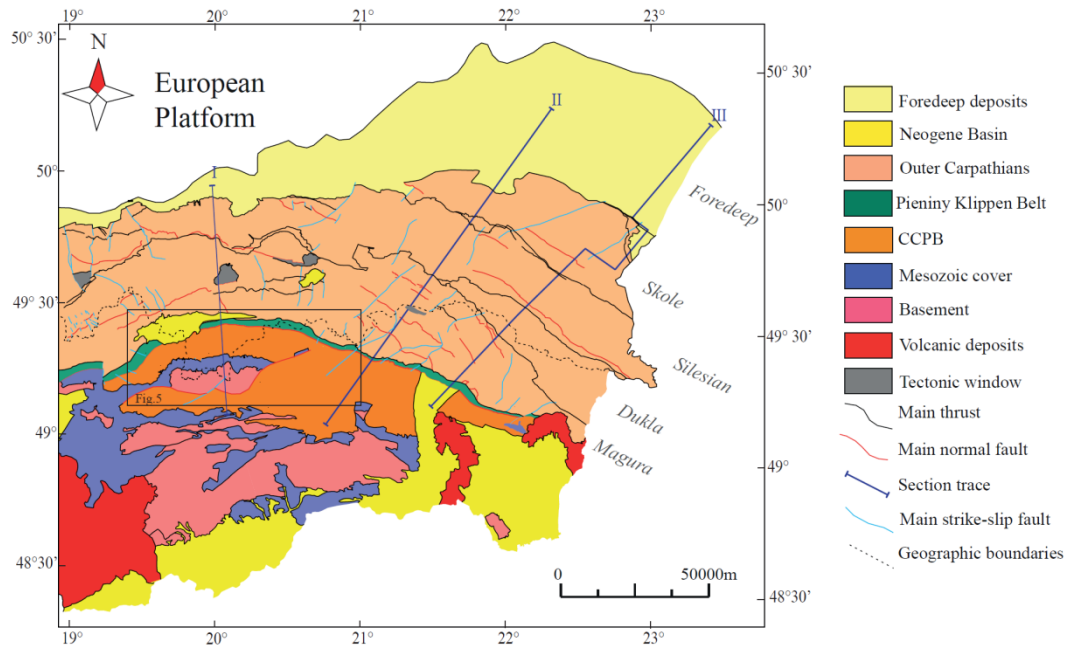


Figure 3.3: Schematic map of the Polish-Slovakian Carpathians showing the main tectonic units and the location of the section traces. Profile III has been offset into two segments following the borehole data. Tectonic windows (in grey) are exposures of the Dukla Units (cropping out extensively more to the southwest).

Our own field data integrated with published datasets and geological maps allowed us to constrain the surface geology and the geometry of deep structures. Flexural slip restoration coupled with 2D forward kinematic modeling is performed in order to check the geometries of the tectonic structures and then validate the cross-sections and the tectonic scenario. Syn and post-tectonic erosion has been simulated, taking into account published low-temperature thermochronometric data including apatite fission track and apatite and zircon (U-Th-Sm)/He ages integrated with new cooling ages from the PKB.

The balanced sections have been constructed across the Polish and Slovakian Carpathians from the foreland basin across the Outer Carpathian accretionary wedge and the PKB, to the Inner Carpathian range. Surface data come from 1:200000 scale geological maps [Nemčok and Poprawa, 1988, 1989; Jankowski *et al.*, 2004; Polák, 2008], 1:50000 scale geological maps [Nemčok *et al.*, 1994], and our own fieldwork, which allowed us to increase the number of dip data and reinterpret some tectonic contacts [see also Mazzoli *et al.*, 2010]. The thickness of the successions are well constrained by geological maps, where both stratigraphic contacts and dip data are shown, boreholes (Bańska PIG-1, Borzęta IG-1 [Marciniak and Zimnal, 2006],

Chabówka-1, Obidowa IG-1, Tokarnia IG-1 [Wójcik *et al.*, 2006], Nowy Targ PGI-1 [Paul and Poprawa, 1992], Zakopane IG-1 [Sokołowski, 1973] and 2 for profile I; Przybyszówka-1 and 2; Rzeszów-1, 2 and 3; Mogielnica-1; Babica-1, Czarnorzeki-1, Zboiska 3 interpreted by Nemčok *et al.* [2006], Zborov-1 interpreted by Nemčok *et al.* [2000], Lipany-2 from Soták *et al.* [2001] and Smilno-1 [Behrmann *et al.*, 2000] for profile II; and Jaksmanice-10 and 26, Leszczyny-1, Bykowce-1; Strachocina-52, Mokre-102 [from Gagala *et al.*, 2012 and references therein], Hanušovce-1 [Behrmann *et al.*, 2000] Kuźmina-1 [Malata and Žytko, 2006], Paszowa-1 [Semyrka, 2009] and Prešov-1 [Čverčko, 1975] for profile III) and published information [Ludwiniak, 2010; Janočko *et al.*, 2006; Nemčok *et al.*, 2000; Oszczypko *et al.*, 2006; Ślęczka *et al.*, 2006]. The geometries of the main tectonic structures have been constrained using seismic lines already interpreted in previous works [e.g. Dziadzio *et al.* 2006; Gagala *et al.*, 2012 and referces therein; Oszczypko *et al.*, 2006]. These data will be described later for each cross-section. The deep architecture of the basement has been traced taking into account the magnetotelluric survey carried out by Stefaniuk, [2006]. Basement morphology is generally controlled by ENE-WSW trending normal faults downthrowing to the south in the western part of the study area, and NW-SE trending normal faults generally lowering the basement to the southwest. Strike-slip faults offset the main basement structures forming a framework in which isolated horsts are surrounded by structural depressions. Magnetotelluric studies, such as that by Ernst *et al.* [1997] suggest also that the Tatra crystalline basement is detached and underlain by a layer of low resistivity sedimentary rocks. Evidence of reverse-slip reactivation of inherited basement normal faults has been documented in some geologic cross-sections and seismic lines [Oszczypko *et al.*, 2006], where Jurassic deposits lay on top of Cretaceous sediments. The occurrence of inversion anticlines [Hayward and Graham, 1989] in Miocene deposits overlying these normal faults suggest a late inversion affecting the basement, which postdates the emplacement of the Carpathian thrust and fold belt. The depth and geometry of the sole thrust is constrained by available seismic lines and already interpreted geological sections. We applied equal area calculation [Chamberlin, 1910, 1919] in order to calculate the depth of the décollement surface where it is not constrained. Although several lithostratigraphic units were

recognized in different pre-shortening sedimentary basins, they are characterized by the similar lithologies with variable sandstone/shale ratio. For the purpose of this work, we group in the same horizon all those lithostratigraphic units deposited during the same time interval. The Upper Cretaceous-Paleocene horizon has been used as regional datum for the restoration.

Once the cross-sections are constructed, flexural slip restoration was performed. This restoration is based on minimum shortening and area conservation assumptions. Each thrust sheet has been unfolded individually using the flexural slip algorithm. The pin line has been traced parallel to the axial plane of the folds. Once unfolded all the thrust sheets and minimized the gaps and/or the overlaps between them, they have been re-folded back to their original position in the cross-section using the Upper Cretaceous-Paleocene horizon as a template. The re-folding allow to fix the geometric inconsistencies in the cross-sections and prepare the section for the sequential restoration.

3.5.1 *Sequential restoration and 2D forward modeling.*

Flexural-slip restoration has been performed in order to prepare the sections for sequential restoration. The structures have been restored taking into account the timing of deformation provided by stratigraphic studies of syn-tectonic deposits and the relationships among the tectonic structures. We applied a vertical simple shear algorithm for listric normal fault restoration in order to deform back the hanging wall along faults with a well-constrained geometry. On the other hand, the fault parallel flow algorithm is best suitable for reverse restoration in shortening settings. Both these algorithms preserve bed area and length. The flexural slip algorithm was also applied to simulate the flexure of the downgoing plate. The undeformed section resulting from the sequential restoration has then been deformed forward in time (from the Ealy Cretaceous to the present-day) in order to validate our structural interpretation and define the structure of the eroded successions. Constraints on the maximum burial and exhumation history have been obtained by thermal modeling based on low-temperature thermochronometric data (apatite fission track and apatite and zircon (U-Th-Sm)/He ages) including both new (Table 1) and published data

[*Anczkiewicz et al.*, 2013, *Andreucci et al.*, 2013; *Zattin et al.*, 2011 and reference therein].

Table 1: Overview of the AFT and AHe age

Sample	Latitude	Longitude	Elevation (m)	Depositional age	AHe w.m.a. $\pm 1\sigma$ (Ma)	AFT central age $\pm 1\sigma$ (Ma)	Mean confined track length \pm SD (μm)
PL 72	49.32298	19.53182	586	Late Cretaceous - Paleocene	7.95 \pm 0.14	45.80 \pm 7.70	10.21 \pm 2.58
PL 75	49.31235	19.48207	570	Late Cretaceous - Paleocene	8.11 \pm 0.09	8.80 \pm 1.70	
PL 82	49.30322	20.79382	608	Late Cretaceous	11.63 \pm 0.11	49.80 \pm 7.10	10.15 \pm 1.85
PL 86	49.42570	20.44130	423	Eocene	10.50 \pm 0.12	10.50 \pm 2.90	
PL 87	49.40512	20.53657	569	Late Cretaceous - Eocene	8.62 \pm 0.15	13.30 \pm 1.80	

3.6 Low-temperature thermochronometric data

Several low-T thermochronometric datasets are available for this study area [*Anczkiewicz* 2005; *Anczkiewicz et al.*, 2005, 2013; *Andreucci et al.*, 2013; *Burchart*, 1972; *Danišik et al.*, 2010, *Král'*, 1977; *Králíková et al.*, 2014a, b; *Struzik et al.*, 2002; *Śmigielski et al.*, 2012; and data herein]. For the IC s. s., apatite fission track (AFT) and apatite (U-Th)/He (AHe) data suggest that the last cooling event is not older than 15 Ma for both the crystalline massifs and the Paleogene deposits of the CCPB [*Anczkiewicz* 2005; *Anczkiewicz et al.*, 2005, 2013; *Danišik et al.*, 2010 and references therein; *Śmigielski et al.*, 2012]. In some particular cases, such as the Tatra Mts., the Middle/early Late Miocene exhumation is locally controlled by the Sub-Tatric normal fault [*Králíková et al.*, 2014a]. On the other hand, the OC experienced an older cooling history (20-15Myr) in their western side, associated with emplacement of the OC accretionary wedge; whereas in the eastern region the tectonic unroofing triggered by low-angle normal faults is the main cause of the younger exhumation (less than 10 Myr) [*Andreucci et al.*, 2013]. To complete frame of the cooling ages, we provide new low-temperature thermochronometric data belonging to the PKB to constrain the timing of cooling of these deposits.

The AFT and AHe datasets available for the study area integrated with our new data from the PKB are represented in Fig. 3.4.

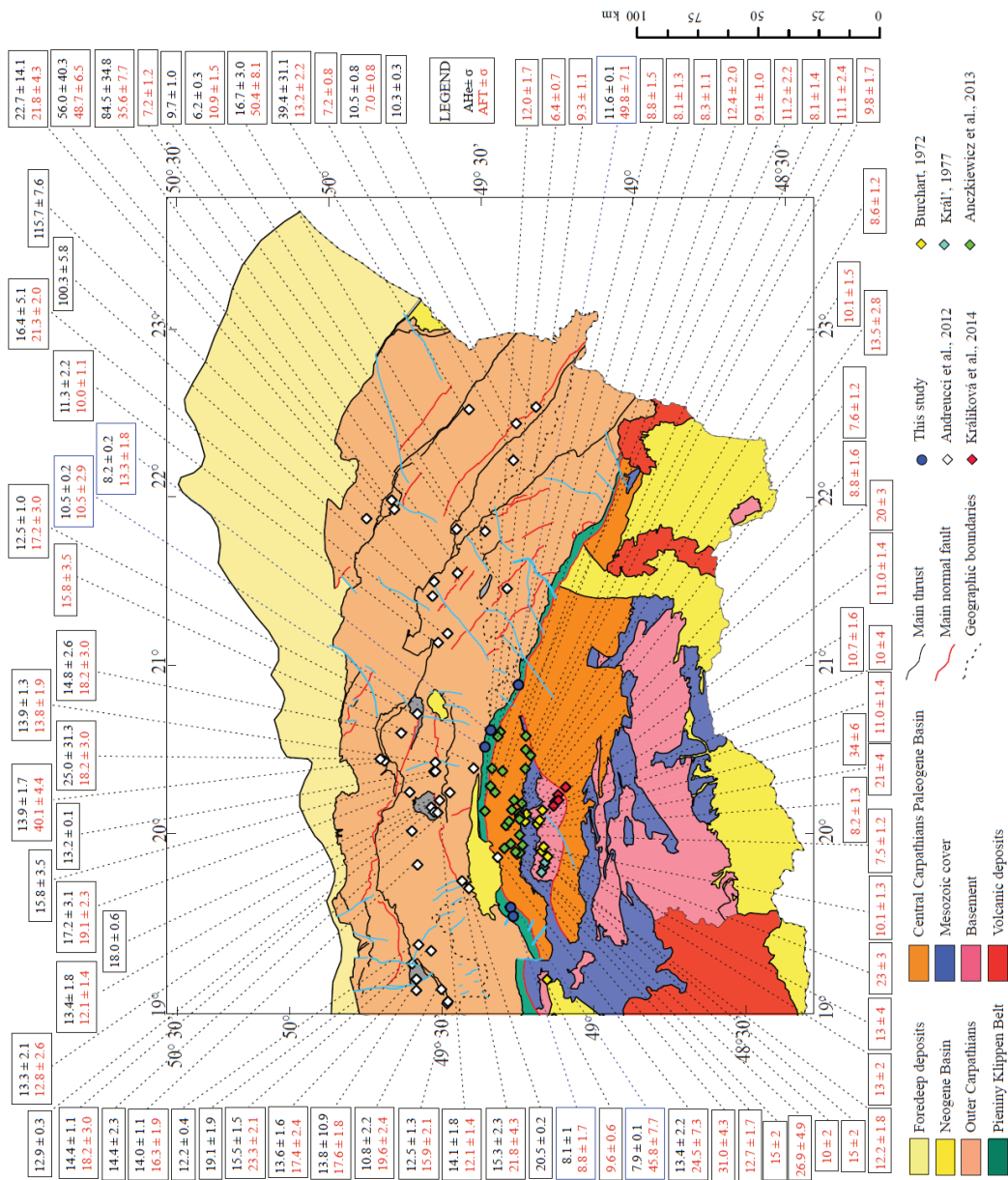


Figure 3.4: Schematic map of the Polish-Slovakian Carpathians showing the spatial distribution and of our new and published samples. AFT central ages and AHe weighted mean ages are indicated for each sample.

3.6.1 New thermochronometric data from the PKB

New AHe and AFT analyses were applied to five samples collected from siliciclastic sandstones and siltstones of the PKB (Fig. 3.5).

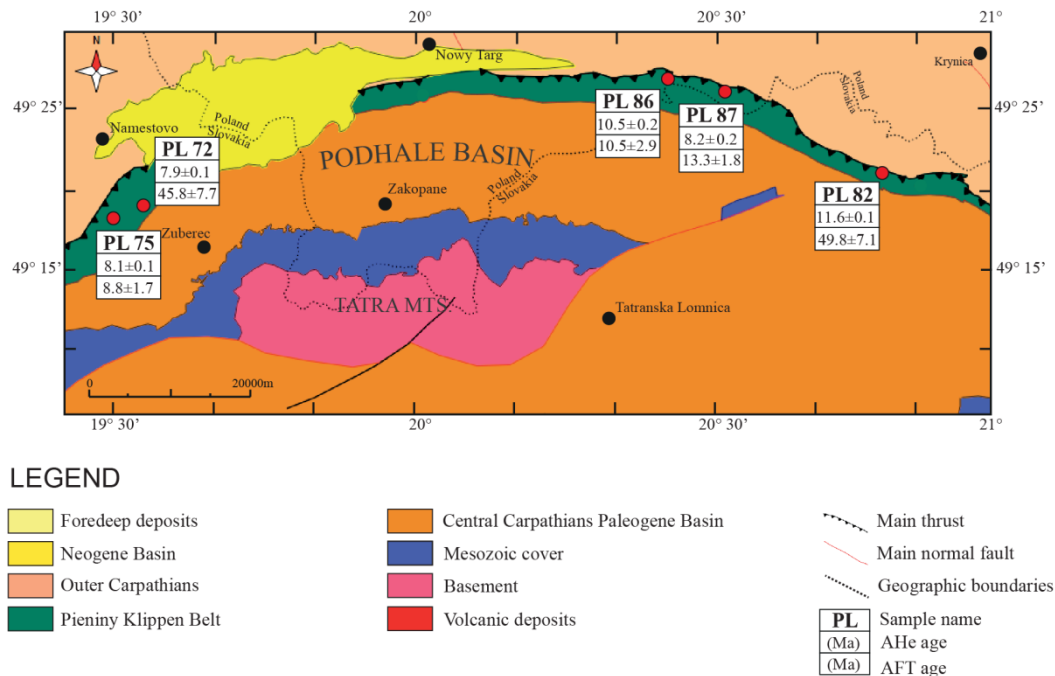


Figure 3.5: Schematic geologic map of the Podhale-Tatra region showing the location of the sampling area along the Pieniny Klippen Belt.

AHe analysis was performed at the Radiogenic Helium Dating Laboratory of the University of Arizona (Tucson), using the procedures described in *Reiners et al.* [2004]. Intact, euhedral, inclusions and coating free apatite crystals, with the smallest dimension $\geq 60 \mu\text{m}$, were preferably selected, handpicked and measured for alpha-ejection correction using the methods described in *Farley* [2002]. In several cases no apatite crystal meeting the criteria listed above was found and slightly abraded, slightly coated or small-inclusion bearing crystals had to be picked. However, no major effect on AHe dates is expected from small inclusions [*Vermeesch et al.*, 2007], and it is in general possible to detect and limit the contingent effect of abrasion and coating [*Spiegel et al.*, 2009; *Andreucci et al.*, 2013]. Therefore, slightly flawed crystals were analyzed relying on their minor and/or detectable and interpretable impact on dates.

Single crystals were loaded into 0.8 mm Nb tubes, and degassed under vacuum by heating with a Nd-YAG laser. The concentration of ^4He was determined by ^3He isotope dilution and measurement of the $^4\text{He}/^3\text{He}$ ratio through a quadrupole mass spectrometer. U, Th and Sm concentrations were obtained by isotope dilution using an inductively coupled plasma mass spectrometer.

AFT analysis was performed at the FT laboratory of the University of Padua. A CN5 glass was used to monitor neutron fluence during irradiation at the Oregon State University Triga Reactor (Corvallis, USA). Central age calculation [Galbraith and Laslett, 1993] was performed with the Radial Plotter software [Vermeesch, 2009]. Chi-square (χ^2) testing assessed the homogeneity of age populations: a population is considered homogeneous for $P(\chi^2)$ higher than 5%. Mean Dpar of single crystals was measured and used as a kinetic parameter. For each sample track densities and length were measured from 20 grains (where possible).

AHe and AFT dates and AFT length data were used to model, for each sample, envelopes of admissible time-temperature paths, using the HeFTy software [Ketcham, 2005]. Timing and rates of cooling obtained by thermal modeling were used, in turn, to constrain the structural model in the last 20 Myr.

3.6.1.1 AHe results

Five replicates were dated for each sample, as shown in Table 2.

Corrected ages range between 6.0 and 49.6 Ma, most of them clustering around 12 and 6 Ma, being younger than depositional ages. The data dispersion among single crystal dates of the same sample is comprised between 20 and 91%. Each sample has minimum ages of 6-9 Ma (1-3 over 5 grains per sample), well-matching the AFT central ages, being 2-4 Myr older. This dataset indicates a very high degree of reset, although incomplete, as shown by the old outlier ages recorded by some crystals .

Table 2: Apatite (U-Th-Sm)/He analytical data. Crossed fields indicate crystals that were considered not reliable and therefore discarded. See the text for details on the reasons for discarding crystals. W.m.a. stands for weighted mean dates: this was calculated using only the youngest crystals (<12 Ma), the corrected dates that were not involved in the calculation of this parameter are indicate by *.

Sample	Replicate	Th/U	Raw date (Ma)	1s ± date (Ma)	Ft (²³⁸ U)	Ft (²³⁵ U)	Ft (²³² Th)	Ft (¹⁴⁷ Sm)	Rs (um)	corr date (Ma)	1s ± date (Ma)	1s ± date %	w.m.a. (Ma)	w.m.a. err. (Ma)	eU (ppm)	eU w/ Sm (ppm)	U (ppm)	dU (ppm)	Th (ppm)	dTh (ppm)	Sm (ppm)	dSm (ppm)	⁴ He/g (nmol)	d ⁴ He/g (ppm)
PL 72	13A156_AC_PL72_Ap1	4.19	6.63	0.35	0.66	0.62	0.62	0.89	41.40	10.32	0.54	5.22			44.83	45.65	22.87	0.34	93.42	1.35	195.52	2.84	1.62	0.08
	13A157_AC_PL72_Ap2	8.02	4.98	0.10	0.67	0.63	0.63	0.89	42.38	7.74	0.16	2.07	7.95	0.14	27.32	27.62	9.62	0.15	75.29	1.07	81.16	1.23	0.74	0.01
	13A158_AC_PL72_Ap3	2.73	10.58	0.24	0.73	0.69	0.69	0.91	52.66	14.78*	0.34*	2.28	-	-	0.10	0.10	0.06	0.00	0.16	0.00	0.41	0.01	0.01	0.00
	13A159_AC_PL72_Ap4	1.49	40.16	0.63	0.61	0.56	0.56	0.87	35.27	66.76*	1.06*	1.59	-	-	127.83	130.98	95.35	1.37	138.21	2.01	698.47	10.22	27.99	0.32
	13A160_AC_PL72_Ap5	1.04	17.23	0.33	0.65	0.61	0.61	0.89	40.01	26.71*	0.51*	1.91	-	-	109.20	111.19	88.20	1.26	89.39	1.29	441.43	6.37	10.22	0.16
PL 75	13A161_AC_PL75_Ap1	2.63	8.18	0.19	0.90	0.89	0.89	0.97	153.40	9.12	0.22	2.36	-	-	1.61	1.64	1.00	0.01	2.58	0.04	7.36	0.11	0.07	0.00
	13A162_AC_PL75_Ap2	6.82	7.88	0.14	0.72	0.69	0.69	0.91	51.38	11.24	0.20	1.79			67.95	69.09	26.51	0.38	176.33	2.51	280.91	4.06	2.92	0.04
	13A163_AC_PL75_Ap3	7.53	4.59	0.11	0.66	0.61	0.61	0.89	40.48	7.27	0.17	2.32	8.11	0.09	50.64	53.00	18.59	0.27	136.40	1.94	530.84	7.63	1.28	0.03
	13A164_AC_PL75_Ap4	14.36	4.92	0.22	0.68	0.63	0.63	0.89	43.07	7.65	0.33	4.38			52.98	53.58	12.35	0.18	172.90	2.48	165.29	2.48	1.42	0.06
	12A165_AC_PL75_Ap5	11.44	4.47	0.10	0.66	0.62	0.62	0.89	40.99	7.08	0.15	2.16			46.54	48.20	12.86	0.18	143.33	2.05	383.06	5.51	1.14	0.02
PL 82	13A166_AC_PL82_Ap1	16.00	8.30	0.15	0.75	0.72	0.72	0.92	58.38	11.36	0.21	1.83			29.46	31.33	6.31	0.09	98.50	1.41	418.65	6.08	1.35	0.02
	13A167_AC_PL82_Ap2	2.80	6.82	0.30	0.60	0.55	0.55	0.87	33.65	11.76	0.52	4.40			42.21	44.60	25.71	0.37	70.24	1.02	523.69	8.02	1.58	0.07
	13A168_AC_PL82_Ap3	5.82	5.18	0.12	0.58	0.53	0.53	0.86	32.53	9.31	0.21	2.24	11.63	0.11	45.67	47.30	19.57	0.29	111.08	1.60	370.20	5.40	1.30	0.03
	13A169_AC_PL82_Ap4	2.01	36.57	0.63	0.75	0.71	0.71	0.92	56.40	49.60*	0.85*	1.72			13.82	14.49	9.46	0.14	18.53	0.26	147.49	2.18	2.77	0.04
	13A170_AC_PL82_Ap5	1.40	8.38	0.13	0.71	0.67	0.67	0.91	49.39	11.86	0.19	1.58			64.32	68.40	48.70	0.69	66.49	0.95	880.74	12.80	2.96	0.03
PL 86	13A176_AC_PL86_Ap1	2.88	7.20	0.42	0.66	0.62	0.62	0.89	41.52	11.12	0.65	5.86			56.58	58.16	34.10	0.49	95.65	1.37	356.40	5.13	2.22	0.13
	13A177_AC_PL86_Ap2	14.52	8.05	0.23	0.70	0.66	0.66	0.90	47.49	11.97	0.34	2.80			59.34	60.08	13.72	0.20	194.15	2.79	199.16	2.88	2.61	0.07
	13A178_AC_PL86_Ap3	41.56	6.82	0.11	0.70	0.66	0.66	0.90	46.77	10.29	0.17	1.62	10.50	0.12	92.04	92.75	8.75	0.13	354.44	5.04	225.99	3.33	3.42	0.04
	13A179_AC_PL86_Ap4	27.64	4.97	0.17	0.67	0.63	0.63	0.89	42.20	7.85	0.27	3.38			39.94	40.54	5.45	0.10	146.78	2.09	158.06	2.28	1.08	0.03
	13A180_AC_PL86_Ap5	4.01	10.00	0.27	0.60	0.54	0.54	0.87	33.55	17.52*	0.48*	2.74			125.88	126.92	65.62	0.95	256.43	3.67	274.70	4.12	6.84	0.17
PL 87	13A181_AC_PL87_Ap1	5.14	5.98	0.17	0.71	0.67	0.67	0.91	48.54	8.67	0.24	2.79			19.24	19.90	8.83	0.13	44.27	0.64	151.16	2.20	0.63	0.02
	13A182_AC_PL87_Ap2	6.16	12.26	0.44	0.69	0.65	0.65	0.90	45.31	18.36*	0.66*	3.61			29.23	30.44	12.12	0.17	72.83	1.06	272.48	4.04	1.97	0.07
	13A183_AC_PL87_Ap3	7.60	4.39	0.27	0.75	0.72	0.72	0.92	58.07	6.00	0.36	6.04	8.62	0.15	6.19	6.32	2.26	0.04	16.74	0.24	29.14	0.49	0.15	0.01
	13A184_AC_PL87_Ap4	2.10	5.84	0.18	0.74	0.71	0.71	0.92	55.83	7.97	0.25	3.10			23.94	24.50	16.16	0.23	33.12	0.48	126.13	1.88	0.76	0.02
	13A185_AC_PL87_Ap5	7.84	8.28	0.44	0.75	0.71	0.71	0.92	56.64	11.42	0.61	5.35			16.35	16.63	5.84	0.08	44.68	0.64	69.90	1.04	0.74	0.04

Analytical data are in general acceptable. However, four grains with suspiciously old dates (with respect to both the overall minimum ages and weighted mean sample ages) and critically high or low analytical values ($\text{He} < 1$ mole/g and $\text{U} < 5$ ppm) were not accounted for in the discussion, and are shown in Tab.2 as crossed fields (PL 72_3; PL 72_4; PL 72_5; PL86_5).

One crystal belonging to sample PL 75, with exceptionally low He content (< 0.1 nmol), was also discarded, in spite of the acceptable crystal features and the age falling within the range of minimum and mean ages (PL 75_1).

3.6.1.2 AFT results

The results of AFT dating are presented in Table 3 and in the radial plots of Fig. 3.6.

Table3: Apatite fission track analytical data*.

Sample	No. of crystals	Spontaneous		Induced		$P(\chi^2)$ (%)	Dosimeter		Age \pm SE (Ma)	Mean Dpar \pm SD (μm)	Minimum age \pm SE (Ma)	No. of confined tracks	Mean confined track length \pm SD (μm)
		r_s	N_s	r_i	N_i		r_d	N_d					
PL 72	20	2.28	167	12.36	906	0.2	11.15	4798	45.8 ± 7.7	1.19 ± 0.10	38.1 ± 4.7	16	10.21 ± 2.58
PL 75	7	1.18	32	31.09	839	64.4	11.69	4798	8.8 ± 1.7	1.25 ± 0.19			
PL 82	20	5.76	432	25.42	1906	0.0	11.73	4798	49.8 ± 7.1	1.34 ± 0.18	16.6 ± 6.9	31	10.15 ± 1.85
PL 86	8	0.59	15	12.15	311	51.0	11.07	4798	10.5 ± 2.9	1.25 ± 0.47			
PL 87	20	1.65	160	30.02	2917	11.4	11.86	4798	13.3 ± 1.8	1.49 ± 0.18			

*Central ages calculated using dosimeter glass CN5 and $z\text{-CN5}=396.08 \pm 2.9$ and the software TrackKey vers. 4.2 [Dunkl, 2002]. r_s : spontaneous track densities ($\times 10^5 \text{ cm}^{-2}$) measured in internal mineral surfaces; N_s : total number of spontaneous tracks; r_i and r_d : induced and dosimeter track densities ($\times 10^6 \text{ cm}^{-2}$) on external mica detectors ($g=0.5$); N_i and N_d : total numbers of tracks; $P(\chi^2)$: probability of obtaining χ^2 -value for n degrees of freedom (where n =number of crystals-1); a probability $>5\%$ is indicative of an homogenous population. Minimum age is the peak age of the youngest age population obtained for partially reset samples using the BINOMFIT software (Brandon 1992). Sample preparation: Apatite grains were separated using heavy liquids and magnetic separation techniques. Mounts of apatite in epoxy were polished and then etched with 5M HNO₃ at 20°C for 20 s to reveal spontaneous fission tracks. Samples were then irradiated with a CN5 dosimeter in the reactor at the Radiation Center of Oregon State Univ. with a nominal neutron fluence of $9 \times 10^{15} \text{ n cm}^{-2}$. After irradiation induced fission tracks in the low-U muscovite detector were revealed by etching with 40% HF at 20°C for 45 min. Samples were analyzed with a Zeiss Axioskop microscope equipped with a digitizing tablet and drawing tube and controlled by the program FTStage 3.11 (Dumitru, 1993). FT ages were calculated using the external-detector and the zeta-calibration methods with IUGS age standards and a value of 0.5 for geometry correction factor. χ^2 test was used to detect whether the data sets contained any extra-Poissonian error.

Up to twenty grains per sample could be analyzed; the chi-square test indicates a variable spread (dispersion of 0 to 40%) of single grain ages, ranging between 245

and 3 Ma. The average D_{par} (diameter of etch figures parallel to the crystallographic c-axis, [Ketcham *et al.*, 1999]) of the samples ranged between 1.19 and 1.49 μm . Measurement of track lengths was possible on samples PL 72 and PL 82 (16 and 31 tracks per sample, respectively). Of the five analyzed samples, PL 72 and PL 82 show a partial reset of the AFT system after sedimentation (part of the single grain ages older or as old as sedimentary age, high age dispersion); PL 87 show an almost complete reset (all the dates are younger than the sedimentary age but the age-dispersion is elevated (20%); PL 75 and PL 86 show a complete reset (very reproducible single grain dates, all younger than the sedimentary age). However, we point out that in these last samples very few grains could be used for track-counting due to the low spontaneous track density. The central ages of reset samples (included PL 87) range between ca. 9 and 13 Ma.

3.6.2 Thermal Modeling

Using the AFT and AHe single grain ages and AFT track lengths, where available, thermal modeling was performed by means of the HeFTy software [Ketcham, 2005] (Fig. 3.7). Due to AHe age dispersion, only the youngest AHe dates were used for modeling (1-3 crystals per sample). For the AFT partially reset samples (PL 72 and PL 82), the maximum post-depositional burial temperature was constrained at 70-85°C; for sample PL 87 (high but incomplete degree of AFT reset), a maximum burial of 90-100°C was imposed; whereas for samples PL 75 and PL 86, a burial temperature range of 85-120°C was imposed (almost complete AFT reset). All Tt paths in Fig. 3.7 show thermal histories characterized by a last cooling event starting at 10 Ma. No maximum values for cooling rates were imposed. Thermal models point out a prolonged (tens of Myr) stay in the AFT and AHe Partial Retention Zones, cooling down at an average rate of 25 °C/Myr between ca. 10 Ma and the present-day. Details on the parameters used for modeling can be found in the caption of Fig. 3.7.

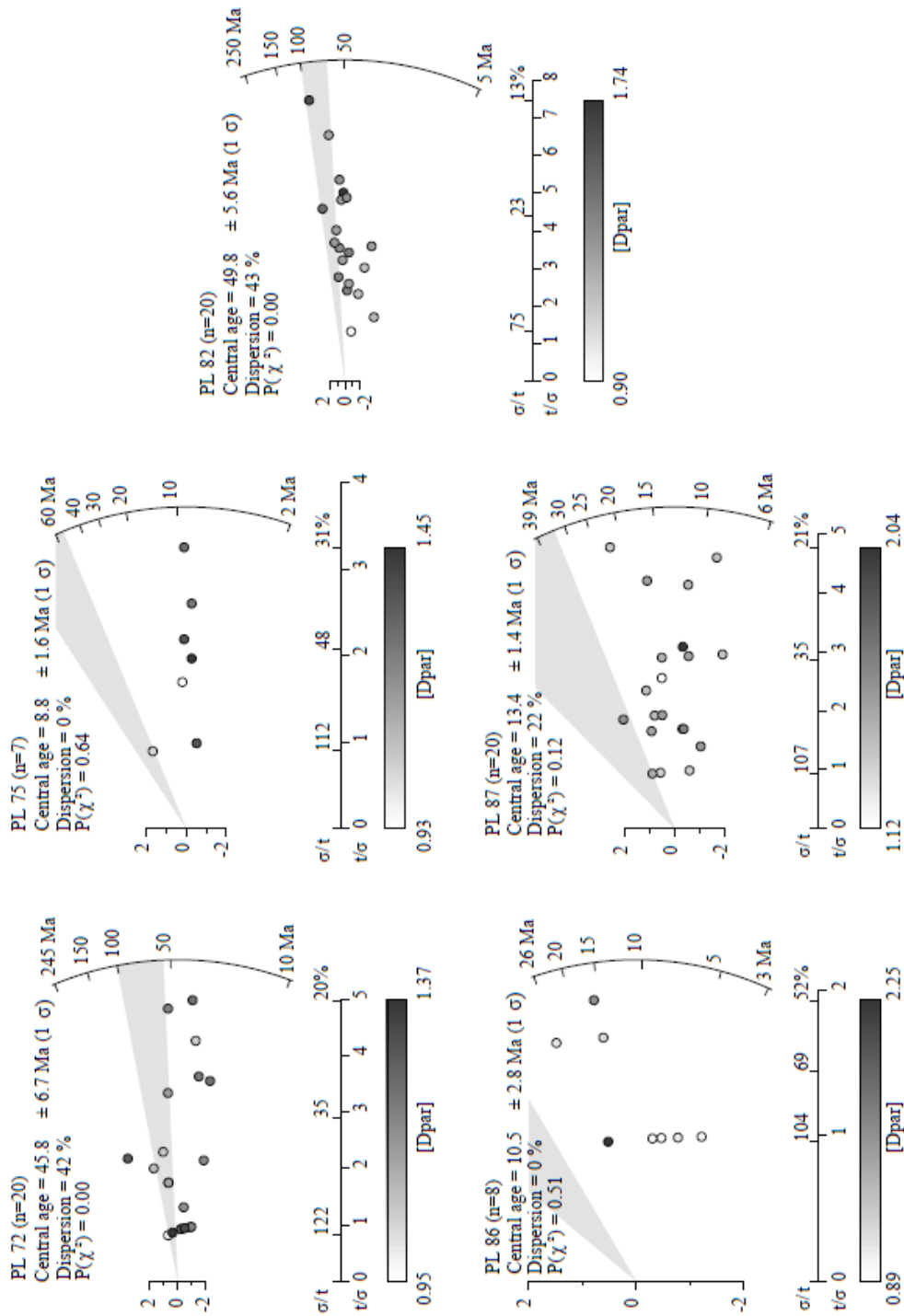


Figure 3.6: Radial plots for AFT samples whose depositional age is indicated by grey area. Standard deviation in single grain age and standard error are indicated in horizontal and vertical axis, respectively. The RadialPlotter software [Vermeesch, 2009] has been used to determine the central age.

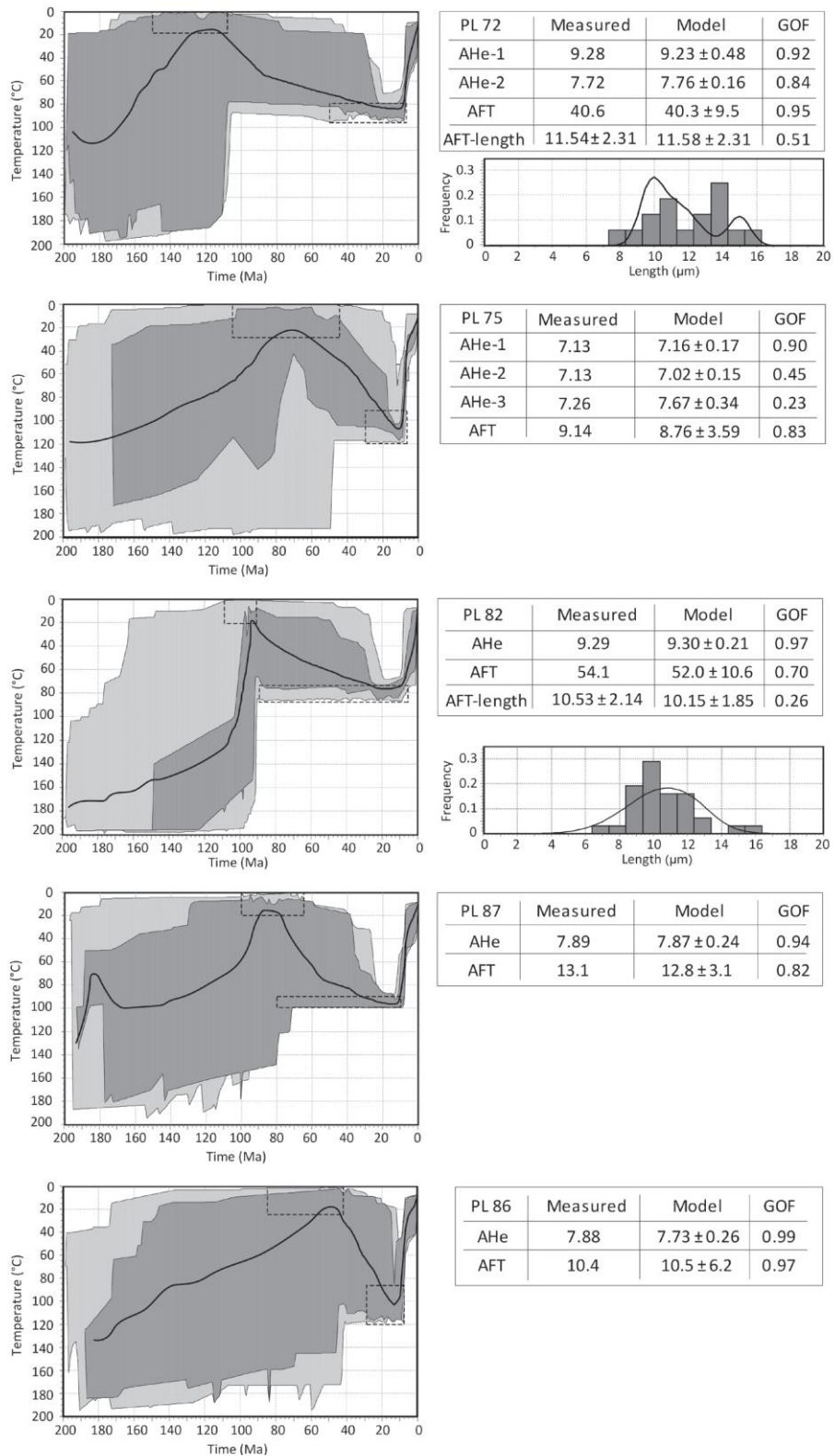


Figure 3.7: Thermal modeling showing the evolution of the Pieniny foreland basin deposits. The black line is the best-fitting path, the light and dark gray area indicate the good path envelope and the acceptable path envelope. Modeling has been performed with the HeFTy software [Ketcham, 2005]. Temperatures between 0 and 20°C were applied during the period corresponding to the stratigraphic age interval.

3.1 Balanced cross sections

The section traces have been chosen to be roughly parallel to the tectonic transport direction, established by the orientation of the major faults. This choice is aimed to avoid major out-of-plane movement that cannot be restored in 2D. The main issue with this assumption (no out-of plane movement) is represented by the evidence for a strike-slip component of displacement along the northern boundary of the PKB [e.g. *Birkenmajer, 1983*]. This strike-slip motion, roughly normal to the main thrust transport direction, implies the occurrence, along the PKB, of a lateral discontinuity in our balanced and restored profiles. However, the amount of strike-slip displacement is probably minor at the scale of our cross-sections, as the PKB forms an arcuate structure (Fig. 3.1) that is unlikely to represent a major wrench fault with consistent strike-slip kinematics all along its roughly semicircular trace. It is worth noting that the arcuate shape of the PKB follows that of the whole Western Outer Carpathian belt, which has been documented by paleomagnetic studies as having suffered only minor or no tectonic rotations around a vertical axis (therefore it did not result by bending of a formerly rectilinear belt [*Szaniawski et al., 2012*]). However, contrasting lateral shear senses have been documented along the PKB, which was first described as sinistral by *Birkenmajer [1986]* and later as dextral by *Jurewicz [2000 a, b]*. The occurrence of contrasting kinematic indicators is consistent with heterogeneous strain produced by shortening and general northward thrusting of the block-in-matrix assemblage constituting the arcuate PKB, rather than large-scale rotation of the Inner Carpathian plate which is implied by a major, consistent strike-slip motion along the belt.

The balanced cross-section lines are located in Fig. 3.3, and shown in Fig. 3.8, 3.9 and 3.10.

3.1.1 Profile I

The profile I (Fig. 3.8a) runs across the Western Polish Carpathians to Slovakia, from Krakow to the Liptov Basin, south of the Sub-Tatra fault. It is almost N-S oriented and normal to the main tectonic structures. The deep architecture of the basement is characterized by several semi-grabens bounded by south-dipping

Mesozoic normal faults in the area beneath the foredeep deposits and the outer part of the Magura Unit. The uncertainties in the interpretation of these structures increase with depth, where the position and the orientation of the tectonic structures involving the basement derive from the restoration of the younger successions in their original pre-shortening position. In the outer sector, the Jurassic deposits covering the basement are unconformably overlain by the Miocene molasse sediments. This unconformity is the result of the Austroalpine phase (so-called “Laramian” inversion in the Carpathian literature [Roure *et al.*, 1993]), which led to the erosion of the Cretaceous cover of the basement and the exposure of the underlying Jurassic deposits. The Neogene molasse has been penetrated by several wells (i.e. Tokarnia IG-1 [Wójcik *et al.*, 2006]) more than 20 km south of the Carpathian thrust front, confirming the large displacement along the leading thrust of the Carpathian chain during the Early Miocene. In its innermost sector, a 26 km thick basement involved thrust sheet occurs (thickness measured without considering syn-thrusting erosion) (Fig. 3.8b). The Outer Carpathians are a thrust and fold belt characterized by a thin-skinned style of shortening, with the sole thrust located along shaly layers intercalated within the Cretaceous succession. The present-day geometry is the result of in-sequence stacking of thrust sheets, which become wider southwards. Starting from the foreland, the Silesian Unit consists of a hinterland dipping duplex, with displacement of individual thrust faults ranging between 200 m and more than 3000 m. The Silesian Unit is also exposed in the Mszana Dolna tectonic window, in the footwall of the surrounding Magura Unit. The Magura Unit is a roof sequence that moved on top of the Silesian duplexes for more than 36 km. This displacement value is obtained from the structural model we used for the reconstruction of the eroded strata, since the location of the present-day Magura front is controlled by erosion. As already suggested by Roca *et al.* [1995], the deformation of the underlying Silesian Unit occurred after the emplacement of the Magura nappes on top of it, producing the deformation of the Magura sole thrust. Both Magura and Silesian Units are affected by normal faults that offset the previously formed thrust and fold structures. These faults mainly reactivate or detach along older thrusts at depth, such as that activating the Magura front or south of the Mszana Dolna tectonic window [Mazzoli *et al.*, 2010]. The Magura - Pieniny tectonic contact is dominantly

steeply dipping, as suggested by several boreholes drilled across it. Nevertheless, its deep structure and kinematics are still a matter of debate, since subsurface data are lacking. In this work we consider this contact a reverse fault that thrusts the Pieniny wildflysch over the Magura Unit [as in *Roca et al.*, 1995], that was later steepened by strike-slip deformation. However, alternative interpretations exist, that invoke left-lateral strike-slip faulting and backthrusting along the northern boundary of the PKB [Birkenmajer 1983, 1985a; Picha *et al.*, 2006; Zuchiewicz & Oszczypko, 2008]. The strike-slip reworking of the PKB is evident at the outcrop scale, although likely minor in terms of absolute displacements. The backthrusting along a N dipping fault is inconsistent with both the map pattern of the tectonic contact and borehole observations, both indicating clearly a S-dipping fault zone. For these reasons we reject the backthrusting hypothesis. Different interpretations have been provided even for the contact bordering the PKB to the south. Our own field mapping indicates the occurrence of a high-angle normal fault putting into contact the Paleogene deposits of the Podhale basin with the Pieniny wildflysch at this location. The Podhale substratum is characterized by four tectonic units produced by the thick-skinned reactivation of basement normal faults as reverse faults. The structural high produced by the imbrication of these basement units is offset by the major Sub-Tatric fault in its southern sector. This structure has been interpreted as a reverse fault by several authors, including *Kotański* [1961], *Birkenmajer* [1986, 2003], *Sperner* [1996], and *Sperner et al.* [2002]. However, this interpretation has been questioned by many authors [Mahel', 1986; Bac-Moszaszwili, 1993; Kohút and Sherlock, 2003; Petřík *et al.*, 2003], who point out a normal dip-slip component of the Sub-Tatric Fault based on the interpretation of a clear reflector visible in the seismic profile 753/92 [Hrušecký *et al.*, 2002], and kinematic indicators provided by mineral fibres (quartz, epidote, and carbonates) and striae on shear surfaces [Jurewicz and Bagiński, 2005]. This extensional dip-slip component of displacement come with previously proposed interpretation for this structure [e.g. *Lexa et al.*, 2000] and is adopted in this study.

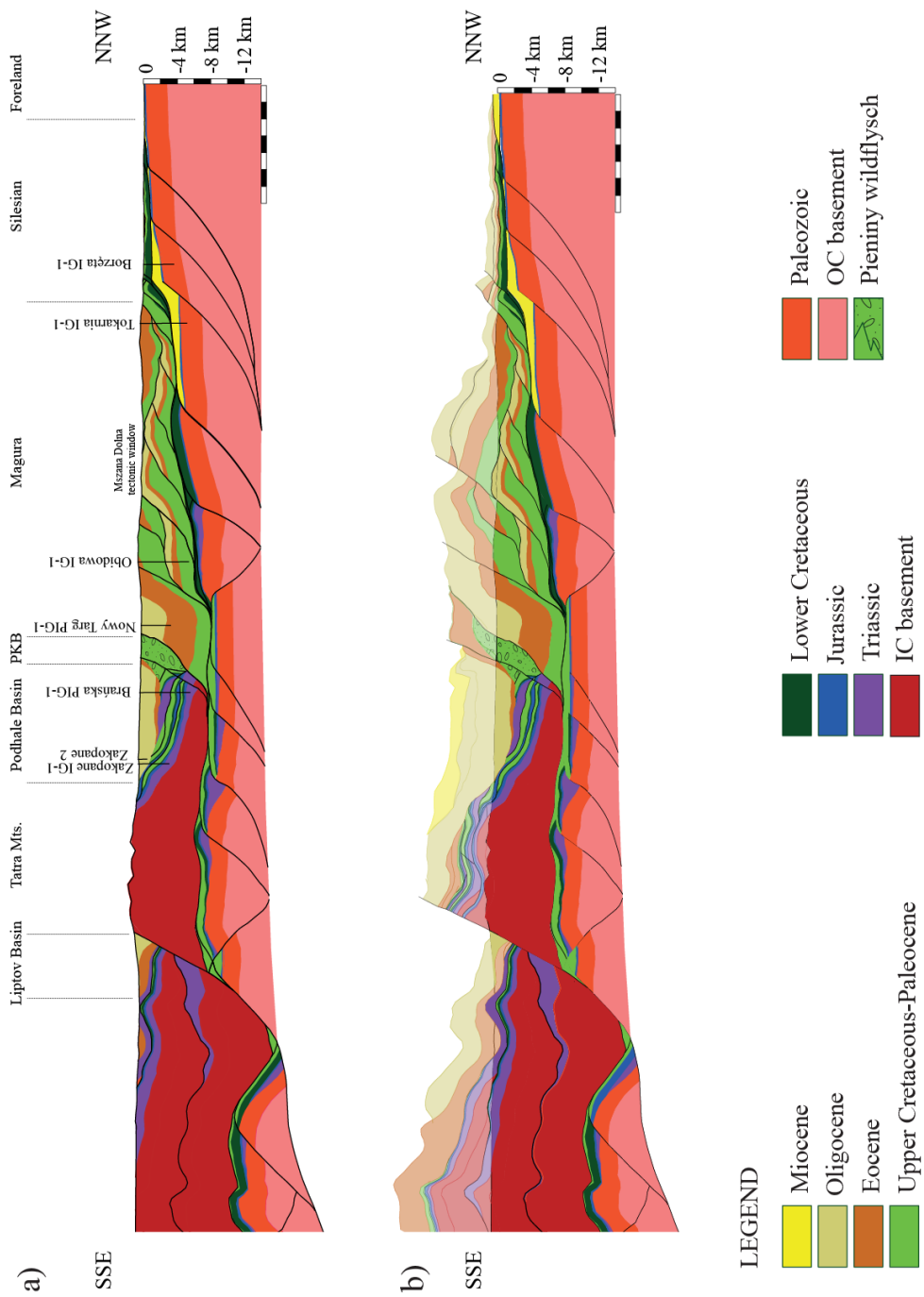


Figure 3.8: (a) Balanced geological section (Profile I) across the Western Polish Carpathians (located in Fig. 3.3). The horizontal scale equals the vertical scale. (b) Thickness of the eroded strata reconstructed above the present-day topographic line represents the minimum value estimated from low-temperature thermochronometric data [Andreucci et al., 2013]. The geometry of the eroded successions is obtained from the forward modeling shown in Fig. 3.12.

Restoration of the pre-orogenic tectonic setting (Early Cretaceous)

In order to restore Profile I to its pre-shortening tectonic setting, the Upper Cretaceous- Paleocene layer is considered the regional datum since it is the best constrained in the Outer Carpathian domain. In addition, this layer can be easily correlated with the Upper Cretaceous horizon representing the youngest deposit of the Inner Carpathian domain. Although the structure of the allochthonous accretionary wedge is well constrained by surface and subsurface data, there are some uncertainties about the extent of the Miocene molasse in the footwall to the Outer Carpathian sole thrust. Some authors suggest a scenario in which Miocene deposits occur beneath the whole Outer Carpathian wedge, although there are no constraints for such an interpretation [i.e., *Nemčok et al.*, 2000; *Oszczypko*, 2006; *Ślęczka et al.*, 2006]. We apply a more conservative criterion, based on the data from the Tokarnia IG-1 well [*Wójcika et al.*, 2006]. We extend the molasse deposits 8 km south of the above-mentioned well, in order to be consistent with the sequential restoration based on minimum shortening. According to this assumption, the Carpathian front records a displacement of about 19 km, considerably less than the ca. 60 km obtained applying the alternative models proposed by *Nemčok et al.* [2000], *Oszczypko* [2006], and *Ślęczka et al.* [2006]. By comparing the present-day geometry of this regional section and the undeformed Early Cretaceous sedimentary basin (Fig. 11a), the amount of shortening can be obtained. It reaches the value of ca. 57 km (46%) for the IC and 73 km (54%) for the OC, without taking into account the Middle Miocene reactivation of the deep basement normal faults causing mild shortening of the foreland basin substratum. The amount of shortening obtained in this study is less than that calculated by *Nemčok et al.*, [2000] for almost the same transect across the Outer Carpathians . Our shortening value, although conjectural, is based on a conservative model that allows us to explain the geometric relationships between the IC, the PKB and the neighboring Magura Unit, which are areas which have no available subsurface data. The sequential restoration provides a 125 km wide IC basin and a 135 km wide OC basin, in which the thickness of the post-rift deposits is mainly controlled by the deep basement architecture.

3.1.2 Profile II

This NE-SW oriented section crosses the eastern sector of the Polish-Slovakian Carpathians, from the foreland basin to the Levoca Basin, one of the minor depressions belonging to the CCPB (Fig. 3.9a). The European Platform underlying the Carpathian belt/foreland system is affected by SW-dipping normal faults. Here, we represent only the major faults that are recognized from magnetotelluric sounding [Stefaniuk, 2006], interpreted seismic lines, and boreholes [see Nemčok *et al*, 2006]. The overall architecture of the cross-section is similar to that shown in the previous profile: the Jurassic deposits, representing the youngest part of the succession of the preserved basement cover, are sealed by the Neogene foredeep deposits. The uncertainties in the interpretation increase at depth, beneath the Magura Unit. The deep basement architecture suggested in this section comes from the sequential restoration that allows us to put back all the detached deposits that built the accretionary wedge to their original position, and construct the basement beneath them. The Neogene molasse forms a wedge-shaped body with southwestward increasing thickness due to the flexure of the lower plate. Directly thrust on top of it, the Skole Unit is made up of upright, horizontal open folds [Fleuty, 1964] produced by detachment folding [Homza and Wallace, 1994]. While the Oligocene and Eocene sequences almost preserve their thickness along the section, the Upper Cretaceous-Paleocene succession becomes thicker towards southwest. This is the only profile that intersects the Subsilesian Unit, which crops out as a narrow belt between the Skole and the Silesian Units. The Subsilesian Unit is deformed by thrust splays showing relatively limited displacement (each displaying ca. 400 m of dip-slip offset) and involving Lower Cretaceous sediments in the inner sector and younger deposits in the external part. The Silesian Unit is characterized by regional open folds, mainly associated with thrusting involving Lower Cretaceous to Oligocene deposits. This unit consists of a hinterland dipping duplex in which individual thrust splays show dip-slip displacements ranging between a few hundreds of meters and 11 km. Also for the Silesian Unit, the Upper Cretaceous and the Oligocene deposits become thicker southwestward. The structure of the inner part of the Outer Carpathians is characterized by the thrust of the Magura Unit on top of the Dukla Unit, which is exposed in the Smilno tectonic window. The number of horses

deforming the Dukla Unit has been inferred from the deformation they produced in the hanging-wall rocks of the Magura Unit, since no seismic profiles clearly show the subsurface structures. The displacement ranges between ca. 1.6 km for the trailing thrust of the Dukla Unit and 18 km for the duplex cropping out in the Smilno area. A noteworthy thickening of the Eocene succession is recorded from the Silesian Unit (ca. 270 m), to the Dukla Unit (ca. 470 m), to the innermost sector where it locally exceeds 3 km. These deposits are affected by low-angle normal faults unraveled by the reinterpretation of some tectonic contacts portrayed in published 1:200000 geological maps [Jankowski *et al.*, 2004]. The trailing edge of the Magura Unit is characterized by the high-angle thrust of the Pieniny wildflysch. Although Hrušecký *et al.* [2006] interpreted the PKB as flower structure, its southern contact is best interpreted as a high angle SW-dipping normal fault, downthrowing the Paleogene and Miocene deposits of the CCPB southward. In this section, the maximum thickness of the accretionary wedge is recorded in the Pieniny wildflysch area where it reaches almost 20 km (Fig. 3.9b). This value is consistent with paleothermal and thermochronological constraints described in section 3.4.

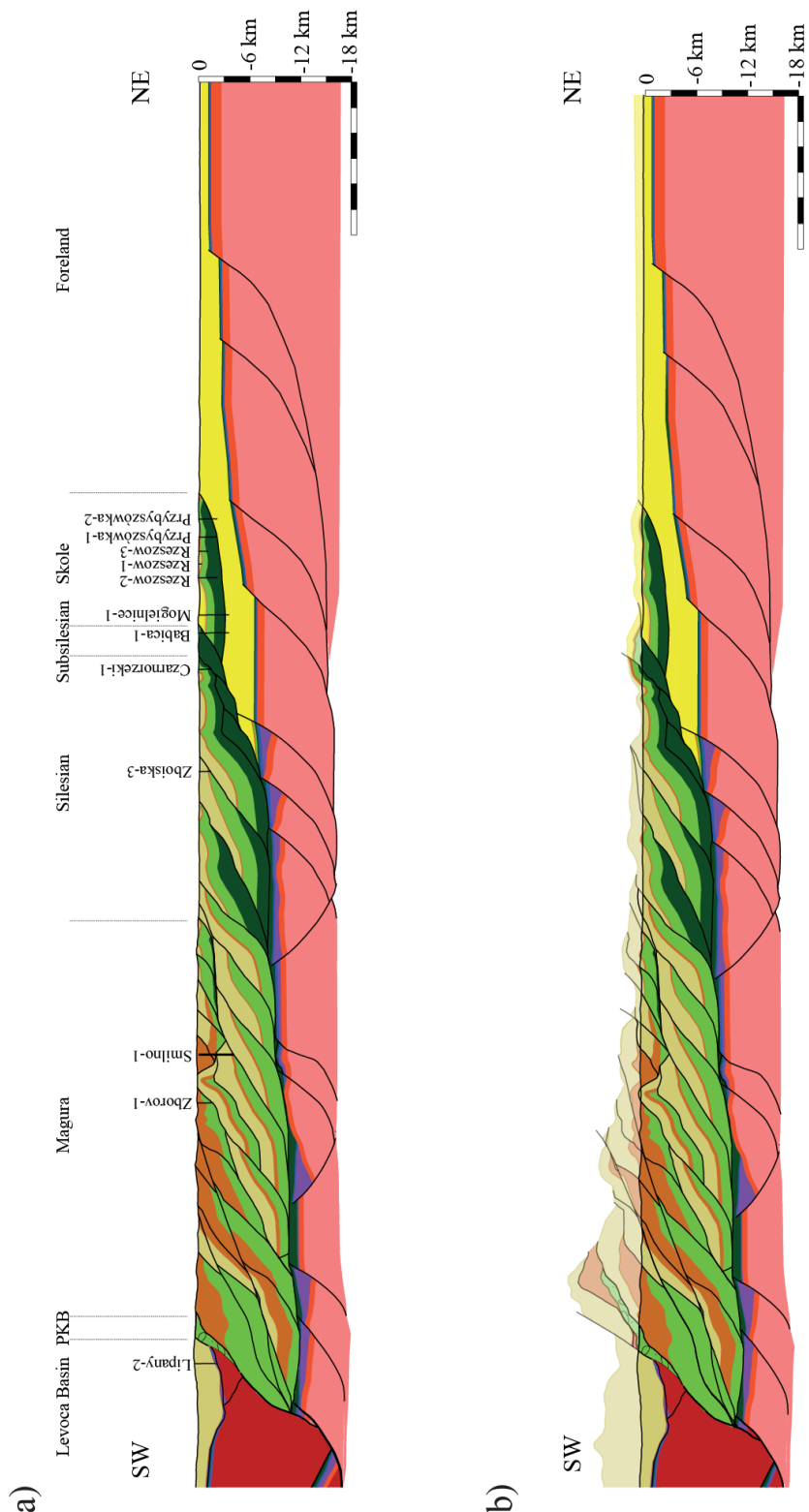


Figure 3.9: (a) Balanced geological section (Profile II) across the Eastern Polish-Slovakian Carpathians (located in Fig. 3). The horizontal scale equals the vertical scale. (b) Thickness of the eroded strata reconstructed above present-day topography represents the minimum value estimated from low-temperature thermochronometric data [Andreucci et al., 2013]. The geometry of the eroded successions comes from the forward modeling we performed in order to validate this section.

Restoration of the pre-orogenic tectonic setting (Late Cretaceous)

The sequential restoration of Profile II has been performed by applying the same assumptions as for Profile I. We used the Upper Cretaceous-Paleocene horizon as a regional datum and, in addition, the available constraints on the position of footwall cut-offs beneath the Skole Unit thrust. Boreholes located along this profile [Myśliwiec *et al.*, 2006] indicate a lack of Upper Cretaceous sediments in the footwall of the sole thrust ca. 5 km southwest of the Carpathian front. Further wells, located southeast of the section trace, indicate the presence of the Skole Unit thrust at a maximum depth of ca. 3 km, gently dipping to the south, and the autochthonous Paleozoic deposits of the European platform directly in its footwall ca. 25 km southwest of the emerging Skole Unit thrust [Nemčok *et al.*, 2006]. Although these constraints did not allow us to infer the position of the Upper Cretaceous footwall cut-off without uncertainties, a conservative solution has been adopted that is consistent with the available subsurface information. Such a solution involved placing the cut-off of the Upper Cretaceous strata ca. 30 km SW of the Carpathian thrust front, in order to avoid huge displacements along the leading thrust. Each thrust sheet building up the Carpathian accretionary wedge has been sequentially restored from the foreland to the hinterland. Some thrusts, such as the trailing thrust of the Magura Unit, seem to not follow the general rule of the up-section propagating ramp, as it cuts down-section into the Upper Cretaceous succession. This apparent down-section propagation is mainly due to the local deformation of the basement after the Inner Carpathian emplacement on top of the lower plate. This tectonic load caused the lowering of the lower plate and the propagation of the subsequent thrust apparently down section. The initial width of the restored Outer and Inner Carpathian basins is of 270 km and 38 km respectively (Fig. 11b), therefore considerably less than the 389 km wide basin proposed by Nemčok *et al.* [2006] for almost the same section. The value of the shortening is about 169 km (63%) for the OC and 10 km (26%) for the IC successions.

3.1.3 Profile III

Profile III (Fig. 3.10a) crosses the easternmost part of the Polish-Slovakian Carpathians. We chose the same transect of Gagala *et al.* [2012] and reinterpreted by

Andreucci et al. [2013] for the OC, extending it further to the southwest in order to include the Pieniny wildflysch and the IC domain. Although data constraining the subsurface geometry of the major thrusts and the thickness of the successions are available, there are uncertainties about the interpretation of the deep structures, as well as about the geometric relationships between the Magura Unit and the Pieniny wildflysch, and the internal structure of the Inner Carpathian Mesozoic nappes beneath the Miocene deposits of the Prešov Basin. While the Stebnik, Skole and Silesian Units are well constrained by seismic profiles and well data [see *Gągała et al.*, 2012 for further details], there are uncertainties about the number of horses deforming the internal part of the Dukla Unit in the footwall of the Magura Unit thrust. We suggest an interpretation that allowed us to construct a balanced section consistent with Profiles I and II in term of structural architecture and amount of shortening. The Middle to Upper Miocene fill of the foredeep basin is characterized by a remarkable thickening southwestwards due to the flexure of the lower plate. The maximum thickness, around 5 km, can be recorded in correspondence of the outermost graben controlled by normal faults in the basement. In this section, the Neogene deposits lay directly on top of the basement, although Jurassic and Upper Cretaceous deposits are known to occur more to the north [*Oszczypko*, 2006]. Magnetotelluric [*Stefaniuk*, 2006] and non commercial seismic profiles show a basement structural high buried by the Silesian thrust sheets, 15 km south of the Paszowa well-1. This morphology influences the geometry of the overlying Silesian Unit thrust, producing its apparent bending as shown in the seismic profiles interpreted by *Gągała et al.* [2012]. No constraints on the architecture of the basement underlying the Dukla and innermost parts of the Silesian Unit are available. The suggested geometry comes from the sequential restoration, as described for the previous two sections. Also in this instance, the OC wedge is characterized by in-sequence thrust propagation. In the outer part, thrusting involves Miocene foredeep deposits of the so-called Stebnik Unit, being detached along the bituminous shales of the Menilite Fm. The inner and tectonically higher Skole Unit forms a leading imbricate fan, whose thrust splays are characterized by variable spacing (from ca. 1000 to 6000 m). A SW-dipping low-angle normal fault offset the inner part of this unit, terminating against a major NE-dipping extensional fault at a depth of ca. 6 km.

The main low-angle normal fault, bordering the Silesian Unit to the south, is responsible for the bending of the Silesian sole thrust and the basement high below it, as well as for significant Late Miocene tectonic exhumation in this area [Andreucci *et al.*, 2013]. The neighboring Dukla Unit consists of several thrust sheets. Thrust spacing within this unit increases to the southwest, while dip-slip displacement of individual splays ranges between ca. 1.5 km and 8 km. The Dukla Unit is partially overridden by the high-displacement Magura Unit. The internal structure of the latter is characterized by the occurrence of several thrust splays whose dip angle increases towards the southwest. The dip-slip displacement along each individual splay ranges from less than 4 km (for the outer thrust ramps) to ca. 19 km for the innermost one. The contact between the Pieniny wildflysch and the Magura Unit is a steep thrust producing the tectonic superposition of the former on top of the latter, as verified by the Hanušovce-1 borehole. The southern boundary of the Pieniny wildflysch is a normal fault dipping to the southwest and following the general trend of the minor normal faults offsetting the Miocene fill of the IC basin. Constraints on the depth of the Oligocene horizon are provided by the Prešov-1 borehole and from available geological cross-sections [Milička *et al.*, 2011]. According to the adopted geological model and the results obtained from forward modeling integrated with paleothermal and low-temperature thermochronologic data, the thickness of the eroded strata has been estimated (see below). The maximum reconstructed thickness occurs in the central part of the OC, where the accretionary wedge reaches 19 km (measured without considering syn-orogenic erosion) (Fig. 3.10b).

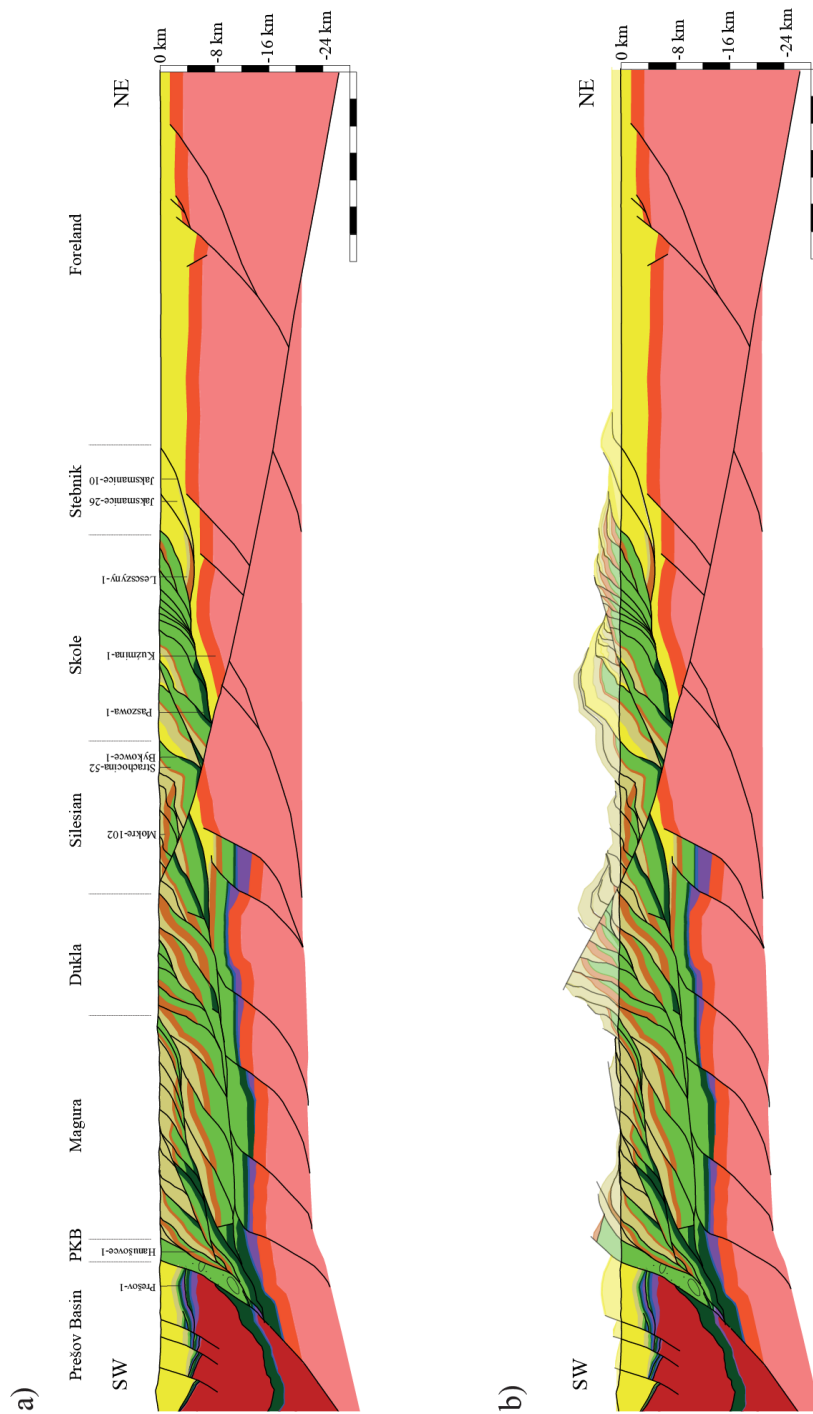


Figure 3.10: (a) Balanced geological section (Profile III) across the Eastern Polish-Slovakian Carpathians [modified after Andreucci et al., 2013]. For location see Fig. 3. The horizontal scale equals the vertical scale. (b) Thickness of the eroded strata reconstructed above present-day topography represents the minimum value estimated from low-temperature thermochronometric data [Andreucci et al., 2013]. The geometry of the eroded successions comes from the forward modeling we performed in order to validate this section.

Restoration of the pre-orogenic tectonic setting (Late Cretaceous)

The sequential restoration has been performed taking into account the same assumptions as for the previously described cross-sections. Considering the uncertainties in the interpretation of basement geometry below the inner part of the allochthonous wedge, the footwall cut-off relative to foreland basin strata correlatable with coeval Stebnik Unit deposits has been placed 61 km south of the Carpathian thrust front, as already proposed by *Gagala et al.* [2012]. The resulting displacement estimated along the Carpathian frontal thrust is of ca. 29 km. Additional displacement has been transferred to the Carpathian leading thrust by the reverse-slip reactivation of preexisting basement normal faults during the Neogene. Unfortunately, the correlation between the neighboring thrust sheets cannot be carried out without uncertainties, since the present-day position of all the emerging leading thrusts is controlled by erosion. We suggest a conservative scenario in order to minimize the shortening and be consistent with the estimate of burial given by the paleothermal and low-temperature thermochronometric indicators. Once restored to their initial configuration, the OC basin reaches a width of 343 km (Fig. 3.11c). This value is considerably less than the ca. 600 km wide basin proposed by *Gagala et al.*, [2012]. This discrepancy results essentially from a different interpretation of the deep structures. The shortening value calculated for the OC successions is around 221 km (64 %). On the other hand, the length of the IC undeformed Late Cretaceous basin equals 116 km, experiencing a shortening around 49 km (42%).

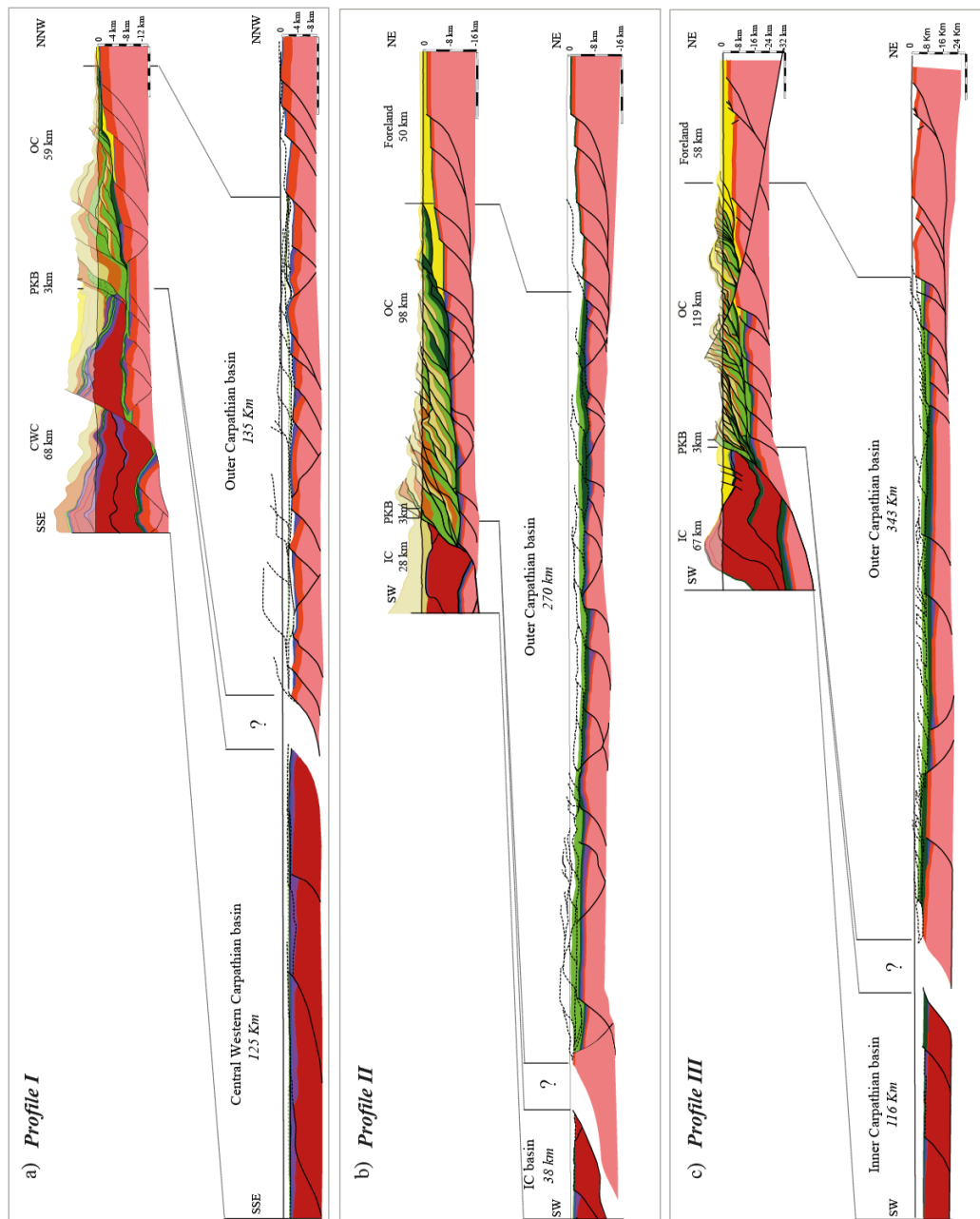


Figure 3.11: Restored cross-sections (a) Profile I at Early Cretaceous time and (b) Profile II and (c) Profile III at Late Cretaceous time. The sections have been sequentially restored based on the minimum shortening assumption. Black dashed lines show trajectories of future thrusts. In the southernmost part of the Profile III the geometry of the eroded Variscan deposits corresponds partially to the outcropping successions, but it is in line with the general geological setting of the specific area.

3.2 Forward modeling

Forward modeling is used in this study to validate the cross-sections that were previously balanced and sequentially restored. The method requires as input parameters the displacement values obtained from the sequential restoration, the thickness of the undeformed successions, as well as the timing of the deformation. The aim of the forward modeling is to produce a final deformed section that is as much as possible, similar to the present-day tectonic setting. We present the 2D kinematic modeling performed on Profile I (Fig. 3.12) in order to show the geological scenario for all the presented profiles. We model the evolution of the Carpathian basin from 145 Ma to the present-day. The Early Cretaceous geological setting is the result of Permo-Triassic rifting and subsequent post-rift Mesozoic sedimentation controlled by the faulted basement architecture (Fig. 3.12a). This pre-shortening geometry comes from the sequential restoration. Shortening started during the Neocomian and involved the inner part of the CWC realm. Deformation then propagated northwards, in the IC realm, producing the reverse-slip reactivation of preexisting normal faults (Fig. 3.12b). The onset of thrusting in the IC is constrained by stratigraphic evidence, the youngest sediments preserved in the IC domain being Turonian in age [Sandulescu, 1988]. The inherited Mesozoic normal faults occurring in the crystalline basement were characterized by variable angles of dip. Their reactivation, during the Austroalpine inversion, caused their propagation into the overlying Mesozoic succession, starting from the Triassic evaporites. The upward propagation into the Mesozoic succession involved a staircase trajectory of the thrusts, which propagated as flat segments along the Triassic evaporites. Thick-skinned deformation produced the imbrication of basement-involved thrust sheets. Subaerial exposure of the IC and associated erosion provided the sediment supply filling the Pieniny foredeep basin, north of the IC front (Fig. 3.12c). Provenance and sedimentological studies [Birkenmajer, 1956b; Roca *et al.*, [1995] document the southern provenance of the olistolithes and olistotromes included in the Pieniny wildflysch, as well as their sedimentological similarity with the IC successions. The erosional event affecting the IC domain is marked by a regional unconformity; the Eocene nummulitic succession lies directly on top of the Mesozoic IC nappes.

During the Late Cretaceous, the emplacement of the IC thrust sheets caused the flexure of the lower plate and the southward deepening of the OC basin, as recorded by the thickening of the Upper Cretaceous-Paleocene succession [Nemčok *et al.*, 2000]. A change in tectonic style occurred during the Paleocene, switching from thick-skinned to thin-skinned thrusting. This change can be likely due the deposition of a shaly formation during the Upper Cretaceous in the OC behaving as décollement surface for all the future thrusts. The deformation front reached the southern margin of the Magura paleogeographic realm during the middle Eocene [Bromowicz, 1999]. Shortening rates increased during the Oligocene, when thrusting propagated further north into the OC paleogeographic realm (Fig. 3.12d-e). The southward thickening of the Eocene and Oligocene strata [Nemčok *et al.*, 2000] suggests an increasing flexure of the lower plate due to the tectonic load provided by the advancing chain. This remarkable change in thickness of the OC Paleogene successions is also confirmed by low-T thermochronometric data [Andreucci *et al.*, 2013]. In-sequence, thin-skinned thrust propagation in the OC domain continued up to the Early Miocene, when shortening migrated at depth into the basement. The reactivation of preexisting basement normal faults in a reverse sense passed further displacement to the sole thrust of the accretionary wedge. During this stage, erosion started to involve the uppermost successions of the inner part of the OC thrust and fold belt. The gravitational instability of the wedge and its subsequent extensional collapse led to the development of normal faults [Mazzoli *et al.*, 2010], some of them reactivating preexisting tectonic contacts. This tectonic event was coeval with rapid erosion during the Late Miocene and was followed by a regional uplift localized in the CWC region (Fig. 3.12f). Comparing the cooling ages obtained for the western sector of the OC [Andreucci *et al.*, 2013] with the new thermochronometric data from the PKB presented in this paper (Fig. 3.5), a remarkable difference in the timing of exhumation can be recognized. Cooling ages ranging between 20 and 15 Myr characterize the western Polish OC successions, whereas a more recent exhumation event (8-15 Myr) involves the PKB deposits. Cooling ages for the PKB are consistent with the published exhumation ages for the IC domain [Burchart, 1972; Baumgart-Kotarba and Král, 2002; Danišik *et al.*, 2008, 2010, 2011], thus suggesting a common cooling event for these two different tectonic domains, as

shown in our structural model. Forward modeling allowed us to not only validate the geological cross-sections and contextualize the thermochronometric datasets, but also to calculate the shortening rate for each step of the reconstructed tectonic evolution. According to our model, the shortening rate for the first convergent tectonic stage (Cretaceous thick-skinned inversion) was of 0.8 mm/yr. A lower rate, 0.5 mm/yr dominated the Paleocene to Early Oligocene time interval. This is in agreement with the Eocene period of relative tectonic quiescence suggested by *Książkiewicz* [1957, 1960] and *Świdziński* [1948]. A remarkable increase of the shortening rate, reaching a value of 6.5 mm/yr, characterized the Late Oligocene-Early Miocene time interval. This was associated with a major change in the style of thrusting, from thick-skinned to thin-skinned. Thrusting was then followed by Middle Miocene normal faulting characterized by an extension rate of ca. 0.6 mm/yr.

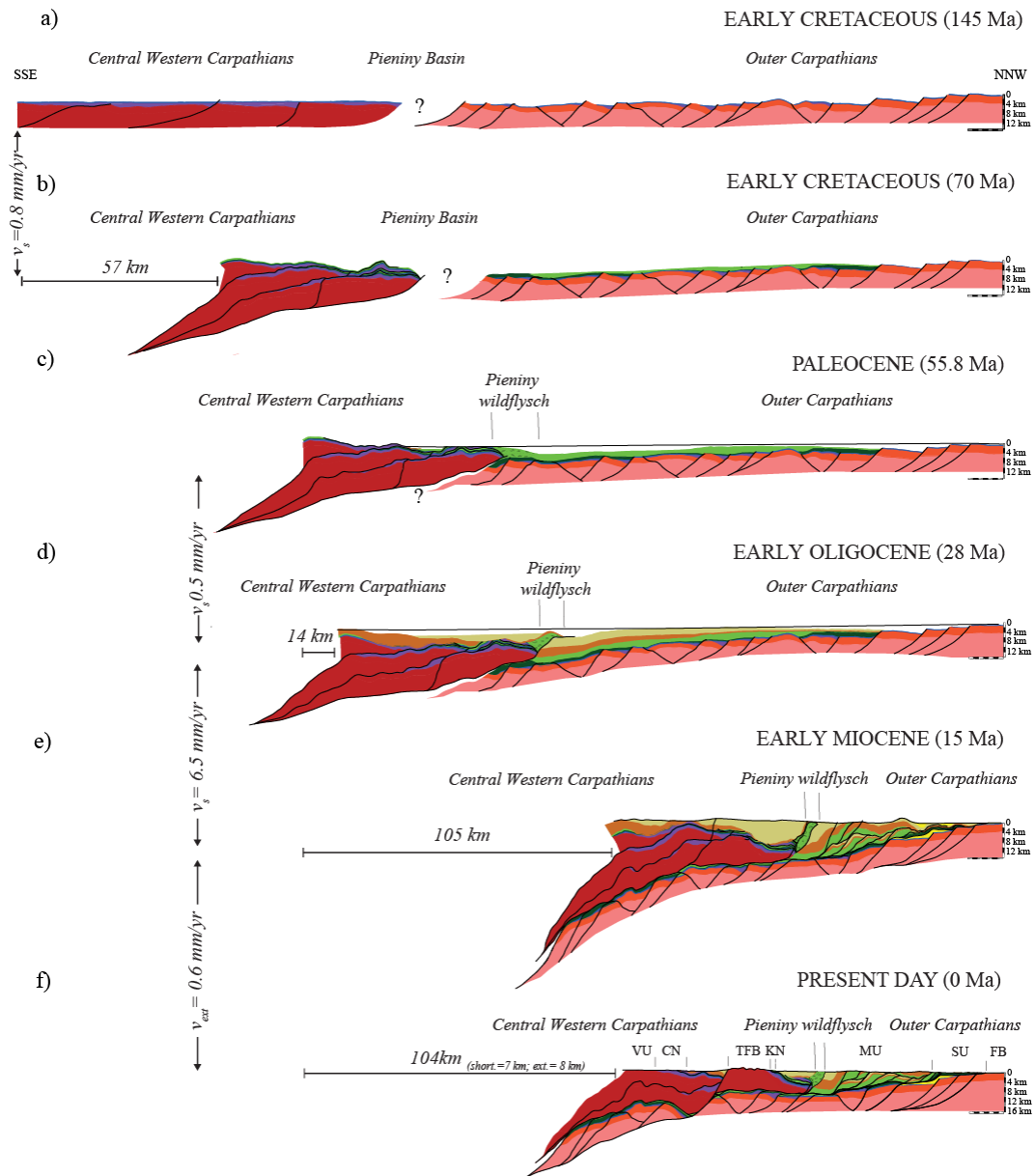


Figure 3.12: Forward modeling showing the evolution of the Carpathian region, from the Central Western Carpathians (CWC) to the foreland. (a) Initial stage at the beginning of the Early Cretaceous, before the deformation of the inner succession of the CWC (that will later produce the Veporic Unit). (b) Basement-involved thrusting in the CWC domain. (c) Thrusting and erosion of the Mesozoic sedimentary cover on top of the Tatricum crystalline basement and subsequent sedimentation in the Outer Carpathian foreland basin. Deposition of the Pieniny wildflysch in the frontal part of the Inner Carpathians. (d) Thrusting of the Pieniny wildflysch on top of the Outer Carpathian successions. (e) In-sequence thrust propagation in the Outer Carpathian domain. (f) Reverse-slip reactivation of Mesozoic normal faults in the basement, and later normal faulting within the accretionary wedge. Erosion of the uppermost successions during the Middle-Upper Miocene. VU: Veporic Unit; CN: Choč Nappe; KN: Križna nappe; TFB: Tatra-Fatra Belt; MU: Magura Unit; SU: Silesian Unit; FB: foreland basin.

3.3 Discussion

Unlike most of the works dealing with the tectonic evolution, time of deformation, and amount of shortening of the OC thrust and fold belt, the aim of this paper is to provide a comprehensive picture of the whole Carpathian orogen-foreland basin system, focusing on the relationships among the IC, PKB and OC. Based on the reappraisal of stratigraphic and structural studies integrated with our own observations, a new scenario is proposed for the tectonic significance of the Pieniny “Klippen Belt” in the Carpathian orogen. Our model involves an Early Cretaceous pre-shortening tectonic setting consisting of a sedimentary basin made of thinned continental crust, on which all the preserved successions of the Inner and the Outer Carpathian domains were deposited, and an unknown – but probably limited if not null – amount of oceanic lithosphere. This paleogeographic setting is consistent with sedimentological evidences: all the successions, from the Upper Cretaceous to the Oligo-Miocene, consist of siliciclastic deposits characterized by almost the same lithology with variable sand/shale ratio. In addition, some marker levels (such as the *Globigerina Marls*, the Menilite bituminous shales, the Upper Cretaceous Puchov-type marls, the Inoceramian-type beds and the Sojmul conglomerates) are continuous throughout the whole Carpathian depositional basin, thus indicating a similar sedimentary environment for both the IC and OC successions [Jankowski *et al.*, 2012]. The lithostratigraphy of the Pieniny and the IC successions (e.g. Křížna Nappe) are also very similar, consisting of ca. 50 m thick Jurassic radiolarites overlying carbonates (Sokolica and Czajakowa Radiolarite on the Podzamcze Limestone [Birkenmajer, 1977]). They do not suggest the presence of oceanic crust flooring the Pieniny Basin, but rather subsidence and deepening in Jurassic times, as already suggested by Kotański [1963a]. Our model is clearly at variance with various palaeogeographic reconstructions proposed in the literature [e.g. Nemčok *et al.*, 2000; Nemčok *et al.*, 2006; Oszczytko, 2006; Picha *et al.*, 2006] implying low shortening values and no relevant differences of the IC and OC original position in terms of latitude. The most obvious difference concerns the number of sedimentary basins originally present in the Carpathian region. All previously proposed palaeogeographic settings involve several deep-water basins, roughly NW-SE

oriented, separated by ridges with almost the same orientation (from north to south: Skole and Silesian Basins, Silesian Ridge, Magura Basin, Czorsztyn Ridge and Pieniny Basin). This subdivision derives mainly from stratigraphic observations and provenance analysis performed on pebbles and olistoliths found in the OC deposits [Książkiewicz, 1965; Unrug, 1968; Golonka *et al.*, 2000, 2005; Picha *et al.*, 2006; Oszczypko, 2006]. According to these studies, the main source of sediments were: (i) a northern massif located along the European margin for the Skole Basin; (ii) the Silesian Ridge for the inner part of the Silesian Basin and the outer Magura Basin; and (iii) the PKB for the inner part of the Magura Basin [Książkiewicz, 1977; Oszczypko *et al.*, 2005 c]. However, the stratigraphic successions, described in detail in several works [i.e. Ślaczka *et al.*, 2006], suggest the same depositional setting for all of the tectonic units. Accordingly, there is no need to infer the presence of a system of deep-water basins separated by ridges. The observed distribution of turbiditic fans and the provenance of the pebbly deposits could be simply controlled by the Cretaceous reactivation of basement normal faults, either as a result of foreland extension associated with the flexure of the foreland lithosphere, or of early tectonic inversion preceding the imbrication and stacking of the IC units on top of the thinned European Platform and the subsequent flexure of this latter. Uplift of some localized areas within the OC basin probably led to the mobilization of unconsolidated sediments. Following the Austroalpine phase, and the consumption of any oceanic lithosphere possibly interposed between the IC and the OC continental margin, a foredeep basin developed on top of the subsiding European Platform in front of the IC. The related accommodation space was filled by the Pieniny wildflysch, including olistostromes and olistoliths coming from the erosion of the IC Mesozoic nappes. Subsequent thrust propagation into the foreland basin led to the partial tectonic superposition of Pieniny wildflysch units on top of the Magura successions during the Eocene-Early Oligocene. This scenario is in contrast with the interpretation of the PKB as an oceanic basin suture characterized by abrupt lateral changes of facies reflecting different paleobathymetry, from the shallow-water marine deposits belonging to the Czorsztyn Ridge to the distal Czertezik and Niedzica successions and the basinal Branisko and Pieniny successions [e.g. Birkenmajer, 1960, 1986; Birkenmajer *et al.*, 2008]. According to the latter

interpretation, the subduction of the Pieniny Ocean during the Cenomanian, the subsequent Savian shortening event [Andrusov, 1938] and Post-Savian erosion [Birkenmajer, 1960] would have led to the exhumation of the PKB during the Early Miocene. However, our new thermochronometric data indicate that exhumation of the PKB occurred later, in Middle-Late Miocene times. The cooling ages from the PKB are consistent with those of the surrounding thrust belt units, thus confirming that the PKB formed part of the thrust belt and did not undergo a different tectonic evolution marking the existence of a suture zone. The oceanic suture interpretation for the PKB has been questioned also by Roca *et al.* [1995], who suggested a sedimentary origin for this unit and its structural position in the hanging wall of the OC, being in turn partially overthrust by the Tatric nappes to the south. Our reappraisal of the PKB is consistent with the interpretation by Roca *et al.* [1995], and allows reconciling the sedimentologic features of the wildflysch described by Plašienka [2012] with the lateral change of facies observed by Birkenmajer [1960]. Marked lateral lithofacies variations are typically recorded in successions deposited on rifted continental margins, as it has been widely documented for (e.g.) the Umbria-Marche successions in the northern Apennines [Marchegiani *et al.*, 1999]. There, Lower Jurassic peritidal carbonate platform facies (Calcari Massiccio Fm.) and overlying condensed deposits pass laterally to basin successions consisting of the complete Corniola, Rosso Ammonitico, Calcari e Marne a Posidonia, Calcari Diasprigni and Maiolica fms. [Santantonio 1993, 1994]. These facies are straightforwardly comparable with the PKB successions, in which shallow water deposits (ascribed to the “Czorsztyn Ridge”) pass laterally to the pelagic sediments deposits of the Branisko Succession [Birkenmajer, 1986]. Therefore, it may be envisaged that similar successions, uplifted by thrusting and eroded in the IC, sourced the blocks included in the PKB. It is well known that block-in-matrix units containing a wide range of blocks of various age and provenance, such as the PKB, are very unlikely to be of purely tectonic origin, being commonly the result of tectonic reworking of pre-existing sedimentary mélanges [Festa *et al.*, 2012].

The deposition of the Pieniny wildflysch on the flexured foreland lithosphere and its subsequent thrusting on top of the OC successions mark the end of the IC thick-skinned deformation and the closure of any oceanic domain originally present in the

area. The switch in tectonic style from thick-skinned to thin-skinned due to the change in the rheology of the décollement layer, was followed by in-sequence propagation of thrusting in the OC (note that our model is at variance with the interpretation of the Magura Unit as an out-of sequence thrust sheet [e.g. *Gagala et al.*, 2012; *Nemčok et al.*, 2006], for which no convincing structural evidence has ever been provided). This stage was characterized by a dramatic increase in the shortening rate, which passed from a value of 0.8 mm/yr during the Cretaceous, through a tectonically unconstrained period (oceanic subduction?) during the Paleogene (70-28 Ma), to a value of ca. 6.5 mm/yr during Early Oligocene-Early Miocene times. The Oligo-Miocene acceleration of shortening could have been triggered by internal orogen dynamics (presence of an efficient detachment level), by external causes related to the movement of the converging plates, or by a combination of both. Lower shortening rates characterized the latest thrusting stages, when active shortening migrated at depth into the basement. Post-thrusting normal faulting affected the accretionary wedge, probably due to the extensional collapse associated with the deactivation of the sole thrust. Crustal normal faults also occur; these could be related to a regional extensional regime, affecting not only the deformed wedge but also the underlying basement. This is the case for the eastern part of the Polish Carpathians, where low-angle normal faults offset the basement of the foreland. These faults are interpreted to have played a primary role in the rapid unroofing of localized portions of the OC [*Andreucci et al.*, 2013].

The original occurrence and extent of oceanic lithosphere between the IC and OC domains cannot be either supported or ruled out unambiguously. No geophysical evidence exists for a continuous oceanic slab beneath the Western Carpathians, and no in situ ophiolites/high pressure rocks occur in the PKB, which is clearly a sedimentary unit rather than subduction mélange. High-pressure (blueschist facies) rocks have been found only as pebbles and have been interpreted as having been sourced by the oceanic suture cropping out farther south of the IC [*Schmid et al.*, 2008]. The lack of volcanic activity [*Ziegler and Cloetingh*, 2004] is an additional issue suggesting that the Piemonte-Liguria Ocean was originally wider to the west, where the occurrence of basaltic rocks has been documented by *Soták et al.* [1993], substantially narrowing within our study area. Thus, we interpret the region as a wide

rifted continental area during the Early Mesozoic, possibly with a narrow oceanic domain between the IC and OC margins, and the true ocean (i.e. the Meliata-Maliac domain) being located farther south. During the Neogene, the presence of subducting oceanic lithosphere SE of our study area controlled the eastward migration of the strongly arcuate Southern Carpathian belt.

Paleo-barometers and paleo-thermal indicators have been used in previous studies to calibrate the burial and maximum temperature experienced by the PKB successions. X-ray diffraction studies of illite-smectite mixed layers in shales, carried out by *Świerczewska* [2005], suggest maximum temperatures ranging between 110°C and 135°C for the eastern part of the PKB (Grajcarek Unit). A wider range of temperatures has been obtained by *Jurewicz* [1994] from fluid inclusion data on calcite veins. Minimum paleotemperatures are in the range of 40-60 °C, while maximum temperatures are mostly in the range of 160-180 °C. Paleotemperatures that locally exceed 200°C have been inferred by *Wójcik-Tabol* [2003] based on illite “crystallinity” and vitrinite reflectance, indicating anchimetamorphic conditions. Our low-T thermochronometric results are in line with the above-mentioned studies and are in agreement with the few low-T thermochronological data published by *Anzkiewicz and Świerczewska*, [2008], indicating exhumation during the Oligocene-Early Miocene. The burial and exhumation history constrained by AFT and AHe ages suggest that the Pieniny wildflysch underwent heterogeneous burial. The estimated maximum temperatures range between 80 and 120 °C, and the average cooling rate, calculated for the last 10 Ma, is of ca. 25 °C/Myr. Thermochronometry allowed us to constrain our structural model, particularly for the last 15 Ma. AFT and AHe data indicate that the PKB and the IC experienced the same exhumation event due to the Middle-Late Miocene regional uplift.

3.4 Conclusions

In this paper we suggest a new interpretation for the tectonic evolution of the Central-Western Carpathian thrust and fold belt. In particular, a new scenario has been proposed for the Cretaceous paleogeography and for the origin of the so-called Pieniny “Klippen Belt” which, independently of the occurrence and extent of oceanic lithosphere between the IC and OC domains, represents an intensely deformed

sedimentary unit (wildflysch) deposited in the foredeep of the IC rather than a subduction mélangé. According to our sequential restoration, the pre-orogenic tectonic setting consisted of a horst and graben system whose architecture controlled the thickness of syn- and post-rift deposits. The extent of this rifted continental area was variable. Profile I has been restored to a 135 km wide OC basin and 125 km wide IC basin, later experiencing a shortening of 54% and 57%, respectively. The shortening calculated for Profile II amounts to 63% for the OC and 26% for the IC, starting from a 270 km wide OC basin and 38 km wide IC basin. Shortening remains almost constant (64%) in the eastern sector of the OC thrust and fold belt, increasing in the IC region. In Profile III, the OC have been restored to a 343 km wide original basin, whereas the restored IC basin has an original length of 116 km. The Austroalpine tectonic phase affected the southern portion of the study area, causing reverse-slip reactivation of the Mesozoic normal faults and subsequent imbrication and uplift of the basement in the IC region. Following the complete consumption of any oceanic lithosphere originally present in the system, the flexure of the East European Platform produced by the tectonic load and the associated development of the foreland basin in the Outer Carpathians domain created the accommodation space that was filled by the Pieniny wildflysch north of the Inner Carpathian front. The olistoliths and olistostromes included in this wildflysch come from the erosion of the structurally higher Mesozoic successions belonging to the IC domain. Thick-skinned deformation proceeded with a shortening rate of ca. 0.8 mm/yr. Tectonic emplacement of the Pieniny wildflysch on top of Outer Carpathian successions marks the onset of the thin-skinned thrusting. In-sequence propagation in the Outer Carpathian domain started with the high-displacement Magura Unit thrust. The subsequent development of the hinterland-dipping duplexes forming the progressively outer Dukla, Silesian, Subsilesian and Skole units led to the present-day tectonic configuration of the OC accretionary wedge. Further displacement has been partially transferred to the OC frontal thrust by Miocene reverse-slip reactivation of preexisting basement normal faults. Crustal shortening was followed by extension, in some cases unroofing wide portions of the accretionary wedge. Structural observations integrated with low-T thermochronometric data suggest that post-thrusting low-angle normal faults controlled the rapid exhumation of footwall

units in the eastern part of the Polish Carpathians. On the other hand, the western Polish Carpathians were affected by erosion-controlled exhumation coeval with thrusting, apparently without a significant contribution by normal faulting. A Middle-Late Miocene exhumation of the so-called Pieniny “Klippen Belt” has also been unraveled based on low-T thermochronometric data. The new cooling ages provided in this paper, indicate exhumation almost coeval with that recorded in the Inner Carpathian domain, and generally younger than that characterizing the Outer Carpathians. This pattern points to a regional uplift of the former domain in recent times.

3.5 Acknowledgments

The data used to produce the results of this paper are available for free from the corresponding author Ada Castelluccio at ada.castelluccio@studenti.unipd.it. This work was supported by University of Padova (Progetto di Ateneo 2009, CPDA091987)".

4 Chapter IV

This chapter is focused on the methodology applied to the sequential restoration that allows us provide the prediction of the low-T thermochronometric ages along the present-day geological cross-section and the evolution of the isotherms through time. This method is also a way to validate the proposed tectonic scenario by comparing the predicted ages resulting from the sequential restoration and the measured ones. This thermo-kinematic model is performed for the Profile I (see Chapter 2 for the location of the section trace). In the following chapter the final version of the paper submitted to *Lithosphere* is presented.

Coupling sequential restoration of balanced cross-sections and low-temperature thermochronometry: the case study of the Western Carpathians

Ada Castelluccio*^a, Benedetta Andreucci^a, Massimiliano Zattin^a, Richard A. Ketcham^b, Leszek Jankowski^c, Stefano Mazzoli^d and Rafał Szaniawski^e.

^a *Department of Geosciences, University of Padua, Via G. Gradenigo, 6, Padova 35131 Italy;*

^b *Jackson School of Geosciences, The University of Texas at Austin, 1 University Station C1160 Austin, TX 78712;*

^c *Polish Geological Institute-Carpathian Branch, ul. Skrzatów 1, Cracow, 31-560, Poland;*

^d *Department of Earth Sciences, University of Naples “Federico II”, Largo San Marcellino 10, Napoli, 80138 Italy;*

^e *Institute of Geophysics, Polish Academy of Science, Ks. Janusza 64, Warsaw, 01-452, Poland*

4.1 *Abstract*

In this paper, a new approach is applied to validate a proposed scenario for the tectonic evolution of the Western Carpathian thrust and fold belt-foreland system. A balanced section was constructed across the thrust and fold belt, from the Polish foreland to the Slovakia hinterland domain to the south. Its sequential restoration allows us not only to delineate the tectonic evolution, but also to predict the cooling history along the section. In addition, the response of low-Temperature thermochronometers (apatite fission track and apatite (U-Th)/He) to the changes in the thrust and fold belt geometry produced by fault activity and topography evolution are tested. The effective integration of structural and thermochronometric methods provides, for the first time, a high-resolution thermo-kinematic model of the Western Carpathians from the Early Cretaceous onset of shortening to the present-day. The interplay between thick- and thin-skinned thrusting exerts a discernible effect on the distribution of the cooling ages along the profile. Our analysis unravels cooling of the Outer Carpathians since ca. 22 Ma. The combination of thrust-related hanging-wall uplift and erosion comprised the dominant exhumation mechanism for this outer portion of the orogen. Younger cooling ages (13 to 4 Ma) obtained for the Inner Carpathian domain are mainly associated with a later, localized uplift, partly controlled by extensional faulting. Our results, effectively unravelling the response of low-temperature thermochronometers to the sequence of tectonic events and changes in the topographic profile, allow us to constrain the best scenario honouring all available data.

4.2 **Introduction**

The sequential restoration of balanced cross-sections is a powerful tool for calculating the amount of shortening, the slip rate and the depth of the décollement surface in contractional/extensional regimes. It represents also the only way to describe the evolution of the tectonic structures backward and forward in time. Nevertheless, the timing of deformation cannot be inferred without uncertainties by means of the kinematic model alone, particularly in cases where syn-tectonic deposits are not preserved and the thrust fronts are all erosional. One possible

solution is to constrain deformation events integrating 2D kinematic modelling with low-temperature (low-T) thermochronometers. The extrapolation of the beginning of deformation events is valid when the cooling ages are strictly associated with the onset of deformation [e.g. *Stockli et al.*, 2000; *Ehlers and Farley*, 2003; *Stockli* 2005]. In addition, sequential restoration can provide an estimate of the maximum burial experienced by different successions cropping out along the section. However, it needs to be constrained by paleothermal indicators, such as vitrinite reflectance. This latter indicator, together with apatite fission-track (AFT) and apatite U-Th/He (AHe) data, are the main constraints for tracing burial and exhumation histories. The thermal evolution associated with thrusting has been modelled for simple tectonic structures (such as fault bend fold and hinterland dipping duplexes) by evaluating the role of topography, inclination of the thrust ramp, and amount of displacement on the predicted cooling age profile along a geological transect [*Huerta and Rodgers*, 2006; *Lock and Willet*, 2008]. Here we want to contextualise low-T thermochronometric data (AFT and AHe) in the complex kinematic restoration of the Western Carpathian thrust and fold belt, in which Early Cretaceous thick-skinned thrusting was followed by thin-skinned deformation of the most external part from the Eocene to the Middle Miocene. In this paper we are not addressing in detail the issues concerning tectonic styles and deformation processes controlling the Carpathian orogeny; rather, the main aim here is to discuss the methodology applied to a case study and, in particular, how low-T thermochronometry can be a successful tool to validate a selected geological scenario. This approach allows us to convert the temperatures obtained with the thermal modelling already performed for several samples along the chosen transect to the depths reached during the tectonic evolution and refine and validate the proposed geological scenario. We use FETKIN [*Almendral et al.*, 2014], a software dedicated to the forward modelling of thermochronometric ages. For a given kinematic restoration, conveniently integrated with thermal parameters (such as paleo-geothermal gradient, thermal conductivity and specific heat capacity), FETKIN calculates low-temperature thermochronometric ages for different thermochronometers along the present-day topographic profile of a geological cross-section. The sequential restoration can be tested by comparing the predicted thermochronometric ages with those measured on samples collected along the

topographic profile. FETKIN provides also the evolution of the isotherms through time, allowing one to estimate the maximum temperatures experienced by the outcropping successions. This study follows the workflow already applied by *Mora et al.*, [2014] on the Eastern Cordillera of Colombia. In particular, we want to evaluate the influence of fault geometry and activity, and of topography evolution, on expected thermochronometric age patterns, and also reach the best result in terms of correspondence between thermo-kinematic model and real data.

4.3 Geological setting

The Western Carpathians are the eastern continuation of the Alpine orogenic system (Fig. 4.1a), which originated from the collision between the Adriatic and Euro-Asiatic plates during the Late Cretaceous to the Miocene. The subduction and subsequent closure of the southern branch of the Alpine Tethys [sensu *Schmid et al.*, 2008] caused the deformation of the innermost successions and, during the Paleogene, the imbrication of the outer successions and their relative emplacement on top of the European Platform. The complex architecture of the Carpathians can be simplified by dividing them into two tectonic domains: the Outer Carpathians (OC) and the Inner Carpathians (IC) [*Książkiewicz*, 1977] (see legend in Fig. 4.1b). The OC consist of a fold and thrust belt made of Upper Jurassic to Lower Miocene deposits [*Książkiewicz*, 1962, 1977; *Bieda et al.*, 1963; *Mahel' and Buday*, 1968; *Koszarski and Ślęczka*, 1976]. It is formed by several thrust sheets (Magura, Dukla Silesian, Subsilesian, Skole units) made of siliciclastic deposits with variable sandy/shale ratio (Fig.4.2). The IC are formed by Variscan basement with its Mesozoic cover piled up as a result of the Austroalpine orogeny.

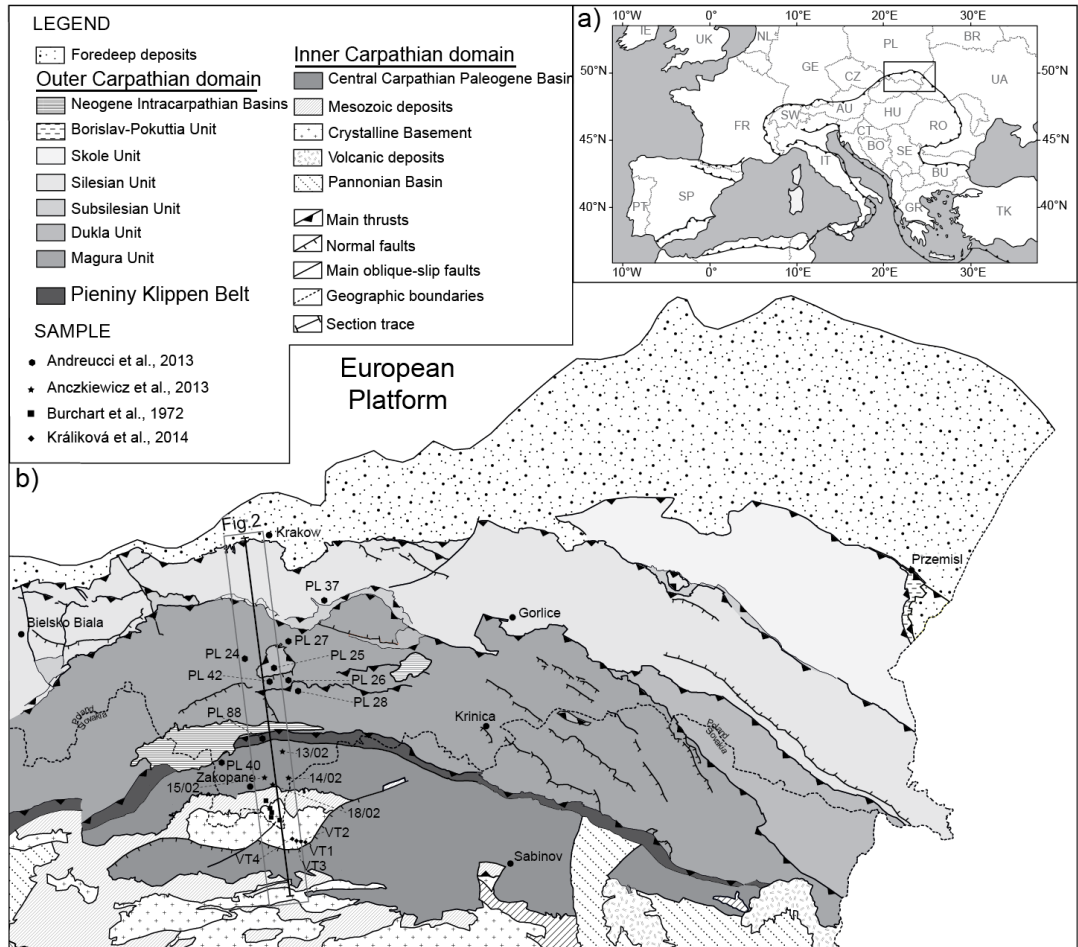


Figure 4.1:(a) Geographic map showing the location of the study area. (b) Tectonic map of the Polish and Slovakian Carpathians, showing location of the modelled profile and of samples used for the validation of the thermo-kinematic model.

The Mesozoic nappes are partially buried under the Paleogene deposits of the Central Carpathian Paleogene Basin (CCPB, Fig. 4.1b). The IC and OC are separated by the Pieniny Klippen Belt (PKB) a narrow belt of shared Mesozoic to Eocene rocks, assumed to be the suture of the Vahicium ocean [Mahel', 1981]. A heated debate exists about the evolution of the Carpathians and the origin of the above-mentioned suture. Many authors [e.g. Birkenmajer, 1960, 1986; Picha *et al.*, 2006; Birkenmajer *et al.*, 2008] suggest the original occurrence of oceanic crust between these two domains, in spite of the lack of any evidence at the surface. More recent papers [Jurewicz, 2005; Malinowski *et al.*, 2013, Roca *et al.*, 1995] cast doubt about the presence of oceanic crust between the IC and OC, rather suggesting that thinned continental crust floored the PKB domain.

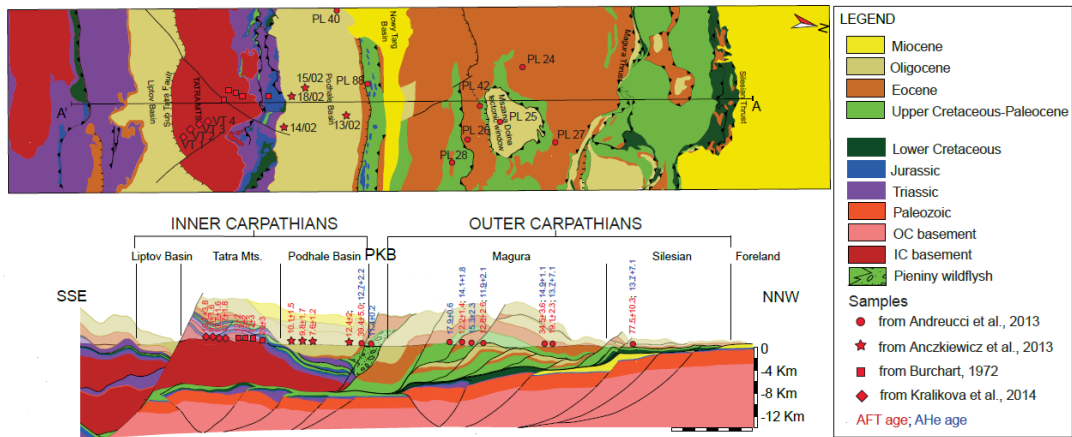


Figura 4.2:(a) Geological map of the area surrounding the cross-section trace. (b) Balanced section across the Western Carpathians with samples projected in their own structural position [Burchart 1972; Aczkiewicz et al., 2013; Andreucci et al., 2013; Králíková et al., 2014]. The constraints for section construction are from our own mapping integrating 1:200000 scale geological maps [Nemčok and Poprawa, 1988-89; Polák, 2008], the 1:50000 scale geological map by Nemčok et al. [1994], dip data, boreholes (Bańska PIG-1, Borzęta IG-1 [Marciniak and Zinnal, 2006], Chabówka-1, Obidowa IG-1, Tokarnia IG-1 [Wójcik et al., 2006], Nowy Targ PGI-1 [Paul and Poprawa, 1992], Zakopane IG-1 [Sokolowski, 1973]), seismic and magnetotelluric profiles [Stefaniuk, 2006].

The stratigraphy of the OC, IC and PKB is summarized in Fig. 4.3, in which an attempt to correlate the deposits belonging to different formations has been made.

Deformation history

For the purpose of this work, we propose a conservative scenario in which the Outer and the Inner Carpathian successions were deposited in sedimentary domains floored by thinned continental crust (Fig. 4.4a). As we cannot quantify the width of the postulated oceanic basin, which could be very narrow or even inexistent, our undeformed stage includes an undefined original separation between the IC to the OC paleogeographic realms. Early Cretaceous shortening involved the southern part of the sedimentary basin [Voigt and Wagneich et al., 2008], producing the reactivation of Mesozoic normal faults as reverse faults (Fig. 4.4b). Thick-skinned thrusting propagated northward during the Late Cretaceous [Maluski et al., 1993] up to the Paleocene. This Early Alpine orogenesis affecting the IC domain is marked by a regional unconformity separating the Paleogene deposits of the CCPB (Eocene Nummulitic Fm.) from the underlying Mesozoic nappes [e.g. Janočko et al., 2006; Soták et al., 2001].

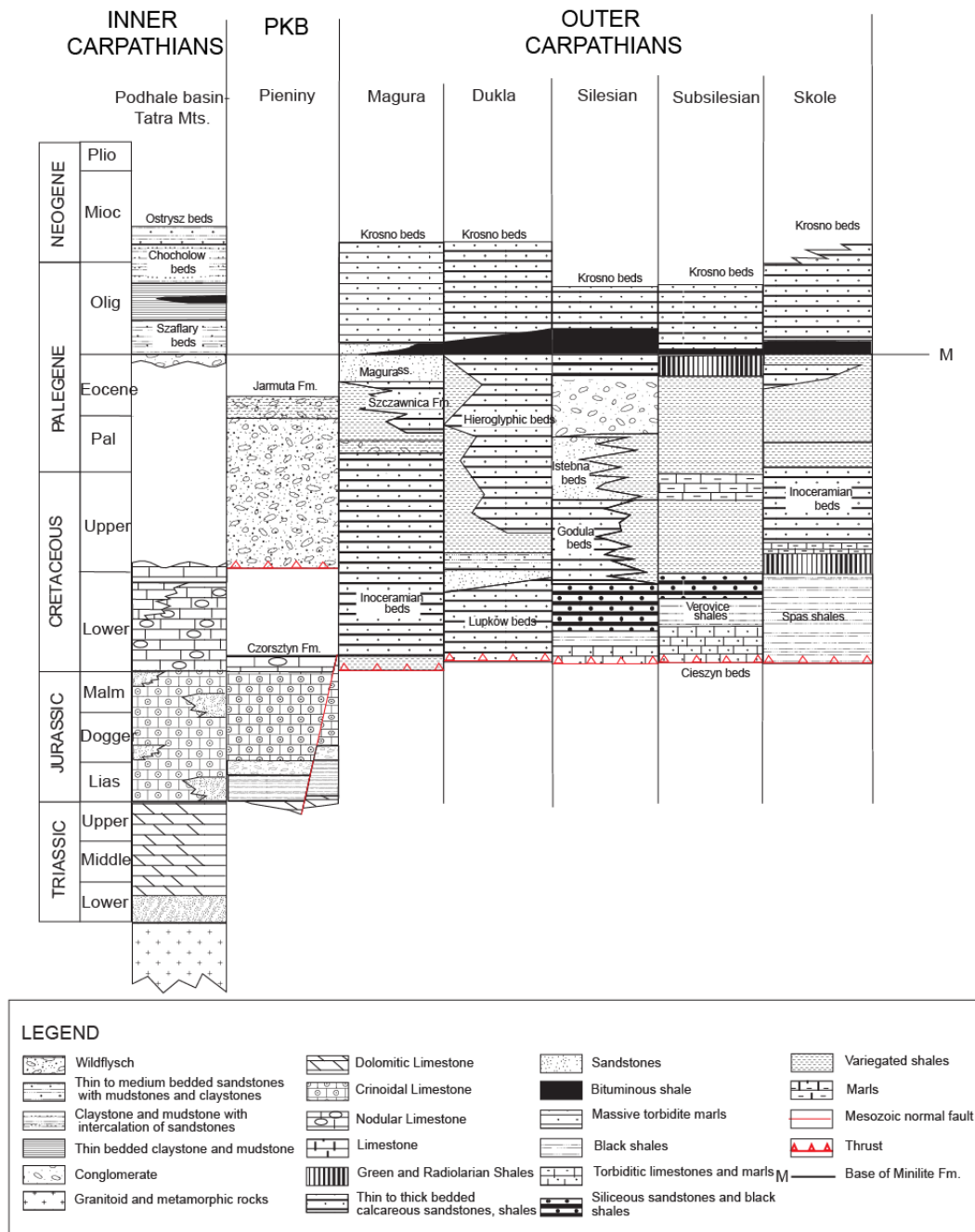


Figure 4.3: Correlation chart for the main tectono-stratigraphic units of the Western Carpathians. The successions are not represented with true thickness.

Imbrication within the IC belt proceeded with a shortening rate of 0.8 mm/yr, decreasing during the Late Cretaceous-Paleocene. The flexural subsidence affecting the European Platform as a result of the IC emplacement produced the development of a large foreland basin. This was filled in its proximal part with olistoliths and olistostromes produced by reworking of Mesozoic successions. These blocks, whose

southern provenance has been demonstrated by *Roca et al.* [1995], originated from the subaerial exposure and subsequent erosion of the IC successions (Fig. 4.4c). The above-mentioned Mesozoic mega-blocks, contained in an Upper Cretaceous-Paleocene matrix, are the main components of the so-called Pieniny wildflysch [*Plašineka and Mikuš*, 2010]. Although this is said to be associated with the tectonic emplacement of oceanic slivers by (e.g.) *Picha et al.* [2006], the model presented by the latter authors actually implies the occurrence of continental crust beneath the Pieniny wildflysch (as was already suggested by *Jurewicz* [2005]) and a sedimentary rather than tectonic origin of the mélangé forming the PKB. The Pieniny wildflysch overthrusts the northern OC successions during the middle Eocene [*Bromowicz*, 1999] (Fig. 4.4d). This tectonic episode marks the end of thick-skinned shortening and the onset of the thin-skinned thrusting involving the OC domain. During the Oligocene, thrusting propagated northward, detaching the OC successions along the Upper Cretaceous shaly deposits, with a shortening rate of 6.5 mm/yr (Fig. 4.3e). The increasing shortening rate could be due to the enhanced quality of detachment, or to regional changes in plate convergence rates, or both. During the Oligocene-Middle Miocene, thrusting and subsequent erosion of the OC successions occurred coevally with sedimentation of the Podhale wedge-top basin deposits south of the PKB. During the Middle-Late Miocene, shortening affected the basement, inverting the inherited Mesozoic normal faults cutting through the lower plate [*Oszczypko et al.*, 2006]. The stacking of thrust sheets increased the gravitational instability of the Carpathian accretionary wedge, leading to the nucleation of normal faults, some of them reactivating reverse structures (Fig. 4.4f). Although some normal faults (such as the Sub-Tatra fault bordering the Liptov Basin to the north) show large displacements, they are not the main mechanism triggering the exhumation in this sector of the Carpathian belt [*Andreucci et al.*, 2013]. Thrust-related uplift and erosion were dominant in the OC, whereas exhumation of the IC was mainly associated with a Middle-Late Miocene regional uplift, locally controlled by normal faulting, and related enhanced erosion [e.g. *Králiková et al.*, 2014].

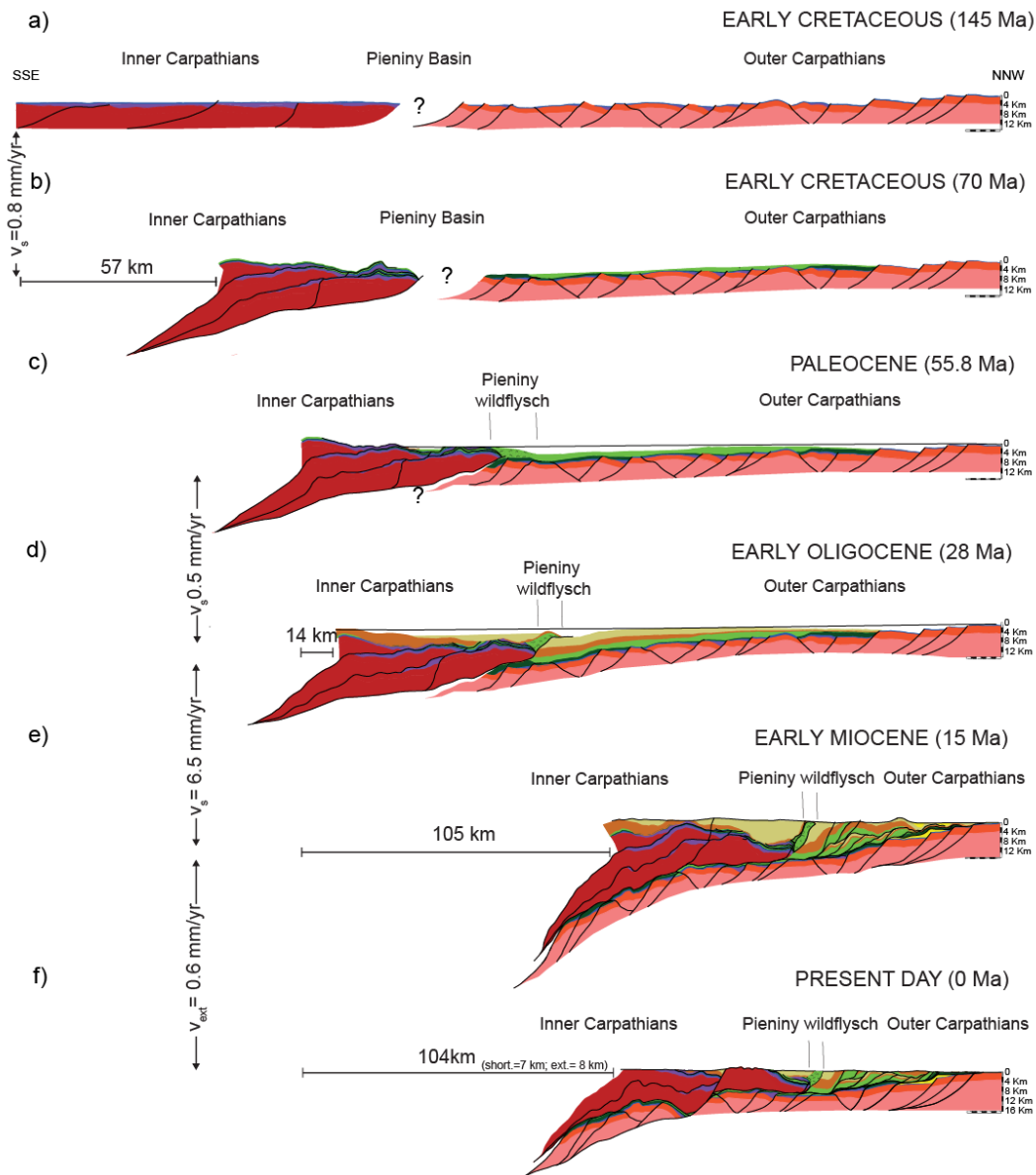


Figure 4.4: 2D forward modelling of the balanced cross-section from the Early Cretaceous to the present-day, performed using Move package, developed by Midland Valley Ltd. Displacement values used as input data come from the sequential restoration. Vertical simple shear and fault parallel flow algorithms were used to restore/forward model the normal faults and the reverse faults, respectively. The flexural slip algorithm was applied to simulate the flexure of the lower plate.

4.4 Methods

The balanced cross-section has been integrated with paleothermal and low-temperature thermochronometric data (Fig. 4.2). AFT, AHe and ZHe ages [Andreucci *et al.*, 2013; Anczkiewicz *et al.*, 2013; Králiková *et al.*, 2014b and

references therein] data are the main constraints for tracing the thermal history of each sample projected into our cross-section. Thermal models have been performed by HeFTy [Ketcham 2005] and together with the illite-smectite [Środoń *et al.*, 2006] and vitrinite reflectance (R_0) [Andreucci, 2013; Wagner, 2011] data allowed us to infer the amount of maximum burial for each sample. Temperature values were converted into burial depths using a constant geothermal gradient of 18°C/km [Andreucci *et al.*, 2013; Hurai *et al.*, 2006; Swierczewska, 2005] (Fig. 4.5).

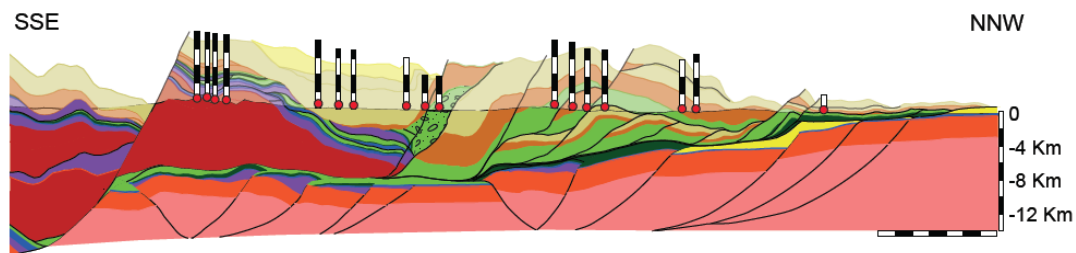


Figure 4.5: Balanced cross-section, showing sample location and maximum burial obtained by thermal modeling of AFT and AHe data [Andreucci *et al.*, 2013; Králiková *et al.*, 2014] integrated with illite/smectite values and vitrinite reflectance data [Andreucci, 2013; Środoń *et al.*, 2006; Wagner, 2011].

Once we constructed and sequentially restored the balanced cross-section, we chose ten steps of the restoration to be exported as ASCII files into FETKIN. The following main steps were considered: (i) 145 Ma as the initial undeformed stage before the Early Alpine orogeny; (ii) 70 Ma as the end of the imbrication of the IC Mesozoic cover (iii) 28 Ma as the time of PKB thrusting on top of the OC Oligocene deposits; (iv) 15 Ma as the end of thrusting; and (v) 0 Ma as the final setting. Further intermediate steps were chosen at 56, 38, 23, 22, and 20 Ma, and the relative setting at each stage were calibrated by means of stratigraphic observations. The sequential restoration was further calibrated by processing each reconstructed step with FETKIN [Almendral *et al.*, 2014]. This software solves the transient advection-diffusion equation in two dimensions [Carslaw and Jaeger, 1986]. Starting from the velocity field generated from the kinematic restoration, FETKIN calculates the temperature distribution honoring the structural setting at each time step. Applying an iterative workflow we changed erosion rate, paleotopography and fault geometry in order to achieve the best fit between modeled and measured data. No changes of

the thermal parameters and timing of the deformation were applied, as these parameters are reasonably well constrained in the literature [Andreucci *et al.*, 2013, and references therein]. Once assigned the topographic profiles, geothermal gradient (18°/km), thermal conductivity (2.2 W/m*°C), density (2.7 g/cm³) and specific heat (1000 kcal/(kg* °C)) to the horizons, we defined the bottom boundary conditions. The depth of the lower boundary is set at 44 km b.s.l and the assigned temperature is 774 °C. The final result is the modeling of the isotherms at each time step of the kinematic restoration.

For each point on the present-day topographic profile, forward modeling of the thermochronometric ages was carried out by FETKIN for different low-temperature thermochronometers (in our case AFT and AHe) based on the annealing kinetics for AFT [Ketcham *et al.*, 1999] and for AHe [Farley, 2000]. The predicted ages were then compared with the measured data. In addition, FETKIN calculates the t-T path for each point of the present-day topography. These paths can be compared with thermal histories obtained from the HeFTy inverse modeling to further verify the validity of the predicted ages (Fig. 4.5).

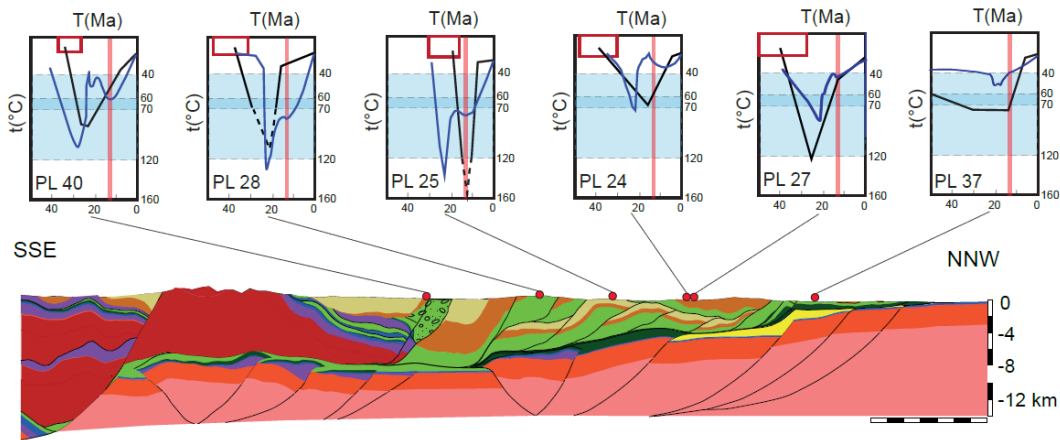


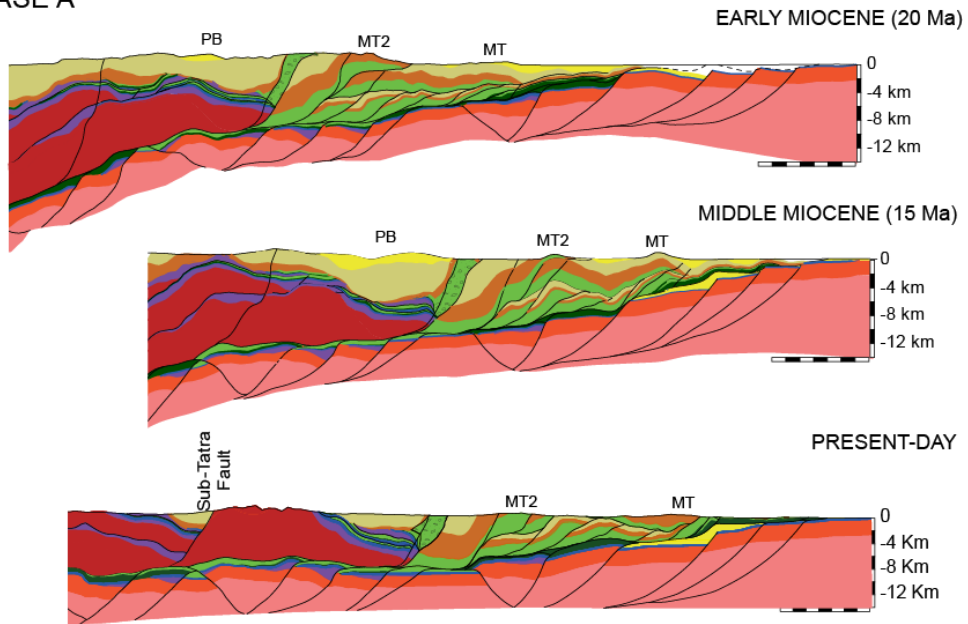
Figure 4.5: Comparison between the T-t path resulting from HeFTy inverse modeling best-fit path (black line) with the thermal path modeled with FETKIN (blue line) for the same location. The red boxes represent the depositional constraints and the red bars correspond to the end of thrusting. The good match between the two paths highlights the validity of the methods.

4.5 Modelling topography evolution: constraints and assumptions

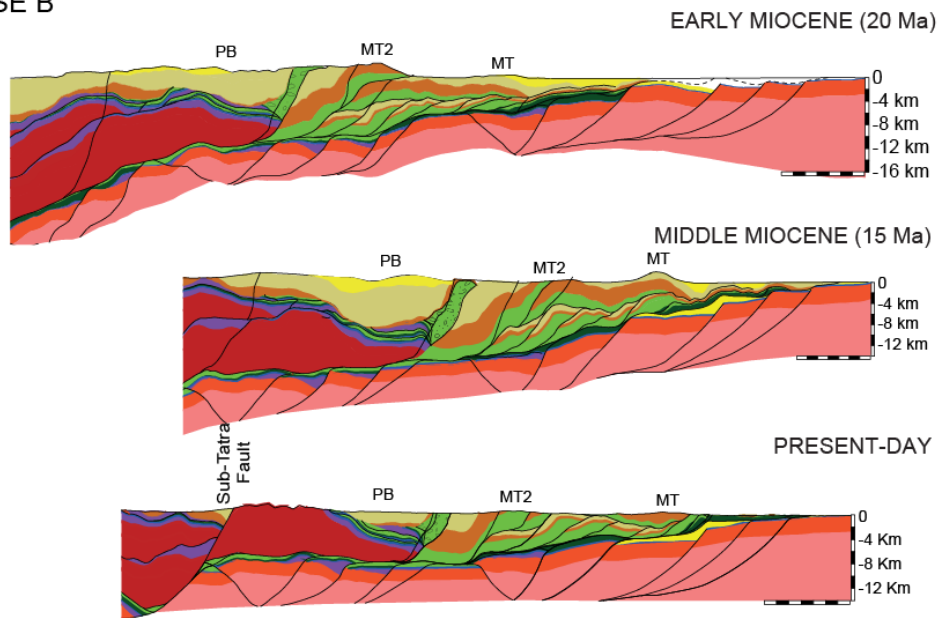
An iterative procedure was used to test the structural model, which was repeatedly processed by means of FETKIN. Each iteration involved modification of paleotopography and fault geometry to evaluate their influence on the cooling age prediction and thus to obtain the best fit of the predicted age profiles with the measured data. This allowed us also to calibrate the evolution of the paleotopography in the last 20 Myr. During its early stage (Early Cretaceous-Paleocene) the Carpathian thrust and fold belt-foreland system was mainly submerged. Since the Eocene, when it emerged, it started undergoing subaerial erosion. This event and its associated erosional surface are well-constrained by a regional unconformity recognized in several wells drilled in the CCPB (e.g. Bránska PIG-1 [Marciniak and Zimnal, 2006], Zakopane IG-1 [Sokolowski, 1973] and further boreholes described by Sotak *et al.*, [2001]), whereas the evolution of the topography during the Oligocene to recent time is poorly constrained. Starting from the comparison between the present-day topography and the corresponding geological structures, we made an attempt at defining the topographic evolution through time by taking into account the structures progressively developing at each stage. A similar approach was applied by Huerta and Rogers [2006], who simulated the evolution of topography corresponding to the frontal part of a thrust system. A topographic high develops with the onset of thrusting directly above the ramp. During thrusting, the relief becomes steeper as the backlimb and forelimb of the ramp anticline are laterally eroded. Following the end of thrusting, erosion keeps acting, minimizing the topographic relief. We apply the same assumptions to our cross-section. Analysis of the present-day topography along the studied cross-section shows that a very smooth relief characterizes the OC region. The main relief of the OC (in any case less than 1000 m a.s.l.) occurs in the frontal part of the Magura Unit, in the hanging wall of the Magura Thrust (MT). Substantial relief also developed above the ramp of the high-displacement Magura Thrust 2 (MT2) occurring within the Magura Unit. The highest peak (ca. 3000 m a.s.l.) of the Western Carpathians is located in the Tatra Mt. region of the IC, consisting of crystalline rocks more resistant to erosion. This present-day

pattern is extrapolated to the past, modelling the topographic profile in order to maintain the main relief of the OC in correspondence of the MT and MT2 faults (Fig. 4.6).

a) CASE A



b) CASE B



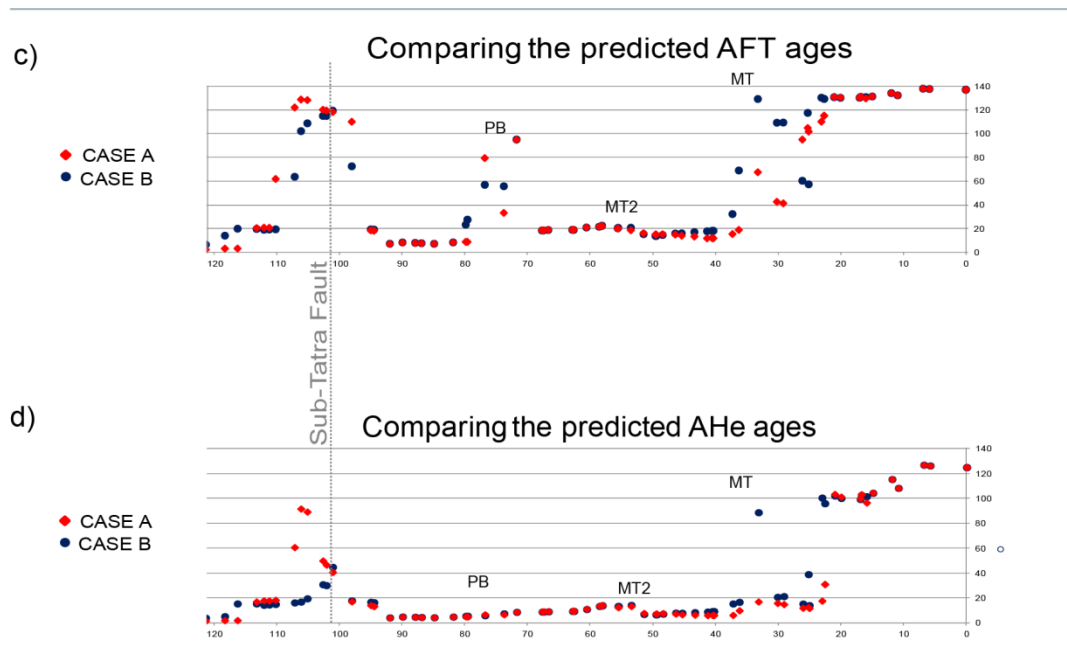


Figure 4.6: Sequential restoration for Case A, represented forward in time (from 20 Ma to the present-day). (b) Sequential restoration for Case B, represented forward in time (from 20 Ma to the present-day). (c) Comparison between AFT thermochronometric ages predicted according to Case A (red squares) and Case B (blue dots). (d) Comparison between AHe thermochronometric ages predicted according to Case A (red squares) and Case B (blue dots). Abbreviations stand for: PB = Podhale Basin; MT2 = Magura Thrust 2 (i.e. high-displacement thrust within the Magura succession); MT = Magura Thrust.

The inferred Early Miocene topography (at 20 Ma) is characterized by a more pronounced structural relief, with respect to the present day, as a result of active thrusting at the time. At 15 Ma, thrusting combined with erosion results in a reduced width of the topographic highs, producing steeper slopes and narrower reliefs. For the two cases shown in Fig. 4.6 a, b, we applied minor changes to the topographic profiles (width and elevation of the relief) in order to achieve the best fit between the predicted AFT and AHe ages and the measured ones.

4.6 Testing two different case histories

We compare two different scenarios (Case A and Case B; Fig. 4.6a, b) differing in the paleotopographic evolution for the last 20 Myr and the geometry of the Sub-Tatra normal fault, which represents the most relevant extensional structure in terms of displacement. The implications of the two different cases are discussed in terms of

topography development, subsidence, and fault geometry. The final result is a thermo-kinematic model in which the selected geological scenario has been consistently integrated with an admissible thermal history.

Case A

In Case A (Fig. 4.6a), we simulated syn-thrusting erosion affecting the innermost part of the OC during Early Oligocene to Early Miocene times. The eroded deposits were carried downslope to the outer zones, accumulating on top of the MT hanging wall block, during the Early Miocene. The resulting inferred mean erosion rate is 1.10 mm/yr. The northward propagation of thrusting and the related flexure of the lower plate, caused by the tectonic load of the accretionary wedge, produced the accommodation space later filled by Middle Miocene deposits, while the highest part of the chain was still affected by erosion. After the end of thrusting at ca. 15 Ma [Nemčok *et al.*, 2006], several normal faults developed as a response to the internal gravitational instability of the orogen. In this first case the Sub-Tatra fault, controlling the northern boundary of the Liptov Basin, has been interpreted as a listric normal fault detaching along the sole thrust of the orogenic system (at ca. 7 km b.s.l. in the area).

Case B

In Case B (Fig. 4.6b) syn-thrusting erosion is assumed to have affected both MT2 and MT hanging-wall blocks earlier than the previous case. The deposition of the Lower Miocene syn-thrusting deposits occurred only in the outermost part of the wedge, in front of the high-displacement MT. In this scenario, Early Oligocene-Early Miocene erosion affecting the MT2 hanging-wall block would have occurred at a lower mean erosion rate (0.64 mm/yr) with respect to Case A. Subsidence of the European Platform is inferred to have slowed down during the Early-Middle Miocene, causing the erosion of the Oligocene deposits of the MT hanging-wall block and the deposition of Miocene successions in the frontal part of the section and in the Podhale Basin (PB) located in the inner part.

The Late Oligocene-Early Miocene mean erosion rate calculated for the MT is almost the same as for the previous case (0.42 mm/yr compared to 0.48 mm/yr of Case A). Middle Miocene deepening of the Magura front and its exhumation in more

recent time (8 Ma) resulted in overall lower erosion rates. The inferred Langhian to present-day mean erosion rates range from 0.12 mm/a (Case A) to 0.07 mm/a (Case B). Furthermore, in Case B the Sub-Tatra Fault has been interpreted as a deep basement structure cutting through the lower plate and detaching at a depth of ca. 17 km b.s.l.

4.7 Discussion

Comparing the AFT age profiles resulting from the two previously described scenarios, some important differences can be highlighted (Fig. 4.6c). The change in topography in the hanging wall of the MT, combined with subsidence - more pronounced for Case A - reduces the cooling ages in this specific area. Partially reset AFT ages predicted for Case A are considerably younger than those predicted for Case B, in some case more than 80 Myr. No major changes in the predicted AFT ages occur in the hanging wall of the MT2, although topography evolution is slightly different for the two cases. In the hanging wall of the Sub-Tatra Fault the variation in the predicted AFT ages is mainly due to the change of the depth to detachment. The shallower is the detachment (Case A), the older are the AFT ages predicted along the hanging wall. The change in the geometry of the fault appears to have a more pronounced influence on the AHe cooling ages (Fig. 4.6d). For a deeper detachment, the AHe ages are considerably younger. No major changes are recorded along the AHe profile for the OC, except for the MT hanging wall where the more gentle modelled topography combined with the higher tectonic subsidence for Case A produced a younging of the cooling ages in this sector.

Case B represents the scenario best approximating the measured thermochronometric data. The resulting thermo-kinematic model provides a complete framework of AFT (Fig. 4.7) and AHe (Fig. 4.8) cooling ages along the studied transect. The predicted AFT age profile (Fig. 4.7) highlights two areas that experienced temperatures not higher than $\sim 120^{\circ}\text{C}$. These are: (i) the foreland basin together with the outermost successions of the OC thrust and fold belt (at a distance from 0 to 24 km along the section), and (ii) the Oligocene deposits of the Liptov Basin (from 100 to 108 km). A partial reset of the AFT cooling ages is predicted for the central part of the Podhale Basin (from 70 to 80 km), whilst totally reset AFT ages from the limbs of the

Podhale syncline indicate cooling through the PAZ during the Middle-Late Miocene. Cooling ages predicted by FETKIN match well the AFT ages obtained by *Anczkiewicz et al.* [2013].

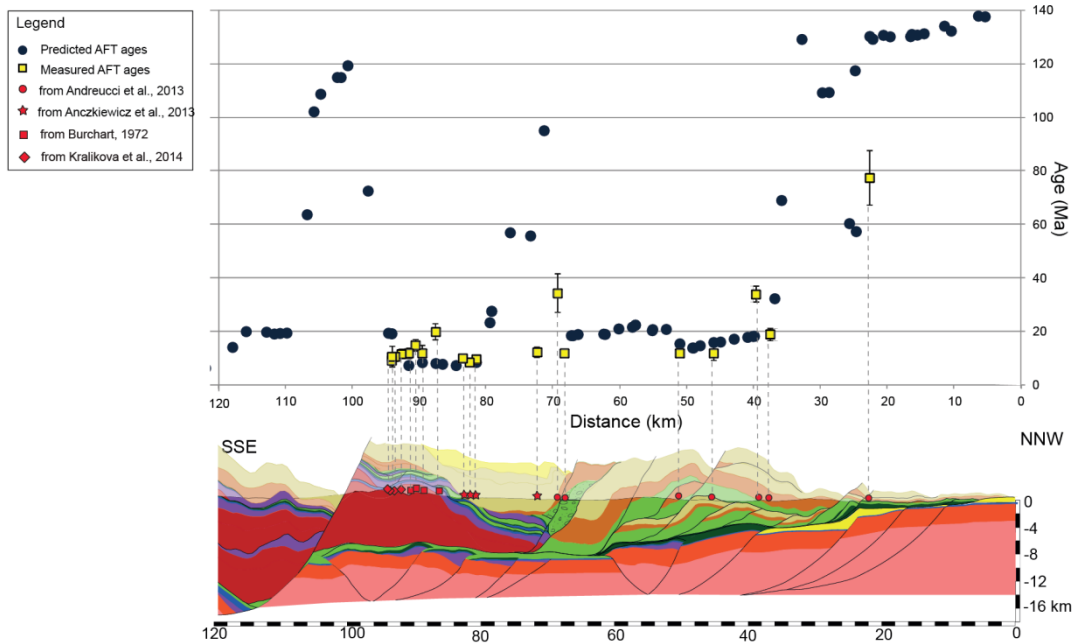


Figure 4.7: Comparison between forward modeled AFT ages obtained by of FETKIN and measured data.

Furthermore, this thermo-kinematic model is consistent with the general trend of increasing temperature towards the backlimb of the Podhale syncline suggested by *Środoń et al.* [2006] and *Wagner* [2011]. The partial mismatch between observed and predicted AFT ages in the central part of this basin is probably due to an underestimation of the thickness of the eroded Oligo-Miocene successions, as the data projected onto the section are from partially reset samples located farther to the west [*Anczkiewicz et al.*, 2013; *Botor et al.*, 2006, 2011].

AFT cooling ages ranging between 14 and 22 Ma are predicted for the OC sector between 36 and 68 km, in line with the cooling ages observed by *Andreucci et al.* [2013]. Here, the general trend of the predicted age profile is controlled by thrust-related uplift and erosion, the oldest ages being located in the hanging wall of the MT2 fault. The youngest ages are from the footwall of the normal fault bounding the Mszana Dolna tectonic window to south, whereas cooling ages become older moving

to the MT front. Younger exhumation ages are predicted for the crystalline basement of the IC, this being consistent with the Middle-Late Miocene cooling documented by *Burchart* [1972], *Král* [1977] and *Králíková et al.* [2014 b]. In the IC, the cooling age profile is locally controlled by normal faulting. The youngest ages are located at the footwall of the Sub-Tatra Fault [*Gross, 1973; Gross et al., 1980*] and are mainly associated with the coeval Middle-Late Miocene regional uplift controlling the cooling of the whole IC domain.

The AHe cooling age profile (Fig. 4.8) shows an overall pattern consistent with the AFT profile. The foreland and the outer part of the Carpathian thrust and fold belt (from 0 to 24 km) and the northern part of the Liptov Basin (from 100 to 106 km) are not reset. As with the AFT profile, a narrow zone in the frontal part of the MT is also not reset (from 32 to 35 km), whereas in its hanging wall the AHe ages are all reset. This means that this entire zone experienced temperatures higher than $\sim 60^{\circ}\text{C}$. A thermochronometer sensitive to very low temperatures, such as the AHe, is particularly effective at unraveling the influence of thrusting on cooling ages. Therefore, for the OC, the relationship between the age profile and the development of the structures forming the thrust and fold belt is clearer than in the AFT profile.

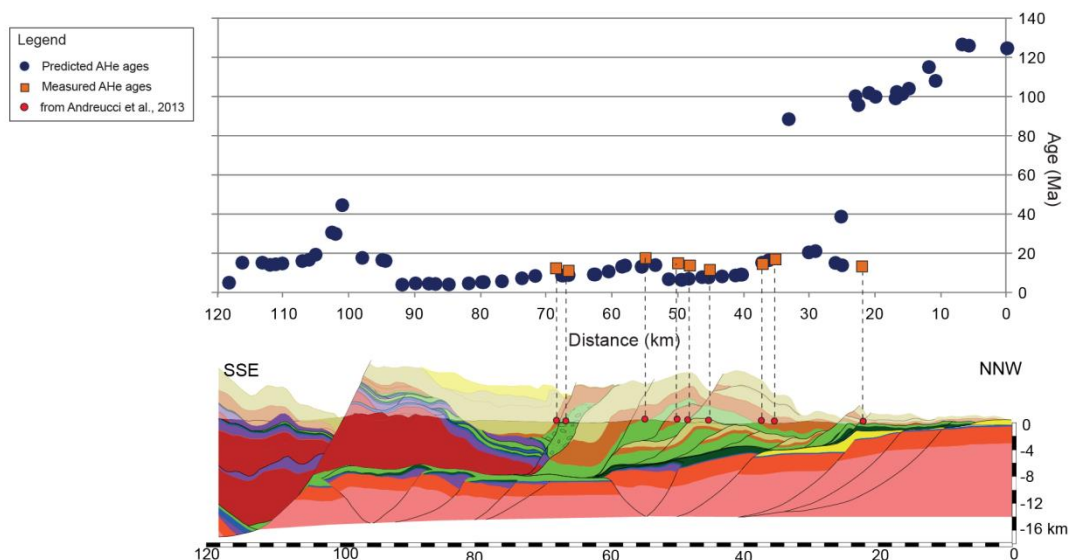


Figure 4.8: Comparison between forward modeled AHe ages obtained by of FETKIN and measured data.

The age gaps recorded along the thermochronometric age profile are indicative of the high-displacement structures. Meaningful examples can be found: (i) at a distance of 26 km along the cross-section, where the younger age (22 Ma) indicates that the hanging wall of the MT moved, at least, up to that point; (ii) at 51 km, where the younger ages mark the location of the MT2 footwall ramp, with the oldest ages located in its hanging wall; and (iii) at 100 km, where a significant age gap is associated with the Sub-Tatra Fault, with its 10 km of dip-slip displacement. According to our model best fitting all available thermochronometric data, totally reset AHe cooling ages range between 8 and 20 km, the youngest ages being located in the Tatra Mts. Region (Fig. 4.8).

The validity of this model is additionally confirmed by comparing the t-T paths resulting from HeFTy and the ones obtained from FETKIN for selected sample on the topographic line. The first differences consists in the detail of the thermal histories. The FETKIN t-T paths are more detailed because they are strictly connected with the sequential restoration. Although well matching the general pattern modeled by HeFTy, in some case the maximum burial is underestimated (i.e. PL 37, PL 27, PL 25). The exhumation of PL 25 and PL 24 starts before the end of thrusting and it is younger than the one computed by HeFTy. These differences influence the age of the first stage of cooling that are generally younger but good matching with the measured data.

4.8 Conclusions

This work represents a successful integration of thermal modelling and kinematic restoration applied to the case study of the Carpathian thrust and fold belt-foreland system. FETKIN has been a key tool in predicting thermochronometric ages and calculating t-T paths along a sequentially restored balanced cross-section. It allowed us to select, validate and refine the most suitable structural model, for which predicted thermochronometric ages match quite well the real data. The obtained thermo-kinematic model points out that exhumation in the Outer Western Carpathians is coeval with the abrupt increase of shortening rate during Early Oligocene to Early Miocene times. This correspondence confirms that thrusting is the driving mechanism in the OC exhumation, as already suggested by *Andreucci et*

al. [2013]. This model is also in agreement with the in-sequence thrust propagation across the OC sedimentary basin suggested by *Roca et al.*, [1995]. Furthermore, the more representative t-T paths traced for some samples along the section (Fig. 6) indicate that the OC did not experience temperatures higher than ~120°C during their thermal history. Slightly higher temperatures are recorded in the crystalline basement cropping out in the IC region, in which cooling during the Middle-Late Miocene is locally controlled by the dip-slip extensional offset associated with the Sub-Tatra Fault.

The comparison between two possible tectonic scenarios points out that the major effects on the thermochronometric age prediction are caused by changes in the geometry of the tectonic structures rather than variations of topographic relief through time. The case of the Sub-Tatra Fault, which is interpreted in this study as a deeply rooted basement structure rather than a shallow-detaching listric fault, reveals that thermochronometry can be a useful tool in constraining the geometry of structures at depth. Our results suggest that integrating AFT analyses with a thermochronometer sensitive to very low temperatures - such as the AHe system - is particularly effective in enhancing structural interpretation and restoration in thrust and fold belts.

4.9 Acknowledgements

We thank Ecopetrol for use and development support of FETKIN.

5 Chapter V

In this chapter two balanced sections crossing the Ukrainian Carpathians have been analyzed. The applied structural model is the same as the one explained in Chapter 3 for the Polish and Slovak Carpathians. Here we do not describe in detail this model but the interaction between this thrust and fold belt and its foreland and the effect of this interaction on the burial history recorded along these geologic transects.

Balanced and sequentially restored sections across the Ukrainian Carpathian thrust and fold belt.

Ada Castelluccio*^a, Benedetta Andreucci^a, Leszek Jankowski^b, Stefano Mazzoli^c,
Rafał Szaniawski^d & Massimiliano Zattin^a

^a *Department of Geosciences, University of Padua, Via G. Gradenigo, 6, Padova 35131 Italy;*

^b *Polish Geological Institute-Carpathian Branch, ul. Skrzatów 1, Cracow, 31-560, Poland;*

^c *Department of Earth Sciences, University of Naples "Federico II", Largo San Marcellino 10, Napoli, 80138 Italy;*

^d *Institute of Geophysics, Polish Academy of Science, Ks. Janusza 64, Warsaw, 01-452, Poland*

5.1 *Abstract*

New regional balanced cross-sections have been constructed across the Ukrainian Carpathians based on field study and available subsurface data. The presented transects cross the foreland basin and the entire thrust and fold belt, including the Transcarpathian Depression. They are not intended to represent a mere picture of the subsurface architecture of this thrust and fold belt, rather they also provide a detailed geological background to the burial and exhumation histories already traced for some specific samples located in this area. The principals of cross-section balancing and sequential restoration, coupled with published transects of low-T thermochronometric data and paleothermal indicators, allow the definition of a tectonic model explaining the kinematic evolution of this belt. The presented cross-sections are the result of the 2D forward kinematic model already applied for the Polish Carpathians, in which the Outer and Inner Carpathian successions can be correlated and ascribed to the same original sedimentary domain and the Pieniny “Klippen Belt” is interpreted as a sedimentary unit (wildflysch) characterized by a block-in-matrix texture rather than a tectonic mélangé. Although poorly constrained at depth, due to the scarcity of seismic data and further geophysical information on the crustal structure, the presented cross-sections, based on the integration of surface geology with numerous well logs, portray a geometrically valid model and provide a geological framework explaining the variation of burial depth along the belt. An estimate of the width of the pre-orogenic sedimentary basin has been also obtained and then compared with the values already available for the western part of the thrust and fold belt.

Keywords: sequential restoration, fold and thrust belt, Late Miocene exhumation, pre-orogenic basin.

Key points

- Balanced cross-section across the Ukrainian Carpathians;
- Fold and thrust belt/foreland system evolution;
- Late Miocene regional uplift.

5.2 Introduction

The evolution of a thrust and fold belt/foreland system can be delineated by means of cross-section balancing and sequential restoration/forward modelling. This technique allows one to define the different stages of the evolution of the chain [Suppe, 1993; Mount *et al.*, 1990; Endignoux and Mugnier, 1990; Zoetemeijer and Sassi, 1992] and provide relevant information to constrain the tectonic subsidence affecting the foreland basin as well as the amount of shortening. In addition, the kinematic restoration allows one to provide a geometrically valid model of the subsurface, where subsurface data are lacking or not available. This work is focussed on the Eastern Carpathians (Fig. 5.1), in particular on the Ukrainian region, that is still poorly known.

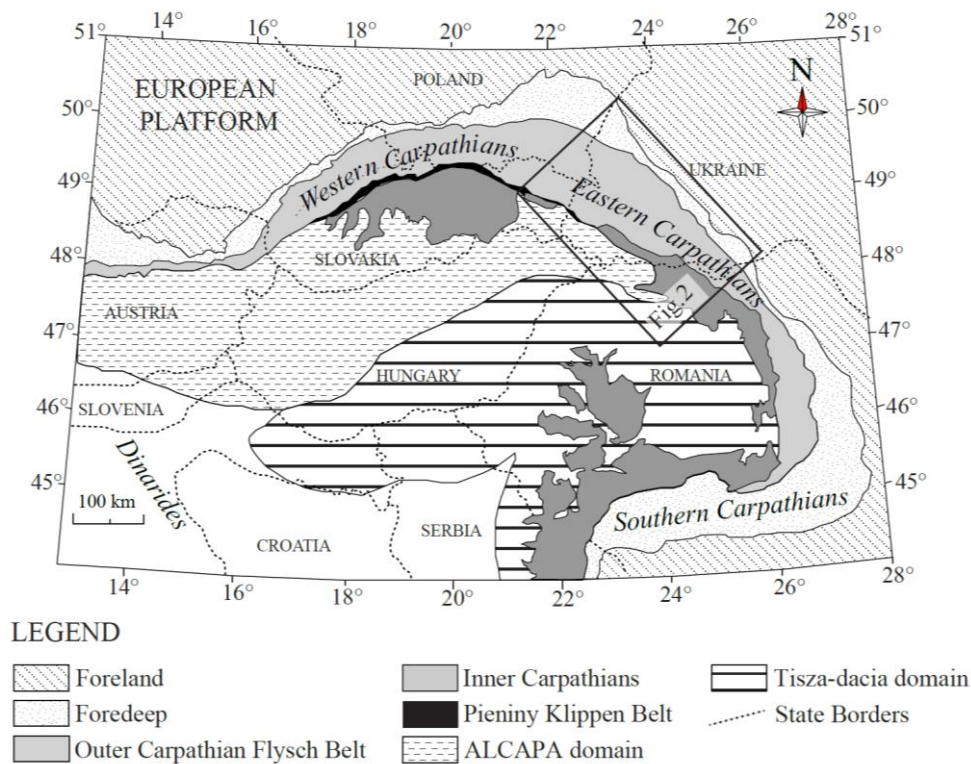


Figure 5.1: General tectonic map of the Carpathian-Pannonian region subdivided into the main tectonic domains: foreland, foredeep, Outer Carpathians, Pieniny Klippen Belt, Inner Carpathians. The Pannonian region is in turn subdivided into two regions representing the units belonging to the ALCAPA terrain (dashed region) and Tisza-Dacia terrain (black striped region).

Most of works focused on the more external part of the chain, dealing with the stratigraphic evolution of the foredeep successions [Joja *et al.*, 1968; Bancila, 1958; Ionesi, 1971; Sandulescu, 1984; Sandulescu *et al.*, 1981a,b and references therein]. Previous structural studies [e.g. Artyushkov *et al.*, 1996; Roure *et al.*, 1993; Oszczypko *et al.*, 2006] proposed several schematic geological sections across the Ukrainian Carpathians; however most of them are located in the foreland area because of the great interest of oil companies. Roure *et al.*, [1993] are some of the few authors publishing a geological transect across the Outer Carpathian flysch belt, furthermore validated by forward kinematic modelling. In such a poorly explored area, we collected new structural data and integrated them with literature data in order to construct balanced and sequentially restored cross-sections and suggest a structural model representing the structures at depth. This is the first attempt across this area to propose regional geometrically valid sections in which the relationships between Inner, Outer Carpathians and Pieniny “Klippen Belt” are shown. We will thus provide a possible scenario for the Ukrainian Carpathian evolution and evaluate the syn-orogenic sedimentation in order to estimate the maximum burial along the section. This latter has been compared with published low-T thermochronometric data (such as Apatite Fission Track (AFT) and apatite and zircon (U-Th-Sm)/He data (AHe and ZHe) and vitrinite reflectance (R_o) [Andreucci *et al.*, 2014] in order to verify the consistency of our tectonic interpretation.

5.3 Geological setting

The Ukrainian Carpathians are a NW-SE oriented thrust and fold belt, representing the north-eastern portion of this curved orogenic belt (Fig.5.2). They formed in response to the collisional event between the European and ALCAPA and Tisza-Dacia microplates during the Alpine orogeny [Sandulescu 1984; Royden 1988; Csontos 1995] from the Middle Cretaceous to the Pliocene [e.g. Sandulescu 1984]. Three main tectonic domains represent the framework of our study area: the Inner Carpathians (IC), the Outer Carpathians (OC) and the Pieniny Klippen Belt (PKB).

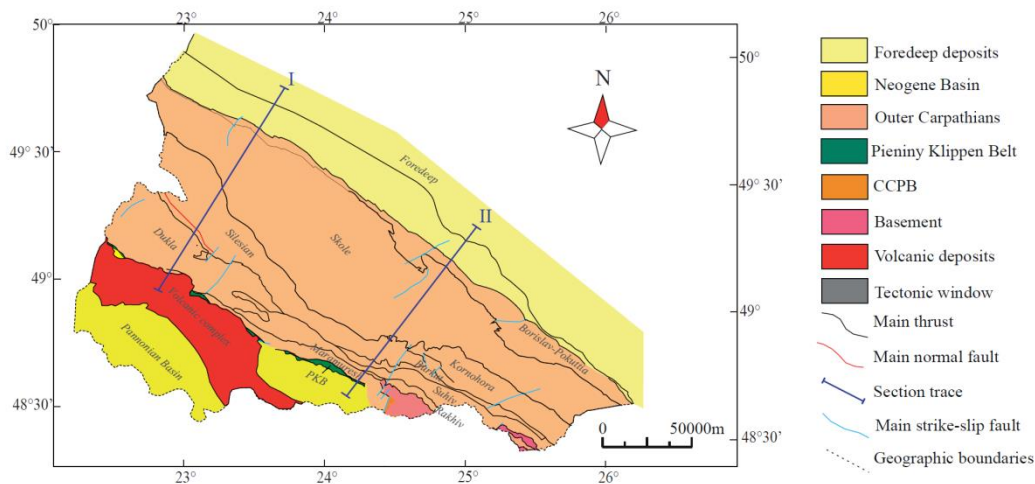


Figure 5.2: Schematic map of the Ukrainian Carpathians showing the main tectonic units and the location of the section traces.

The IC are built up of thick-skinned thrust sheets made of Variscan basement and the overlying Mesozoic deposits, unconformably covered by Paleogene up to Miocene sediments of the Transcarpathian Depression (TD). These successions are involved in the Neogene calc-alkaline volcanisms flowing up along faults oriented parallel to the Outer Carpathian flysch belt [Kaličák and Pospisil, 1990].

The OC are a thin-skinned thrust and fold belt formed by Lower Cretaceous-Lower Miocene turbiditic deposits. These successions are affected by Early Oligocene to the Late Miocene shortening and then emplaced on top of the adjacent margin of the European Platform. This belt is built up of several tectonic units, stacked one on top of the others by the in-sequence propagation of thrusting (Maramuresh, Rakhiv, Suhiv, Burkut, Krasnošora, Čorna Hora, Dukla, Silesian, Skole and Borislav-Pokuttia Units [Jankowski *et al.*, 2007]). Stratigraphic investigations on the marginal foredeep deposits pointed out that the NE-SW convergence ended at 11.5 Ma ago [Nemčok *et al.*, 2006].

The OC are bordered to the south by the PKB, a 600 km long belt, whose paleogeographic setting is still enigmatic. The main component of the PKB are Lower Jurassic-Lower Cretaceous olistoliths and olistotromes embedded in the Upper Cretaceous-Paleocene matrix. Triassic blocks also are present, but they can be found sporadically in the Western Slovakia. Some authors suggest an autochthonous development of these deposits [e.g., Stampfli and Borel, 2002] and some others

[*Birkenmajer, 1986; Golonka et al., 2000*] point out an allochthonous origin in which the PKB is the expression of the subducting Piemont-Ligurian- Vahic ocean at the surface.

5.3.1 The main tectono-stratigraphic units

In the following paragraphs we are going to describe the successions belonging to the IC, OC and PKB. Several regional names are assigned to them sometimes to the same formation. For the sake of simplicity we apply the subdivision adopted by *Jankowski et al. [2012]* in order to describe the composition of these deposits and their relative nomenclature. This allows us to compare the lithologies described for adjacent units (associated with adjacent basins) and highlight the similarities among them. In Fig. 5.3 a more detailed representation of the formation and relative nomenclature is made.

The Outer Carpathians

The OC are built up by several nappes made of siliciclastic deposits thrust on top of the Middle Miocene molasse [*Oszczypko et al., 2006*]. These deposits are grouped into several formations. Some of them can be easily recognized all over the study area. For some others the correlation remains uncertain because of the lack of homogeneous nomenclature. The first attempt to tie the Ukrainian OC stratigraphy has been made by *Jankowski et al., [2012]* achieving the same depositional system for the OC deposits. The **Borilav-Pokuttia Unit** is the most external units of the OC thrust and fold belt. It is detached in correspondence of Lower Cretaceous shaly beds intercalated in the siliciclastic deposits of the Stryi Beds. The sedimentation gets more calcareous during the Eocene, later covered by the Oligocene bituminous shales belonging to the Menilite Fm. This deposit represents an anoxic event occurring both in the Polish, Slovak and Ukraine regions and can be used as marker for stratigraphic correlation. During the Miocene the sedimentation changes abruptly passing into evaporitic layers with lenses of conglomerates.

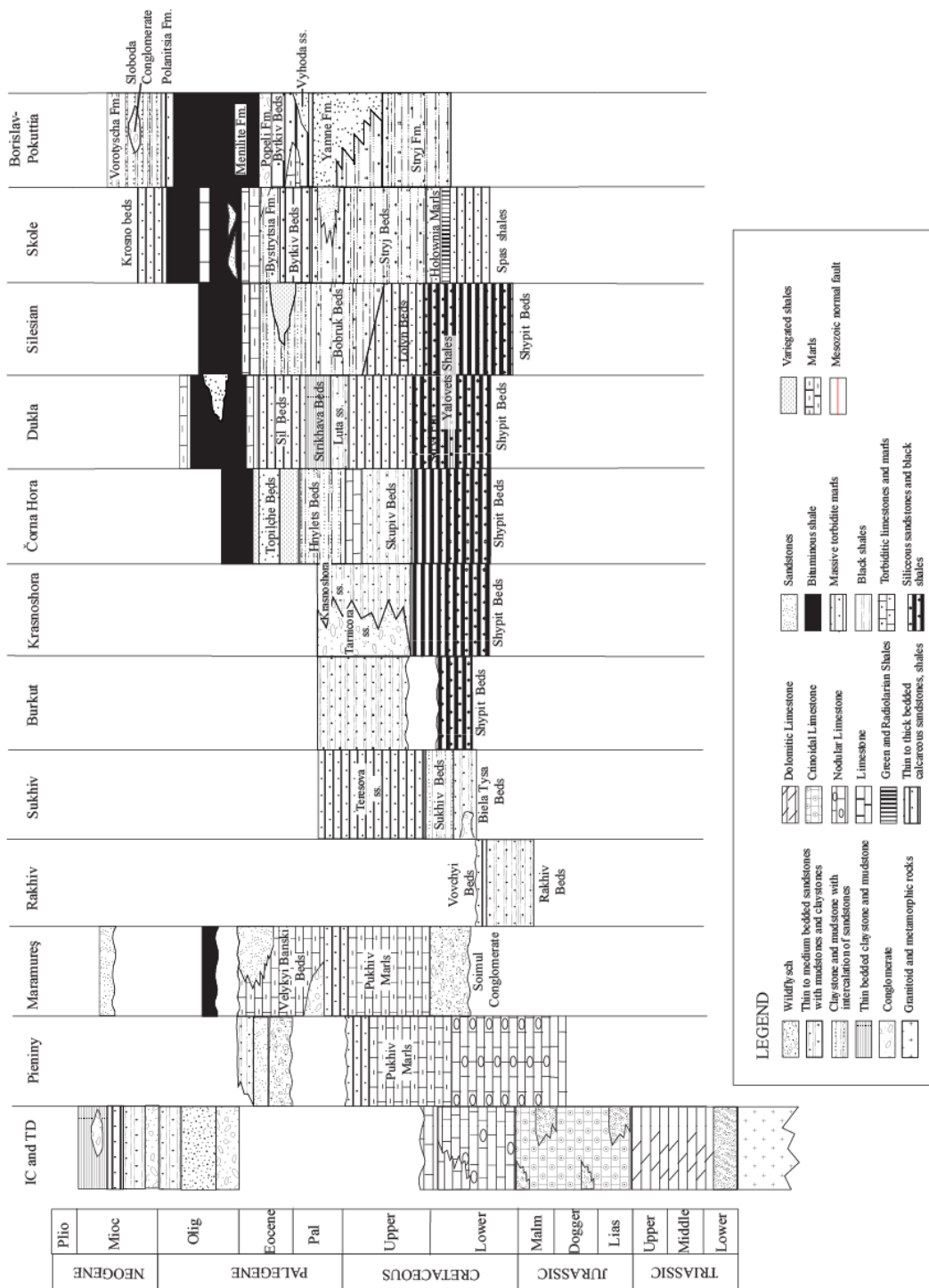


Figure 5.3: Chrono-stratigraphic chart of the main tectonic units constituting the Ukrainian Carpathians. The used nomenclature is the one already applied by Jankowski et al., [2012]. The formations are not represented with their own real thickness.

The structurally upper **Skole Units** has approximately the same stratigraphic record: Lower Cretaceous black shales behaving as décollement surface, passing upward into the thick-bedded siliceous and then calcareous turbiditic deposits. In this case, the Menilite Fm. starts with lenses of sandstones and chert and is covered by 2400 m of Miocene marly shale and thick-bedded sandstones (Krosno Beds). Moving toward the hinterland, the **Silesian** and the upper **Dukla units** show the same lithology, more shaly in correspondence of the detachment level (Shypit Fm.-Lower Cretaceous) and passing gradually upward into thick bedded sandstones, in some case intercalated with marls. The Menilite Fm. closes the Silesian succession and is covered by younger thin-bedded calcareous sandstones and shales in the Dukla Unit. This latter is overthrust by the Čorna Hora Unit, that is not continuous in the whole Ukrainian region. It is located in the southeastern part of the Ukrainian Carpathians. According to some authors [e.g. *Ślaczka* 1959], this unit represents the inner part of the Silesian Unit. Also in this case, the Skypit shales represent the oldest sediments (Barremian–Aptian). The sandy component increases during the Albian getting thin-bedded till the Eocene, when it is intercalated with thin layer of shales. This unit is closed by the Oligocene deposits of the Menilite Fm. and the Transitional Beds, composed by dark brown shales. **Krasnoshora, Burkut and Sukhiv** are the most internal units together with the **Rachiv Unit**. The formers are detached along the Shypit shales and pass upward into Paleocene thick- to thin-bedded sandstones and gray shales, locally intercalated with conglomerates. The Rachiv Unit is formed by Upper Jurassic black shales, calcareous thin- and medium-bedded turbiditic sandstones, and limestones passing upward into a more sandy Lower Cretaceous complex intercalated with conglomerates. Exotic blocks of Mesozoic limestones and diabases are also present. The youngest deposits are represented by black shales and thin bedded calcareous sandstones [*Ślaczka et al.*, 2006]. The trailing edge of the OC flysch belt is bordered by the **Maramureş Unit**. Its lower part is characterized by Mesozoic olistoliths and olistostromes covered by flysch deposits. These mega-block are made of Paleozoic and Proterozoic schists and gneisses, Paleozoic, Triassic, Jurassic, and Barremian–Aptian dolomites and limestones, and Permian–Triassic quartzitic sandstones and conglomerates [*Ślaczka et al.*, 2006]. The Upper Cretaceous-Eocene successions are formed by marls, thin-bedded sandstone and shales, locally interrupted by

conglomeratic lenses. Menilite and Malcov formations, unconformably overlay the above-described Eocene deposits. The sedimentological features of the Maramureş Unit change radically to the SW where it is built by metamorphosed Riphean-Vendian rocks and by sedimentary, volcanic, and epizonally metamorphosed Carboniferous, Triassic, and Jurassic formations. The Cretaceous conglomerates, organogenic limestones, and marls discordantly overlie older rocks [see *Kropotkin*, 1991 for details].

The Pieniny wildflysh

The Pieniny wildflysch (known in literature as Pieniny Klippen Belt, PKB) is a few km wide belt located between the IC and the OC (Fig. 5.2). It is formed by condensed successions for years described as the sedimentary infilling of the northern branch of the Meliata ocean [e.g. *Andrusov* 1945; *Birkenmajer*, 1986, *Plasienska* 2012]. Its peculiar block-in-matrix structure, together with the stratigraphic observations, [*Birkenmajer*, 1956b; *Plašienka and Mikuš*, 2010] indicates the sedimentary [*Festa et al.*, 2012] rather than the tectonic origin of this unit. The main components of the Pieniny wildflysch consists of Mesozoic olistoliths and olistostromes surrounded by a matrix made by shales, sandstones and marls whose age is Upper Cretaceous-Paleocene (even known as Klippen mantle from *Birkenmajer*, [1960]). These mega-blocks are more frequently made of Middle-Upper Jurassic up to Lower Cretaceous deposits [*Andrusov*, 1945; *Slavin* 1963, 1966 and *Rakús*, 1990]. The Jurassic succession starts with Aalenian marly shales covered by Bajocian to Berriasian crinoidal limestones. Several lithofacies can be recognized within these deposits: from the crinoidal limestones to the ammonitico rosso nodular limestones separated by radiolarites and covered by micritic limestones. These successions are closed by the Berriasian *Calpionella Alpina* limestones. These variable facies characterizing the mega-blocks are interpreted as rapid lateral change of facies in the Pieniny basin. This characteristic is peculiar of the Pieniny deposits along all the Carpathian chain but in the case of the Ukrainian sector, the correlation with the Polish Pieniny successions are difficult for some formations. While the nodular limestones can be easily correlated to the successions belonging to the so-called Czorsztyn Ridge, the red siliceous intercalations within it are not a common

facies. These are interpreted as the transitional slope facies of a hypothetical Kamenets Ridge [Lewandowski *et al.*, 2005]. These deposits are overlain by andesitic/basaltic and pyroclastic deposits dated Lower Cretaceous [Matějka, 1929; Andrusov, 1945; Slavin, 1963, 1966; Lomize, 1968].

The Inner Carpathians: the Transcarpathian Depression and its substratum.

The Transcarpathian Depression (TD) is a NW-SE basin, bordering the Pannonian domain to the north-east. It is delimited by the Pieniny wildflysch along its northern flank. It is located in a retro-wedge position and formed during the Miocene extension, while thrusting was still active at the Carpathian front. The basin fill starts with the Oligocene turbiditic deposits. Conglomerates, sandstones and clay passes upwards into siltstones and claystones. The Oligocene/Miocene boundary is marked by the beginning of another turbiditic event depositing 1000 m-thick sequence of clastic deposits [Rudinec, 1978]. The Lower Miocene succession is overlain by Middle Miocene shallow-water to deltaic deposits. It starts with the marine pelites of the Mirkovce Fm. [Zlínka, 1992] intercalated with volcano-sedimentary deposits passing upwards in a more sandy complex with calcareous clay and salt intercalations. The Middle Miocene succession is closed by clay deposits interbedded with sandy lenses and conglomerates. The Upper Miocene is characterized by lacustrine facies. 1000 m-thick alternation of clay, sands, gravel, tuff and coal deposited up to the Lower Pliocene [Vass and Čverčko, 1985].

The pre-Neogene substratum is made by structural units differing in origin and age [e.g. Tözsér and Rudinec, 1975; Sviridenko, 1976; Soták *et al.*, 1993]. The northernmost Mesozoic successions are interpreted as belonging to the Krížna Nappe [Mahel, 1986]. The orientation of the tectonic units buried under the Neogene deposits is NW-SE. They consist of thick-skinned nappes involving deposits from the Precambrian anchimetamorphic basement to the Eocene. The inner units are the Inatchevo-Kritchevo made of Permian to Eocene deposits overthrust by the Tatric and Veporic crystalline basement [Tomek, 1993]. These successions are then affected by folding during the Eocene [Soták *et al.*, 1993].

5.4 Methods

Two balanced sections have been constructed across the Eastern Ukrainian Carpathians (see Fig. 5.2), whose traces have been chosen to be parallel to the main tectonic transport direction. We integrated our own field data with published datasets and geological maps in order to constrain the surface and subsurface geometry.

The cross-sections have been then compared with published thermal models resulting from AFT, AHe, ZHe and R_o [Andreucci *et al.*, 2014] to constrain the maximum burial experienced by some specific horizons along the sections. Once constrained the burial along the sections, we try to figure out a possible geometric configuration for the eroded strata. We use Move package, developed by Midland Valley Exploration Ltd., to build up and validate our cross-sections. The first check of the geometrical consistency of our geological transect has been made performing flexural slip restoration. Each horse has been unfolded using a pin line parallel to the axial plane of individual folds. Once compared with the neighbour thrust sheet and minimized the gaps or overlaps and fixed the geometric problems among them, they have to be folded back to the original position. The horizon used as regional datum/template is the Upper Cretaceous-Paleocene. The section is thus prepared for the sequential restoration. Vertical simple shear algorithm has been applied to restore the displacement along listric normal faults and the fault parallel flow algorithm for the reverse fault restoration. Both these algorithms preserve bed area and length of the horizons. Then we performed 2D forward kinematic modeling to the obtained undeformed section inserting as input the displacement values obtained with the sequential restoration.

The 2D forward kinematic modelling allows us to define the tectonic structures at depth and to infer the geometric configuration of the strata above the present-day topography, also evaluating the relationships between the thrust and fold belt and its foreland basin.

5.5 Balanced cross-sections

Two profiles have been selected across the Ukrainian Carpathians. Although deformation was essentially produced by thrusting and associated folding for both of

them, normal faulting locally affected the accretionary wedge during the Middle-Late Miocene in the area crossed by Profile I (Fig.5.4). On the other hand, no evidences of significant post-thrusting normal faulting was found in the area crossed by Profile II (Fig.5.5), more to the SE.

Data constraints for cross section building.

1:200000 scale geological maps [*Jankowski et al.*, 2004, 2007; *Kaličiak et al.*, 2008] represented the starting point for constructing our balanced cross-sections. These maps have been integrated with our own field data in order to constrain the geometry of the structures. In some cases, the structural survey turns out to be very helpful in the reinterpretation of some tectonic contacts (such as the one bordering to the southwest the Silesian Unit [*Mazzoli et al.*, 2010]). The above-described surface data have been combined with well data, very abundant in the outermost part of this thrust and fold belt. The geometry of the foreland basin and the outer Borislav-Pokuttia unit has been constrained according to the interpretation made by *Osczyzypko et al.*, [2006] for the Werbiz, Derziw, Bilcze-Wolycia, Uhersko, Laniwka and Oparzy wells. The geological interpretation of the deepest structures of the OC thrust and fold belt is in line with that made by *Osczyzypko et al.*, [2006] and *Matenco and Bertotti*, [2000] for the Romanian Carpathians, highlighting the occurrence of three tectonic repetitions of the successions in the inner part of the OC. The detailed cross-sections constructed across the whole Ukrainian foreland [*Osczyzypko et al.*, 2006] provide a comprehensive picture of the relation between the foreland deposits and the underlying European Platform. Unfortunately, poor seismic constrains are available in the inner part of Ukrainian belt. The geometry of the sole thrust and the top of the basement comes from the interpretation of some magnetotelluric profiles published for the neighbour area, in proximity of the Polish border [*Stefaniuk et al.*, 2006]. Geophysical data interpreted by *Osczyzypko et al.*, [2006] shows the occurrence of SW-dipping blind normal faults lowering the top of the basement from 6 down to 20 km b.s.l.

5.5.1 Profile I

Profile I (Fig. 5.4a) crosses the Ukrainian Carpathians from the foreland region to the TD. In the frontal part, the Miocene molassic deposits lay on top of the Upper

Cretaceous and Jurassic cover of the North European Platform. Its thickness increases to the SW reaching 3 km in correspondence of the Carpathian front. The Platform directly below them is cut by SW-dipping Mesozoic normal faults obliterated by the Carpathian sole thrust. After the Mesozoic rifting, these normal faults experienced two reactivation phases: the Laramian inversion [*Roca et al.*, 1995] and the Miocene inversion [*Oszczypko et al.*, 2006 and references therein]. The well-constrained geometry of the basement under the foreland basin has been replaced by a more uncertain reconstruction below the inner part of the OC and PKB. Here it results from the restoration of the OC deposits back to their original position that allows a hypothetical reconstruction of the basement below them. The structural setting represented in the frontal part of the flysch belt is constrained by several exploration wells since this area is of great interest in oil and gas exploration [*Popadyuk et al.*, 2006]. Here, the Skole Unit is detached in correspondence of the shaly layers within the Upper Cretaceous succession and, together with the inner deposits of the Borislav-Pokuttia Unit, are overthrust on top of the anticlines and duplexes deforming the Borislav-Pokuttia successions. Such a high displacement thrust (ca. 50 km) can be activated thanks to the presence of the Miocene Polanitsia Fm. that represents an efficient décollement layer. The inner Dukla and Silesian units are deformed by in-sequence propagation of thrusting. The maximum displacement recorded along some of these splays is around 13 km getting lower in correspondence of the thrust within the Dukla Unit. The main décollement layer is represented by the Lower Cretaceous Spas Shale in the Dukla units; then thrusting propagates north-eastwards in the younger succession in correspondence of the Upper Cretaceous black shales and the Oligocene-Menilite Fm. The depth of the sole thrust reaches ca. 6 km below sea level in the more internal part and remains almost flat, slightly SW-dipping. The OC flysch belt are bordered to the south by the Pieniny faults. This is a high-angle fault inclined ca. 70° south-westward [*Lewadowski et al.*, 2005] thrusting the Pieniny wildflysch on top of the Eocene deposits belonging to the Dukla Unit. Here the Pieniny wildflysch is interpreted as a sedimentary unit deposited in the proximal part of the IC foreland basin where the olistoliths and olistotromes together with the slumping affecting the Upper Cretaceous-Paleocene sandy-shaly matrix are thought to be the effect of the subaerial

erosion of the IC range. The Upper Miocene volcanism [Pécskay *et al.*, 2000] located in correspondence of the WNW–ESE fault system [Kaličák and Pospisil, 1990] makes the interpretation of the deep structures of the IC very difficult. Our interpretation is based on the detailed geological section compiled by Elečko *et al.*, 2008 in addition to the 1:200000 geological map [Kaličiak *et al.*, 2008]. This transect shows the presence of the Paleogene-Neogene deposits (from the Eocene to the Upper Miocene) within the TD unconformably overlaying the Mesozoic cover of the IC basement. If any imbrications of the Mesozoic cover occurred, this cannot be detected just from the well data as they reach only the upper part of this cover. The youngest deposits of the TD are affected by Late Miocene high angle normal faults characterized by relatively low displacement ranging between 200 and 500 m. Moving to the NE, a high-displacement low-angle normal fault borders the Silesian Unit to the SW, increasing its dip angle at depth, in correspondence of the more competent lithology of the crystalline basement. In the construction of our balanced section we adopted a more conservative and simple solution to complete the subsurface information gap occurring in the area of the PKB where there are not seismic profiles showing clearly the geometrical relationship between the IC, PKB and OC and where the setting is furthermore complicated by the calc-alkaline intrusion in the IC arc.

The eroded strata reconstructed above the present-day topography (Fig.5.4b) are consistent with the burial depth estimated by the Andreucci *et al.*, 2014. The frontal part of the Skole Unit is buried under less than 3 km thick sediments. Burial increases to the SW where the syn-thrusting Miocene sediments get thicker. The maximum burial is produced by the stacking of several thrust sheets developed within the Dukla Unit where the tectonic burial is ca. 6 km and the thickness of the wedge reaches the maximum values of ca. 11 km.

Restoration of the Late Cretaceous pre-orogenic basin.

The sequential restoration allows us to reconstruct the geometry of the sedimentary system back to the Late Cretaceous (Fig.5.6a). The Upper Cretaceous-Paleocene horizon is considered as regional datum for the restoration, as it is well constrained at the surface and common to both the IC and OC. We restore, at first, the 8 km displacement along the NE-dipping normal fault and the normal faults involving the

IC deposits. Then we proceed with the restoration of all the thrust sheets back in their original position. In order to restore the frontal thrust leading the Borislav-Pokuttia Units on top of the Miocene molasse, we assume that, 15 km southwest of the frontal thrust, the Miocene deposits floor the Carpathian belt (as suggested by the Biskiw-1 well [Osczyzko *et al.*, 2006]). Then the first footwall cut-off is put in correspondence of the basement low directly to the south of the last recorded Miocene deposits. The displacement recorded for the leading thrust is ca. 26 km, considerably less than the 50 km estimated by Osczyzko *et al.*, [2006]. Once restored all the structures we calculated the amount of shortening separately for the IC and OC domains. Independently from the occurrence of any oceanic crust between these two domains, the IC experienced a shortening around 37% and their original sedimentary basin extends for 37 km. The Pieniny wilflysch deposited on the thinned continental crust of the European Platform and its shortening is included in the one calculated for the OC. These latter has been restored to a 245 km width basin and the relative computed shortening is ca. 156 km (63%). These values are not comparable with other works [e.g. Artyushkov *et al.*, 1996; Roure *et al.*, 1993] since they restored only the outer part of the Ukrainian Carpathians or provide a merely schematic regional profiles.

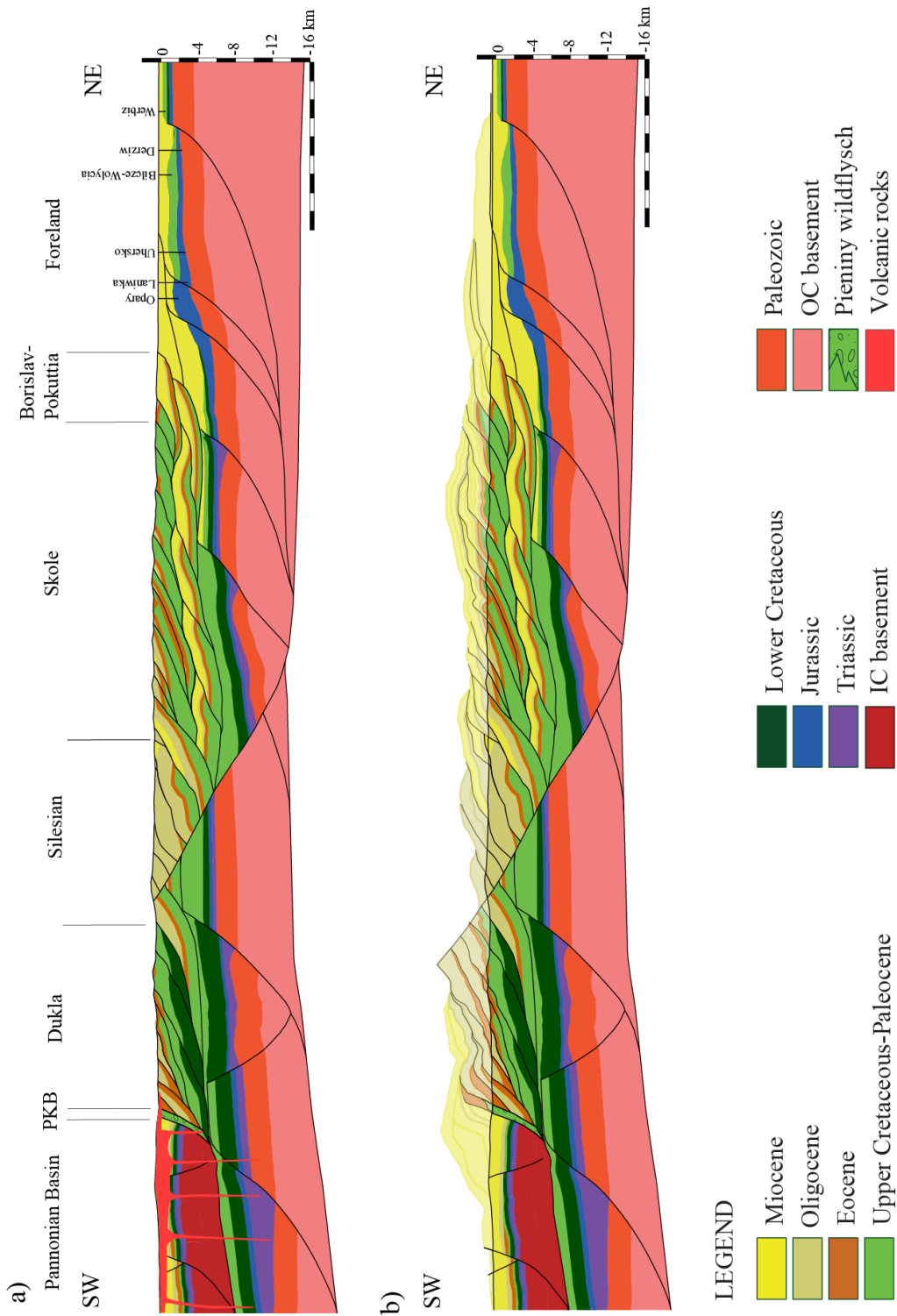


Figure 5.4: Balanced geological section (Profile I) across the Ukrainian Carpathians (located in Fig. 5.3). The horizontal scale equals the vertical scale. (b) Thickness of the eroded strata reconstructed above the present-day topographic line represents the minimum value estimated from vitrinite reflectance and low-temperature thermochronometric data [Andreucci et al., 2014]. The geometry of the eroded successions is obtained from 2D forward modeling.

5.5.2 Profile II

The profile II (Fig.5.5a) crosses the Ukrainian Carpathians from the foredeep basin to the Miocene deposits of the TD without crossing any volcanic complex. The Miocene sediments of the Carpathian foredeep deposited directly on top of the Mesozoic cover of the East European Platform. The thickness of the molasse increases to the south and is controlled by the flexure of the European plate produced by the advancing Carpathian belt. These Miocene deposits are folded and thrust in proximity of the Carpathian front forming the so-called Miocene folded foredeep. The frontal part of this belt is well constrained from several exploration wells drilled in correspondence of the Borislav and Bytkiv–Babche oil-gas fields. These wells show the repetition of the whole succession from the Upper Cretaceous Stryj Fm to the Polianycia shaly deposits [Popadyuk *et al.*, 2006]. The hinterland-dipping duplexes deforming the Borislav-Pokuttia Unit are overridden by the Skole Unit. This latter is deformed by several splays propagating northwards. Their displacement ranges between a few hundred meters to 2 km. The maximum values is recorded by the Skole leading thrust, moving on top of the Borislav-Pokuttia duplexes for ca. 35 km. Every thrust sheets is affected by internal fault propagation folds. The décollement level is represented by the Lower Cretaceous Spas Shales and in the more external part by the Upper Cretaceous red radiolaritic shales. The Skole Unit is bordered to the south by an oblique-slip fault with 1.5 km of normal displacement. The Silesian Unit overthrusts the Skole succession for ca. 35 km. It is internally deformed by fault propagation folds with thrusts developing in the hinge zone of the so-formed anticlines. The Silesian Unit is at turn overthrust by a leading imbricated fan composed by the adjacent Krasnoshora, Burkut and Maramureş units detached in correspondence of the Lower Cretaceous shales. The internal structure of the OC accretionary wedge is characterized by the stacking of three major high-displacement nappes producing a thickening of the accretionary wedge in its central part. This is in agreement with the maximum burial estimated by Andreucci *et al.*, [2014]. According to these authors, the Skole Unit in its central sector is buried by about 7 km (Fig.5.5b). This value decreases going toward the foreland and the Maramureş zone where it reaches 3 km. The trailing edge of the

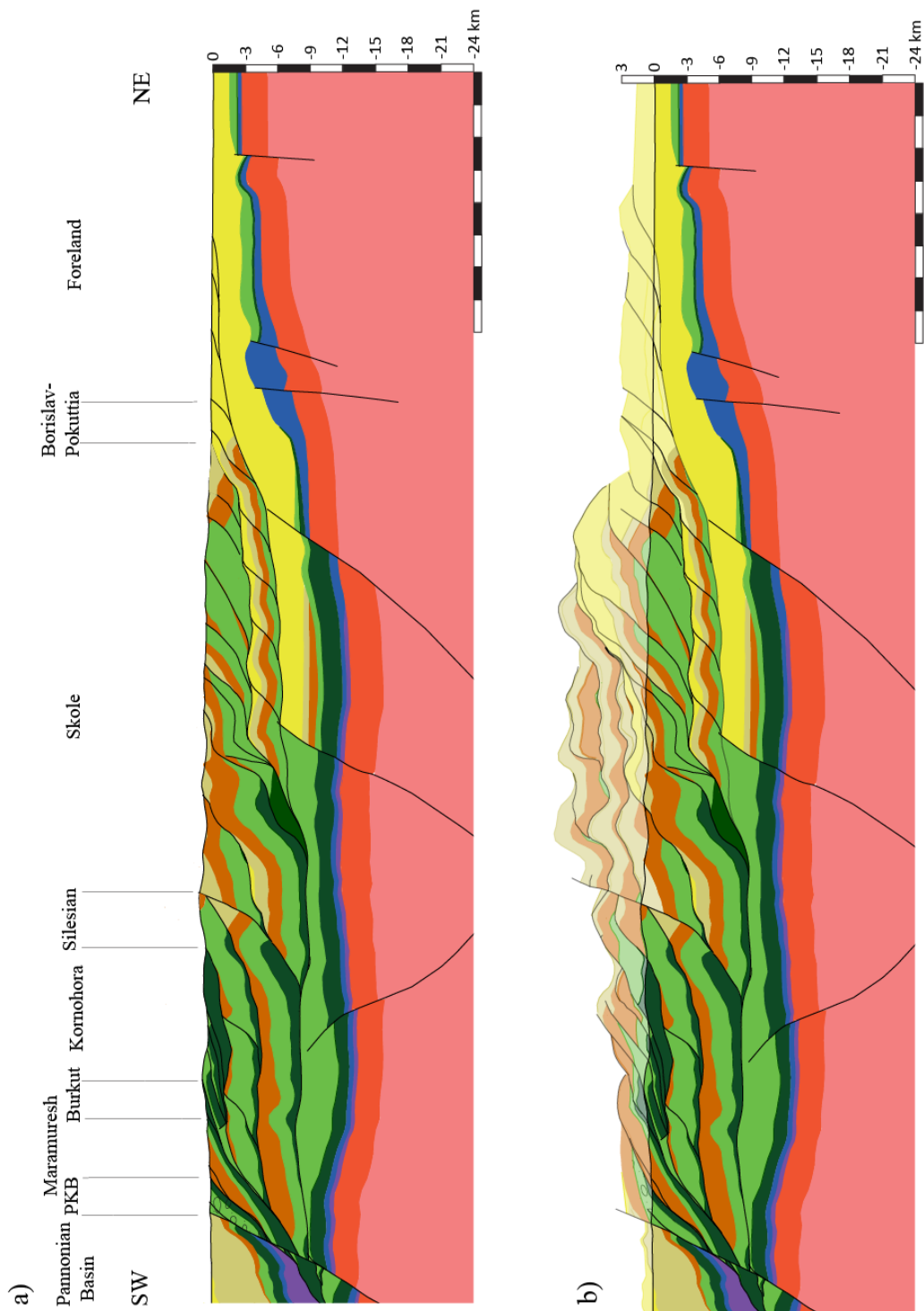


Figure 5.5: Balanced geological section (Profile II) across the Ukrainian Carpathians (located in Fig. 5.3). The horizontal scale equals the vertical scale. (b) Thickness of the eroded strata reconstructed above the present-day topographic line represents the minimum value estimated from vitrinite reflectance and low-temperature thermochronometric data [Andreucci et al., 2014]. The geometry of the eroded successions is obtained from 2D forward modeling.

OC accretionary wedge is bordered by the Pieniny wildflysch thrust on top of the Maramureş Unit. Some detailed but superficial geological transect [Słaczka *et al.*, 2006] show in both of the above-mentioned units Mesozoic olistoliths and olistostromes including the Triassic Keuper sandstones, the Upper Jurassic red crinoidal limestone and the Upper Jurassic-Neocomian white organic limestones bounded by Upper Cretaceous-Paleocene flysch deposits. The general trend recorded in the Pieniny area is given by SW high-angle dipping strata reflecting the geometry of the thrust. The Pieniny wildflysch is partially covered by the Badenian deposits of the TD. The structure below the TD is constrained by only a few wells located in the Eastern Slovakia [Milička *et al.*, 2011]. They show the occurrence of SW-dipping Eocene deposits below the TD directly on top of the Mesozoic and Paleozoic basement rocks. Our reconstruction is the result of the forward modelling that allows one to define the thickness and geometry of the strata buried under the Paleogene deposits.

Restoration of the Late Cretaceous pre-compressive basin.

The restoration of the Profile II (Fig. 5.6b) follows similar assumptions as those made for profile I: use of the Upper-Cretaceous-Paleocene horizon as regional datum and minimum shortening. Starting from the more recent structures we restore the normal component of the displacement along the oblique-slip fault between the Skole and Silesian unit. Then we proceed to the restoration of the more external thrusts from the folded foredeep units toward the hinterland. No constraints exist on the location of the footwall cut-off of the frontal thrust. We suppose it located 30 km south of the Borislav-Pokuttia leading thrust. Therefore, its displacement is of ca. 23 km. Comparing the present-day geological section with the initial undeformed flysch basin resulting from the sequential restoration, an estimate of the amount of shortening can be done for the Inner and Outer Carpathians, separately. The Pieniny wildflysch has been considered as deposited on the continental crust of the European Platform and included in the computation of the shortening affecting the OC basin. It amounts to 140 km (64%) without taking into account the Upper Miocene reactivation of the Mesozoic deep basement normal faults. In the southern part, the width of the IC undeformed basin is around 11 km, experiencing a shortening of ca. 54%.

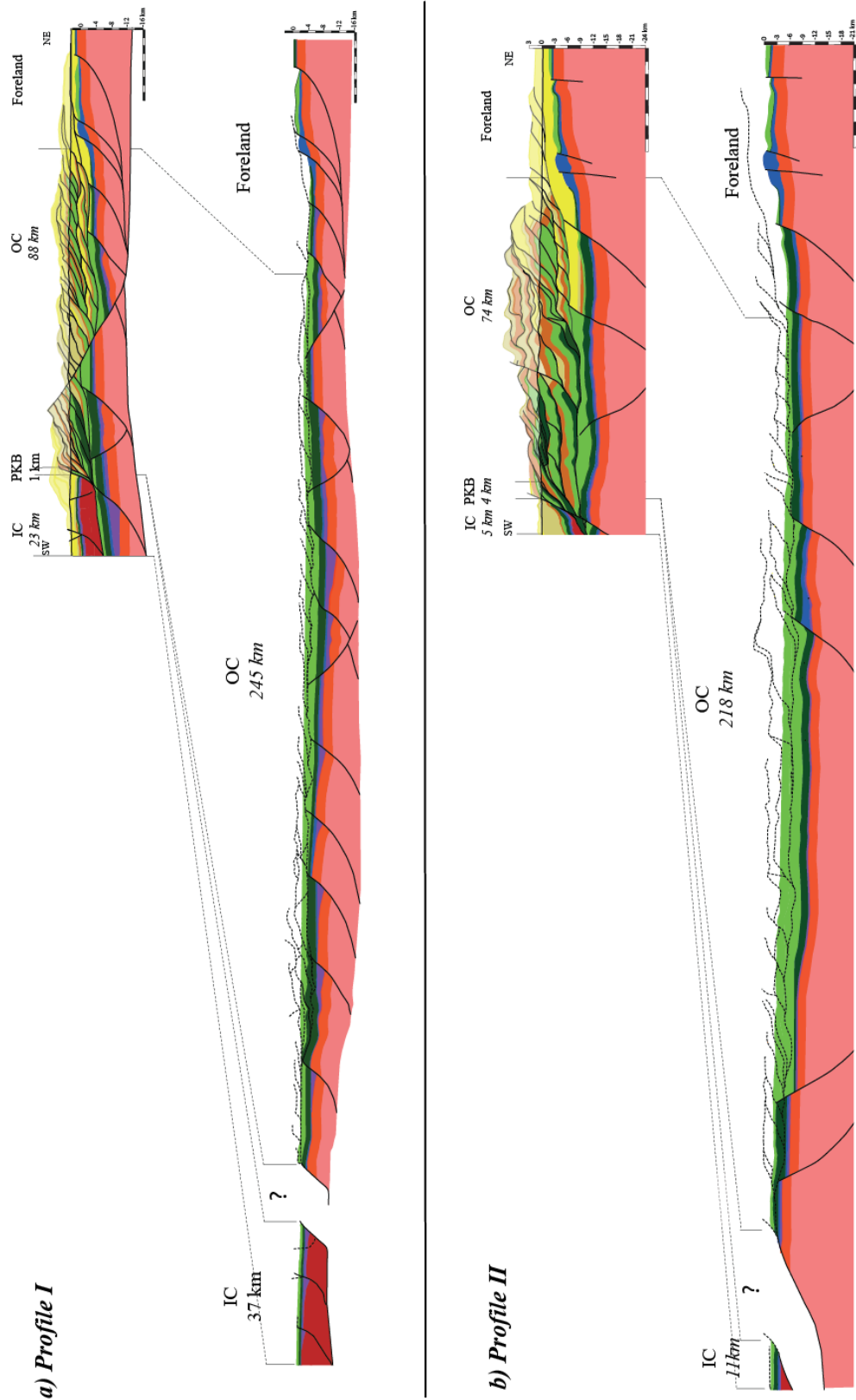


Figure 5.6: Restored cross-sections (a) Profile I and (b) Profile II at Late Cretaceous time. The sections have been sequentially restored based on the minimum shortening assumption. Black dashed lines show trajectories of future thrust.

5.6 Discussion

The Ukrainian Carpathians remained an unexplored area for years. Most of the previous works [Artyuchkov *et al.*, 1996; Kotarba and Koltun, 2006; Oszczypko *et al.*, 2006; Popadyuk *et al.*, 2006] focussed on the foreland basin recently drilled by exploration wells. They provide useful constraints on the thickness of the foredeep deposits, depth of the basement, geometry of the frontal thrust and occurrence of any tectonic repetition due to high-displacement thrust faults. The representation of the subsurface geology is in most of the cases schematic and not supported by a suitable geometric validation except in the case of Roure *et al.*, [1993]. They carried out a geological section across the Romanian Carpathians where more subsurface data are available and they calculated a shortening value of 133 km for the Skole (Skiba) and the foreland deposits. Our starting point is represented by a scenario that is completely different from what commonly accepted in literature. In fact, we exclude the occurrence of any oceanic crust below the Pieniny wildflysch. According to our reconstruction this latter is floored by continental crust representing the southern margin of the Eastern European Platform. In addition, stratigraphic evidences [Birkenmajer, 1956 b; Ślęcka *et al.*, 2006] suggest the occurrence of Mesozoic olistoliths and olistostromes, whose lithology is comparable with the Mesozoic cover of the IC. They can be likely interpreted as belonging to the proximal part of the foreland basin formed in the frontal part of the IC range. These mega-blocks are embedded in Upper Cretaceous flysch deposits deformed by large slumps. The northern continuation of these deposits is represented by the Maramureş Unit. This latter preserves the same characteristics as the Pieniny wildflysch: olistoliths and olistostromes at the bottom, covered by Eocene marls and sandstones. All of these deposits have been already interpreted to be the southern continuation of the Magura flysch [Sandulescu *et al.* 1981], in line with our geological reconstruction. A good correlation has been made among the OC successions so far interpreted as belonging to different tectonic and paleogeographic units, that is corresponding to adjacent basins separated by grabens. Jankowski *et al.* [2012], first suggested a common sedimentary system, unifying even the nomenclature of the various formations. The changes in thickness of these formations recorded along our cross-sections are the

results of the interplay between the emplacement of this thrust and fold belt and the flexure of the foreland. The first deepening of this basin can be recorded during the Eocene when the thrust front reached the OC domain. In some localized area, such as the innermost OC, the Oligocene sedimentation does not occur as it represented the Carpathian front at that time. The Oligocene deposits start to be thicker in correspondence of the Silesian deposits where the deepening of the foreland basin allowed the accumulation of more than 3 km thick deposits. In the southern Ukraine even the Skole successions record such a thickening of the Oligocene deposits. Here fault propagation folds and the subsequent thrusting produced the stacking of ca. 7 km of folded flysch deposits. This burial, even recorded by R_o and ZHe data [Andreucci *et al.*, 2014], slightly decreases in correspondence of the Skole front. According with the geometric reconstruction of the eroded strata, the Miocene deposits increases their thickness in correspondence of the frontal part of the Skole Unit. The stratigraphic thickness of the Miocene deposits gets lower in the frontal part of the belt, from the Borislav-Pokuttia Unit to the present-day foreland. The building of the OC thrust and fold belt could be occurred in the submarine environment till the Late Miocene when the last cooling event has been recorded by the AFT, ZHe and AHe.[Andreucci *et al.*, 2014]. These data have cooling ages almost homogeneous all over the area. When totally reset these ages range between 6 and 10 Ma suggesting a regional uplift as the main mechanism triggering this Upper Miocene cooling. Even if the north-western part of this thrust and fold belt is affected by a remarkable NE-dipping normal fault, in this area it seems to not influence the cooling ages of this sector that have the same values both at its footwall and hanging-wall. The nucleation of fault has to predate or be at least coeval with the Late Miocene regional uplift affecting this area.

5.7 Conclusions

The tectonic evolution of the Ukrainian Carpathians and the burial depth recorded along this thrust and fold belt have been constrained integrating our field data with published structural and paleothermal datasets. After the first Mesozoic rifting phase,

controlling the thickness of the formations till the Late Cretaceous, the sedimentation and the thickening/thinning of the younger successions are controlled by the emplacement of the IC range on top of the southern margin of the Eastern European Platform and the Oligo-Miocene imbrications of the OC successions. This is partially the reason of the variation of the burial depth recorded along the balanced cross sections. These latter show two different scenario for the northern and southern part of the Ukrainian Carpathians. The northern part, near the Polish border, is locally affected by post-thrusting normal faulting. The NE-dipping normal fault bordering the Silesian Unit to the SW, seems not influence the cooling ages of the horizons located both in its footwall and hanging wall. The cooling ages are almost coeval (Late Miocene), suggesting that the normal faulting has to be younger or coeval with the regional erosion affecting this area. Moving to the south-east, near the Romanian border, there are no evidences of post thrusting normal faulting. The most recent structures are represented by oblique-slip faults oriented parallel to the main transport direction. The discontinuous burial characterizing the Profile I is here replaced by a regular increase of the burial in the central part of the OC accretionary wedge, mainly controlled by thrusting. A different scenario in terms of burial can be delineated for the TD where the burial depends mainly by the sedimentation. In addition, the sequential restoration provides also the width of the pre-orogenic undeformed basin. The Profiles I and II have been restored to a 245 km and 218 km-wide OC basin, respectively, whereas the IC undeformed basin are considerably less wide, ca. 35 km and 11km respectively for Profile I and II.

6 Discussion

In this work a thermo-kinematic model of the Carpathian thrust and fold belt-foreland system is presented. This model is the result of an integrated method that combines fieldwork and kinematic modelling with the low-T thermochronometry and the 2D thermal modelling. New AFT and AHe data from the Pieniny wildflysch are also presented to complete the wide dataset already available for this area. This work has a dual aim: on one hand it wants to be a first attempt to represent the tectonic and thermal evolution of both the IC and OC domains at regional scale; on the other hand it tests the validity of a new approach consisting in the combination of the kinematic model and thermochronometry with FETKIN.

The here proposed thermo-kinematic model highlights the occurrence of four main phases in the Carpathian evolution from the Permo-Triassic rifting to the Early Cretaceous-Middle Miocene shortening and the post-compressional orogenic collapse.

Mesozoic rifting (from the Permo-Triassic to the Late Jurassic).

The rifting phase occurring in the Carpathian-Pannonian region during the Permian-Early Triassic (Figure 6.1) coincided with the closure of the Paleo-Tethys to the south. The subsequent opening of the Vardar Ocean produced the separation of the Adriatic plate into two main plates. According to the most accepted interpretation, this rifting phase lasted till the Early Cretaceous giving rise to the development of some branches of this ocean (e.g. Meliata, Penninic-Vahic, Magura oceans) fragmenting the Adriatic plate in several continental terrains [see *Csontos et al.*, 2004 for more details]. In particular, the Magura Ocean and the southern Pieniny Basin opening between the stable European Plate and the ALCAPA and Tisza-Dacia microplates reached the maximum width during the Tithonian when it became the westward prolongation of the Vahic-Penninic Ocean. Since no oceanic remnants are preserved in the Western Carpathian region (as discussed in the Chapter 3), such a big extension can be thought as affecting the continental crust, making it thinner but without developing any oceanic crust between the European and Adriatic plates. If oceanic domain had developed it should have been very narrow. This could explain the lack of its remnants at surface Independently from the occurrence of an oceanic

basin, our model shows an Early Cretaceous palaeogeographic setting (Fig.3.12) in which the sedimentation of the IC (ALCAPA and Tisza-Dacia terrain units [Wessely 1988]) and OC (belonging to the European domain) Mesozoic successions occurred on thinned continental crust. The analysis of the stratigraphy described in detail in Chapter 3.4 shows the occurrence of deeper facies in the IC realm, suggesting a deepening of the Early Cretaceous basin to the south. Furthermore the correlation charts represented in Chapter 3.4) show that the OC and IC deposited in the same sedimentary domain.

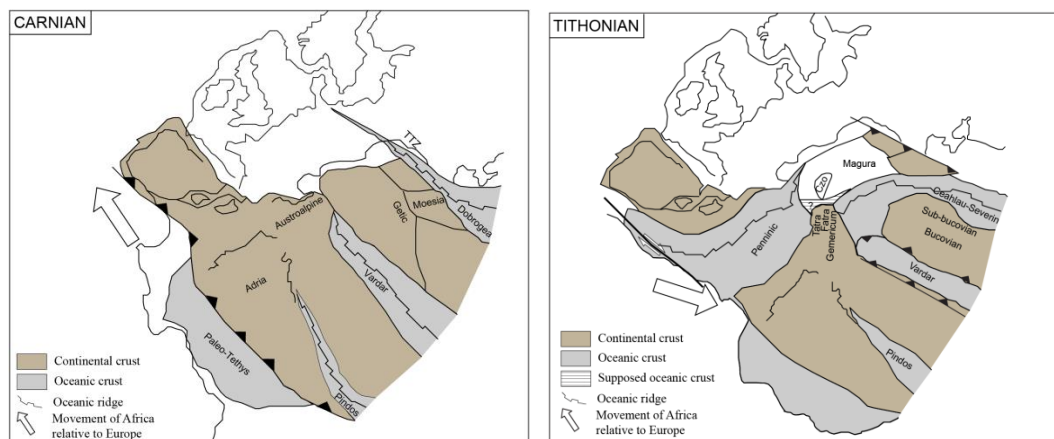


Figure 6.1 Schematic paleogeographic setting showing the position of the unit during the Carnian and Tithonian [modified after Csontos and Vörös, 2004]

Thick-skinned tectonic inversion (Early-Late Cretaceous).

After the Mesozoic rifting the so-formed normal faults were inverted during the Early and Late Cretaceous in correspondence of the northern margin of the Adria Plate. This resulted from the relative movement of the Africa Plate respect to the European Platform, oriented W-E. This period is thought to be the moment of the Western Carpathian oroclinal bend [Plašienka, 1998], even if more recent paleomagnetic data [Szaniawski et al., 2013] suggest an original curved shape of the belt without invoking the occurrence of any major rotation of the inner domains. The Eo-Alpine tectonics caused the formation of the IC thick-skinned tectonic system, in which thrusting propagated northward, toward the present-day Western Carpathian domain [Plašienka, 1998]. In the eastern sector the Tisza-Dacia microplate collided

with the southern margin of the European Platform during the Aptian [Vörös, 2001]. In this case the imbrication of the IC successions starts later and recorded a NE vergence. The inverted faults preserves a high inclination in the basement, and then they got flat in correspondence of the less competent Triassic evaporates. These faults produced the imbrication of the basement and the stacking of nappes made of its Mesozoic sedimentary cover. The so-formed IC range got exposed to the subaerial erosion only during the Eocene when a regional unconformity, described in several wells listed in the Chapter 3.5, developed all over the IC region.

Sedimentation and imbrication of the Pieniny wildflysch (Late Cretaceous-Paleocene)

The general eastwards movement of the Africa Plate respect to the European Platform produced the rotation of the ALCAPA and Tisza-Dacia blocks and the subsequent migration of these latter to the north and northeast. This movement caused the closure of the supposed Pieniny oceanic basin [e.g. Dewey *et al.*, 1989] and the emplacement of the IC nappes on top of the European Platform [Fig. 6.2]. As discussed in Chapter 3.4, an open debate exists on the origin and geodynamic meaning of the Pieniny Basin. For years interpreted as an oceanic basin [e.g. Birkenmajer *et al.*, 1960; Golonka *et al.*, 2000; Oszczypko, 2004; Picha *et al.*, 2006], this idea is later replaced by the hypothesis of a basin floored by thinned continental crust [Roca *et al.*, 1995; Jurewicz, 2005]. In our model this latter hypothesis has been supported. The sedimentological features of the Pieniny wildflysch has been already described by Plašienka and Mikuš, 2010 where the block in matrix texture has been highlighted. These olistoliths and olistostrome consists mainly of Mesozoic rocks. Triassic blocks, even if not abundant, have been described in the Pieniny Mts., in Western Slovakia and Ukraine. They are made of dolomites, dolomitic limestones, sandstones and gravel [Ślęczka *et al.*, 2006]. The Jurassic blocks are made of crinodal limestones and red radiolarian cherts and nodular limestones [Birkenmajer, 1960] whereas the lithologies of the Lower Cretaceous unit are characterized by white organic limestones. Upper Cretaceous variegated marls and thin bedded flyschoid deposits are the main component of the Pieniny matrix deformed by slumping and shearing internal to the basin. The sedimentation in the Pieniny basin

ends during the Middle Eocene with the sedimentation of sandstones, conglomerates and flysch deposits. Comparing these lithologies with the ones building up the Mesozoic nappes of the IC domains there is a good correlation suggesting the southern provenance of these mega-blocks. [Birkenmajer 1956 b and Roca *et al.*, 1995]. The same sedimentological characteristics can be recognized in the Maramureş Units (Ukrainian Carpathians) that in our reconstruction represent the northward continuation of the Pieniny foredeep basin. Thus, the Pieniny wildflysch represents the deposits of the IC foredeep basin in its proximal part. The IC belt was the only source of sediments at that time, feeding the foredeep basin with the Mesozoic deposits eroded from its structurally uppermost units. The Pieniny wildflysch overthrust the OC successions during the Early Oligocene. This high angle thrust represents the northern boundary of the Pieniny wildflysch along all the Carpathian belt.

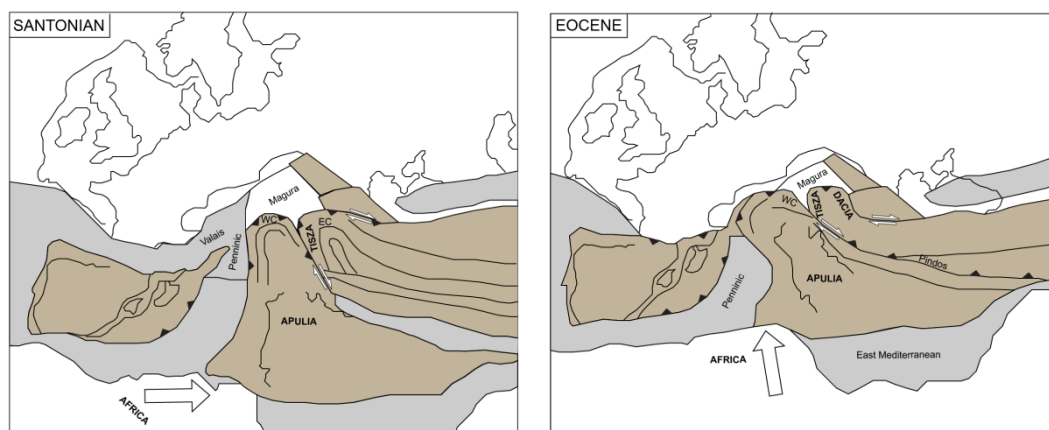


Figure 6.2: Schematic paleogeographic setting showing the position of the unit during the Santonian and Eocene [modified after Csontos and Vörös, 2004]

Thin-skinned thrusting: OC building and deep-basement fault inversion (Early Oligocene-Middle Miocene)

Starting from the Late Eocene [Fodor *et al.*, 1992] until the Oligocene, a continental escape of the ALCAPA terrain from the Alpine sector took place [Csontos *et al.*, 1992; Fodor *et al.*, 1992, 1998; Kázmér and Kovács, 1985]. The major movement is transferred to the boundary between the Dinarides and Alpine terrains. This is followed by the Early Miocene opposite rotation of the ALCAPA and Tisza-Dacia

plates [Márton *et al.*, 1992; Márton and Fodor, 1995; Márton and Márton, 1999; Panaiotu, 1998], which is supposed to be the mechanism triggering the thrusting in the OC sedimentary basin. Here thrusting involves the Meso-Cenozoic successions of the OC basin, detaching in correspondence of the Lower Cretaceous shale. High displacement thrusts, as the one flooring the Magura succession are followed by lower displacement thrusts producing hinterland dipping duplexes at the Magura footwall. In Ukraine fault propagation folds replaced the development of horses in the hinterland of the accretionary wedge. In the earliest stage the shortening involved also the deep basement normal faults forming anticlines in the Middle Late-Miocene molassic deposits [Oszczypko *et al.*, 2006]. In some cases the displacement was transferred to the Carpathian sole thrust.

Exhumation: timing and processes (Early-Late Miocene)

Thrusting in the OC propagated northward till the Middle Miocene and then the tectonic transport direction shifted toward northeast ceasing in the western part. [Nemčok *et al.*, 2006]. In the eastern part the end of thrusting is dated by stratigraphic observations at the beginning of the Late Miocene. After the emplacement of the Carpathian thrust and fold belt on top of the southern margin of the European Platform, its internal gravitational instability lead to the formation of normal faults, some of them reactivating older tectonic contacts. High angle normal faults cut through the Carpathian flysch belt in the Polish region, in particular the western region. In the central sector of our study area, in proximity of the Polish and Ukrainian border, the normal faults become less steep, controlling the exhumation of the accretionary wedge. This is also confirmed by low-temperature thermochronometry [Andreucci *et al.*, 2013] that provides cooling ages younger than the end of thrusting. In this region the young cooling ages are furthermore associated with Upper Miocene rapid cooling rates interpreted as due to a tectonic unroofing. In the Western Polish Carpathians erosion is controlled by thrust-related uplift. In this region new data have been carried out from the Pieniny wildflysch, dating its last cooling at the Late Miocene. This age is coeval with the cooling recorded by the IC succession suggesting a common thermal history for both the domains due to a later localized uplift. The thermo-kinematic model performed by FETKIN highlights that

the erosion in this sector is consistent with the in-sequence propagation of thrusting in the OC region and that the Pieniny wildflysch and the IC region recorded the youngest cooling ages partially controlled by the Sub-Tatra fault. The Eastern Carpathians, in particular the Ukrainian region, experienced an Upper Miocene cooling event due to isostatic uplift. Here there are no evidences of post-thrusting normal faulting and the most recent event involve the formation of oblique-slip faults, trending almost parallel to the main tectonic transport direction.

7 Conclusions

- The IC and OC successions, and the Pieniny wildflysch were deposited in continental passive margin basins. These could have been separated by an hypothetical oceanic domain (Meliata ocean) of which there is no present-day direct record (in the form of ophiolites). In this work, a conservative hypothesis has been proposed, suggesting the inexistence or the reduced extent of this oceanic embayment;
- The Pieniny wildflysch is here interpreted as a sedimentary unit constituting the proximal part of the IC foredeep basin. In the Ukrainian region the Maramureş Unit represent its continuation towards northeast;
- AFT and AHe ages from the Pieniny wildflysch record a non homogeneous burial along this belt, as some AFT ages are not reset. Middle-Upper Miocene exhumation is interpreted to be triggered by a regional uplift involving the Pieniny wildflysch together with the IC domain.
- The OC flysch belt can be subdivided into three different tectono-thermal domains: the Western, the Eastern Polish Carpathian and the Ukrainian Carpathians. The first domain is characterised by syn-thrusting erosion. The high-angle normal faults developed after the end of thrusting, are not the main mechanism triggering the exhumation of the accretionary wedge. On the other hand, the tectonic unroofing controlled by post-thrusting normal faults affect a wider area of the Eastern Carpathian region. The Ukrainian Carpathians, especially the south-eastern part, are not involved in the post-thrusting normal faulting. The exhumation here is due to a regional isostatic uplift.

- The estimated burial along the belt generally increases toward the hinterland in the western sector of the study area. In the easternmost side of the Polish Carpathians and the Ukrainian region the central part of the OC record the maximum thickness.
- The calculated shortening of the OC basin is 54% for the western part of the study area getting higher (ca. 63-64%) moving to the east. The width of the undeformed basin is ca. 135 km in correspondence of the Profile I, reach its maximum extent in the central part (ca. 343 km) and become narrower in the Ukrainian sector where it reached the 220 km. The shortening calculated for the IC is lower, ranging from 38% to 54% the maximum value recorded by Profile II in Ukraine;
- The here tested FETKIN demonstrated to be a successful tool in validating the selected structural model and predicting thermochronometric ages even starting from structurally complex scenarios.

•

8 References

Almendral, A., W. Robles, M. Parra, A. Mora, and R. Ketcham, FETKIN: Coupling kinematic restorations and temperature to predict exhumation histories: AAPG Bull., doi:10.1306/07071411112.

Anczkiewicz A. (2005), Verification of maximum paleo-temperatures on the basis of smectite illitization estimated for the Tatra Mts., Podhale Basin and adjacent area of the External Carpathians using fission track method. PhD. Thesis, Inst. Nauk Geol. Pol. Akad. Nauk, Osrodek Badawczy, 123 (in Polish).

Anczkiewicz, A., M. Zattin and J. Środoń (2005), Cenozoic uplift of the Tatras and Podhale basin from the perspective of the apatite fission track analyses, Pol. Towarzystwo Mineralogiczne – Prace Specjalne, 25, 261-264.

Anczkiewicz, A., J. Środoń, and M. Zattin (2013), Thermal history of the Podhale Basin in the internal Western Carpathians from the perspective of apatite fission track analyses. Geol. Carpath., 64 (2), 141-151, doi: 10.2478/geoca-2013-0010.

Anczkiewicz, A., and A., Świerczewska (2008), Thermal history and exhumation of the Polish Western Carpathians: evidence from combined apatite fission track and illite-smectite data, presented at 11th International Conference on Thermochronometry, Anchorage, Alaska.

Andreucci, B., (2013), Thermochronology of the Polish and Ukrainian Carpathians, PhD thesis.

Andreucci, B., A. Castelluccio, S. Corrado, L. Jankowski, S. Mazzoli, R. Szaniawski and Zattin, M. (2014), Interplay between the thermal evolution of an orogenic wedge and its retro wedge basin: an example from the Ukrainian Carpathians, *GSA Bull.*, *in press*.

Andreucci, B., A. Castelluccio, L. Jankowski, S. Mazzoli, R. Szaniawski, and M. Zattin (2013), Burial and exhumation history of the Polish Outer Carpathians:

Discriminating the role of thrusting and post-thrusting extension, *Tectonophysics*, 608, 866-883, doi.org/10.1016/j.tecto.2013.07.030.

Andrusov, D. (1931), Étude géologique de la zone des Klippes internes des Carpathes occidentales. I: Introduction, II: Stratigraphie (Trias et Lias), *Rozpr. St. Geol. Úst.*, 6.

Andrusov, D. (1938), Etude geologique de la zone des Klippes internes des Carpathes occidentales. III: Tectonique, *Ibidem*, 9.

Andrusov, D. (1945), Geologický výskum vnútorného bradlového pásma v Západných Karpatoch: časť IV, Stratigrafia doggeru a malmu. časť V. Stratigrafia kriedy, *Pr. Štátneho Geol. Úst.* 13, 1- 176.

Andrusov, D. (1950), La zone des Klippes entre la Vlára et Zilina. *Geol. Sborn Slov. Akad. Vied*, 1, 2-4.

Andrusov, D. (1974), The Pieniny Klippen Belt (The Carpathians of Czechoslovakia), in *Tectonics of the Carpathian-Balkan region*, *Geol. Inst. D. Štúr*, edited by M. Mahel', pp. 145-158, Bratislava.

Artyushkov, E. V., M. A. Baer and N. A. Mörner (1996), The East Carpathians: Indications of phase transitions, lithospheric failure and decoupled evolution of thrust belt and its foreland, *Tectonophysics*, 262, 101-132.

Bac- Moszaszwili, M. (1993), Structure on the western termination of the Tatra massif, *Ann. Soc. Geol. Pol.*, 63, 167-193. (In Polish with English summary).

Bancila, I. (1958), *Geologia Carpatilor Orientali*. Ed. stiintifica, Bucarest, 367 pp. (in Romanian).

Baumgart-Kotarba M. and J. Král (2002), Young tectonic uplift of the Tatra Mts.(fission track data and geomorphological arguments), presented at 17th Congress of Carpathian-Balkan Geological Association, Bratislava, Slovakia.

Behrmann, J.H., S. Stiasny, J. Milicka and M. Pereszlenyi (2000), Quantitative reconstruction of orogenic convergence in the northeast Carpathians, *Tectonophysics* 319, 111-127, doi:10.1016/S0040-1951(00)00020-2.

Bieda, F., S. Geroch, L. Koszarski, M. Książkiewicz, and K. Żytka (1963), *Stratigraphie des Karpates externes polonaises: Biul. Inst. Geol.*, 181, 5-174.

Birkenmajer, K. (1956 b), Sedimentary characteristics of the Jarmuta Beds (Maestrichtian) of the Pieniny Klippen Belt (Central Carpathians), *Bull. Acad. Polon. Sci.*, 3, 4, 10, Varsovie.

Birkenmajer, K. (1957 c), Remarks on the sedimentation of the Aalenian Flysch and the Jarmuta Beds (Senonian) of the Pieniny Klippen Belt. *Ann. Soc. Geol. Pol.*, 26, 2, Krakow.

Birkenmajer, K. (1958 d), Przewodnik geologiczny po pienińskim pasie skałkowym, in Pieniny Klippen Belt of Poland, Geological guide (in Polish), *Wyd. Geol.*, Warszawa.

Birkenmajer, K. (1960), Geology of the Pieniny Klippen Belt of Poland (A review of latest researches), *Jb. Geol. Bundesanst.*, 103(1), 1-36. Wien.

Birkenmajer, K., (1977), Jurassic and Cretaceous lithostratigraphic units of the Pieniny Klippen Belt, Carpathians, Poland, *Stud.Geol. Pol.*, 45, 1-158.

Birkenmajer, K. (1983), Strike-slip faults in the northern boundary zone of the Pieniny Klippen Belt, Carpathians, *Stud. Geol. Pol.*, 77, 89-112.

Birkenmajer, K. (1985a), Stage of structural evolution of the Pieniny Klippen Belt, Carpathians. *Stud. Geol. Pol.* 88, 7-31.

Birkenmajer, K. (1986), Stage of structural evolution of the Pieniny Klippen Belt, Carpathians. *Stud. Geol. Pol.*, 88, 7-32.

Birkenmajer, K. (2003), Post-collisional Late Middle Miocene (Sarmatian) Pieniny Volcanic Arc, Western Carpathian, Bull. Pol. Acad. Sci., Earth Sci., 51, 79-89.

Birkenmajer, K. (2008), The Szopka Limestone Formation- a new lithostratigraphic name for Upper Liassic beds of the Pieniny and Branisko successions, Pieniny Klippen Belt (West Carpathians) Stud. Geol. Pol., 131, 229-235.

Birkenmajer, K., and J. Dudziak (1988), Age of Palaeogene flysch in the Pieniny Klippen Belt, Carpathians, Poland, based on calcareous nannoplankton, Bull. Pol. Acad. Sci. Earth Sci., 36, 15-24.

Birkenmajer, K., P. Gedl, R. Myczyński and J. Tyszka (2008), “Cretaceous black flysch” in the Pieniny Klippen Belt, West Carpathians: a case of geological misinterpretation, Cretaceous Res., 29, 535-549, doi: 10.1016/j.cretres.2007.04.011.

Botor, D., I. Dunkl, M. Rauch-Włodarska and H. von Eynatten (2006), Attempt to dating of accretion in the West Carpathian Flysch Belt: apatite fission track thermochronology of tuff layers. Proc. of VI Internat. Conference. Central European Tectonic Studies, Zakopane. Geolines, 41-43.

Botor, D., I. Dunkl, M. Rauch-Włodarska and H. von Eynatten (2011), Timing of tectonic subsidence, accretion and exhumation of the Western Carpathian Flysch by apatite fission track and (U-Th)/He thermochronology. European Geosciences Union General Assembly (EGU) Vienna.

Brewer, J. (1981), Thermal effects of thrust faulting. Earth and Planetary Science Letters, 56, 233-244.

Bromowicz, J. (1999), Olistoliths-a proof for the Middle Eocene mobility of the Magura Basin, paper presented at International Geological Conference “Carpathian Geology 2000”, Smolenice.

Brown R. W., & M. A Summerfield (1997), Some uncertainties in the derivation of rates of denudation from thermochronologic data, Earth Surface Processes and Landforms, 22, 3, 239-248.

Burchart, J. (1972), Fission-track age determination of accessory apatite from the Tatra mountains, Poland. *Earth Planet. Sci. Lett.*, 15, 418-422.

Burtan, J., J. Chowaniec, and J. Golonka (1984), Wstępne wyniki badań nad egzotycznymi skałami węglanowymi z zachodniej części polskich Karpat fliszowych (Preliminary results of studies on exotic carbonate rocks in the western part of the Polish Flysch Carpathians), *Biul. Inst. Geol.*, 346, 147-159.

Carslaw, H. S., and J. C. Jeager (1986), *Conduction of Heat in Solids* (2. utg). London, UK: Oxford University Press.

Carslaw, H. S. and J. C. Jeager (1986), *Conduction of heat in solids* (2. utg.) London, UK: Oxford University Press.

Chamberlin, R. T. (1910), The Appalachian folds of Central Pennsylvania, *J. Geol. Chicago*, 18, 228-51.

Chamberlin, R. T. (1919), The building of the Colorado Rockies. *J. Geol. Chicago*, 10, 95-144.

Ciarcia, S., S. Mazzoli, S. Vitale, and M. Zattin (2012), On the tectonic evolution of the Ligurian accretionary complex in southern Italy, *Geol. Soc. Am. Bull.*, 124, 463-483, doi: 10.1130/B30437.1.

Ciarcia, S., S. Vitale, A. Di Staso, A. Iannace, S. Mazzoli, and M. Torre (2009), Stratigraphy and tectonics of an Internal Unit of the southern Appennines: implications for the geodynamic evolution of the peri-Tyrrhenian mountain belt, *Terra Nova*, 21, 88-96.

Cieszkowski, M., N. Oszczytko and W. Zuchiewicz (1987), Late Cretaceous submarine slump in the Inoceramian Beds of the Magura nappe at Szczawa, Polish Western Carpathians, *Ann. Soc. Geol. Polon.*, 57, 189-201.

Csontos, L., A. Nagymarosy, F. Horváth, M. Kovác (1992), Cenozoic evolution of the Intra Carpathian area: a model, *Tectonophysics*, 208, 221–241.

Csontos, L., and A. Vörös (2004), Mesozoic plate tectonic reconstruction of the Carpathian region, *Palaeogeography, Palaeoclimatology, Palaeoecology*, 210, 1-56, doi:10.1016/j.palaeo.2004.02.033.

Čverčko, J. (1975), Preliminary report about results of the deep structural well Prešov-1, Mns. Geofond, Bratislava (in Slovak).

Dahlstrom, C.D.A. (1969a), Balanced cross sections, *Canadian Journal of Earth Sciences*, 6, 743-757.

Danišik, M., J. Kadlec, C. Glotzbach, A. Weisheit, I. Dunkl, M. Kohút, N.J. Evans, M. Orvošová, B.J. McDonald (2011), Metamorphism, exhumation and topographic evolution in orogenic belts by multiple thermochronology: a case study from the Nízke Tatry Mts., Western Carpathians. *Swiss J Geosci.*, 104, 285-298.

Danišik, M., M. Kohút, I. Broska and W. Frisch (2010), Thermal evolution of the Malá Fatra Mountains (Central Western Carpathians): insights from zircon and apatite fission track thermochronology, *Geol. Carpath.*, 61, 19-27.

Danišik, M., T. Pánek, D. Matýsek, I. Dunkl and W. Frisch (2008), Apatite fission track and (U-Th)He dating of teschenite intrusions gives time constraints on accretionary processes and development of planation surfaces in the Outer Western Carpathians, *Z. Geomorphol.*, 52(3), 273-289.

Dal Piaz, G. V., S. Martin, I. M. Villa, G. Gosso, R. Marschalko (1995), Late Jurassic blueschist facies pebbles from the Western Carpathian orogenic wedge and paleostructural implications for Western Tethys evolution, *Tectonics*, 14, 4, 874-885.

Dewey, J. F., M. L. Helman, E. Turco, D. W. H. Hutton, S. D. Knott (1989), Kinematics of the Western Mediterranean, in *Alpine Tectonics*, edited by M. P. Coward, D. Dietrich, R. G. Park, Spec. Publ.-Geol. Soc. Land., 45, 265-283.

Dodson MH. (1973), Closure temperature in cooling geochronological and petrological systems, *Contrib. Mineral. Petrol.*, 40, 259-74.

- Dzuleński, S., and R. Gradziński (1960), Source of the Lower Triassic Clastics in the Tatra Mts., *Bull. Acad. Polon. Sci.* 8, 45-48.
- Duddy I.R., P.F. Green, G.M. Laslett (1988), Thermal annealing of fission tracks in apatite 3. Variable temperature behaviour, *Chem. Geol.*, 73, 25-38.
- Dunkl, I., (2002), TRACKKEY: a Windows program for calculation and graphical presentation of fission track data, *Computational Geosciences* 28,2, 3-12.
- Endignoux, L., and J. L. Mugnier (1990), The use of forward kinematic model in the construction of balanced cross sections, *Tectonics*, 9, 1249-1262.
- Elliot, D. (1983), The construction of balanced cross-sections, *Journal of Structural Geology*, 5, 101.
- Endignoux, L. and J. L. Mugnier (1990), The use of a forward kinematic model in the construction of balanced cross-sections, *Tectonics*, 9, 1249-1262.
- Ernst, T., J. Jankowski., V. Semenov , A. Adam, M. Hvozدارa, W. Jówiak, J. Lefeld, J. Pawliszyn, L. Szarka and V. Wesztergom (1997), Electromagnetic Soundings across the Tatra Mountains., *Acta Geophys. Pol.*, 45, 33-44.
- Faccenna, C., T. W. Becker, F. P. Lucente, L. Jolivet, and F. Rossetti (2001), History of subduction and back-arc extension in the central Mediterranean. *Geophys. J. Int.*, 145, 809–820.
- Faccenna, C., M. Mattei, R. Funiciello, and L. Jolivet (1997), Styles of back-arc extension in the central Mediterranean, *Terra Nova*, 9, 126 - 130.
- Faccenna, C., C. Piromallo, A. Crespo-Blanc, L. Jolivet, and F. Rossetti (2004), Lateral slab deformation and the origin of the western Mediterranean arcs, *Tectonics*, 23, TC1012, doi:10.1029/2002TC001488.
- Farley K. A. (2000), 'Helium diffusion from apatite: General behavior as illustrated by Durango fluorapatite', *Journal of Geophysical Research*, 105, B2, 2903-2914.

Farley K. A. (2002), (U-Th)/He dating: techniques, calibrations, and applications, in Noble Gases in Geochemistry and Cosmochemistry, Rev. Mineral. Geochem, vol. 47,. edited by D. Porcelli et al., pp. 819-44, Mineral. Soc. Am., Geochem. Soc., Chantilly, VA, doi: 10.2138/rmg.2002.47.18.

Festa, A., Y. Dilek , G.A. Pini, G. Codegone, K. Ogata (2012), Mechanisms and processes of stratal disruption and mixing in the development of mélanges and broken formations: Redefining and classifying mélanges, Tectonophysics 568 – 569, 7-24.

Filo, I., and Z. Siranova (1998), Hornad and Chrast Member - new regional lithostratigraphic units of the Sub-Tatric Group, Geologicke Prace, Spravy, 103, 35-51.

Fodor, L., Á. Magyari, M. Kázmér, A. Fogarasi (1992), Gravityflow dominated sedimentation on the Buda paleoslope (Hungary): record of Late Eocene continental escape of the Bakony unit, Geol. Rundsch., 81/3, 695– 716.

Fodor, L., B. Jelen, E. Márton, D. Skaberne, J. Car, M. Vrabec (1998), Miocene–Pliocene evolution of the Slovenian Periadriatic fault: implications for Alpine Carpathian extrusion models, Tectonics ,17 (5), 690– 709.

Fleuty, M. J. (1964), The description of folds, Geological Association Proceedings, 75, 461-492.

Froitzheim, N., D. Plašienka and R. Schuster (2008), Alpine tectonics of the Alps and Western Carpathians, in The geology of Central Europe, II: Mesozoic and Cenozoic, edited by McCann T., Geol. Soc. Publ. House, London, pp. 1141-1232.

Ğagala, Ł., J. Vergés, E. Saura, T. Malata, J. Ringenbach, P.Werner, P. Krzywiec (2012), Architecture and orogenic evolution of the northeastern Outer Carpathians from cross-section balancing and forward modeling, Tectonophysics 532-535, 223-241, doi:10.1016/j.tecto.2012.02.014.

- Galbraith, R.F., and G.M. Laslett (1993), Statistical models for mixed fission track ages. *Nucl. Tracks* 5, 3-14, doi: 10.1016/1359-0189(93)90185-C.
- Gallagher K. (1995), Evolving temperature histories from apatite fission-track data, *Earth Planet. Sci. Lett.*, 136, 421–35.
- Gibbs, A. (1983), Balanced cross-section construction from seismic sections in the areas of extensional tectonics, *Journal of Structural Geology*, 5, 153–160.
- Gleadow, A. J. W. (1981), Fission-track dating methods: what are the real alternatives?: *Nuclear Tracks*, 5, 1-2, 3-14.
- Gleadow A.J.W., I.R. Duddy, P.F. Green, J.F. Lovering (1986), Confined track lengths in apatite: a diagnostic tool for thermal history analysis, *Contrib. Mineral. Petrol.*, 94,405-15.
- Gleadow, A.J.W., and P.G. Fitzgerald (1987), Uplift history and structure of the Transantarctic Mountains: New evidence from fission track dating of basement apatites in the Dry Valleys area, Southern Victoria Land, *Earth and Planetary Science Letters*, 82, 1-14.
- Golonka, J. (2000), *Cambrian-Neogene Plate Tectonic Maps*, 1-125, Wyd. Uniw. Jagiell., Kraków.
- Golonka, J., L. Gahagan, M. Krobicki, F. Marko, N. Oszczytko and A. Ślęczka (2005), Plate-tectonic evolution and Paleogeography of the Circum-Carpathian Region, in *The Carpathians and their Foreland: Geology and Hydrocarbon Resources*, AAPG Mem.,84, edited by J. Golonka and F. J. Picha, pp. 11-46.
- Green, P. F. (1995), Comparison of zeta calibration baselines for fission track dating of apatite, zircon and sphene, *Chemical Geology: isotope Geoscience Section*.
- Green, P. F., I. R. Duddy, A. J. W. Gleadow, and J. F. Lovering (1989a), Apatite Fission Track Analysis as a Paleotemperature Indicator for Hydrocarbon Exploration, in *Thermal History of Sedimentary Basins-Methods and Case Histories*: New York, Springer Verlag, edited by Naesser, N. D., and T. McCulloh, 181-195.

Green, P. F., I. R. Duddy, G. M. Laslett, K. A. Hegarty, A. J. W. Gleadow, , and J. F. Lovering, (1989b), Thermal Annealing of Fission Tracks in Apatite: 4. Quantitative Modelling Techniques and Extension to Geological Timescales: Chemical Geology (Isotope Geoscience section), 79, 2, 155-182.

Green P.F, I.R. Duddy, A.J.W. Gleadow, P.R. Tingate, G.M. Laslett (1986), Thermal annealing of fission tracks in apatite, 1. A qualitative description, Chem. Geol., 59, 237–53.

Gross, P. (1973), On the character of the Choč-sub-Tatra fault. Geol. Práce, Spr, 61, 315-319 (in Slovak).

Gross, P., E. Köhler (Eds.), A. Biely, O. Franko, V. Hanzel, J. Hricko, G. Kupčo, J. Papšová, Z. Priehodská, V. Szalaiová, P. Snopková, M. Stránska, I. Vaškovský and L'. Zbořil (1980), Geology of the Liptovská kotlina Basin, GÚDŠ, Bratislava, 242 (in Slovak).

Gross, P., E. Köhler, and O. Samuel (1984), A new lithostratigraphical division of the Inner-Carpathian Paleogene, Geol. Práce, 81, 103-117. [In Slovak with English summary]

Gross, P., E. Köhler, J. Mello, J. Hasko, R. Halouzka, & A. Nagy (1993), Geology of Southern and Eastern Orava, Bratislava, pp. 292, D. Stur Inst. Geol.

Hayward, A. B., and R. H. Graham (1989), Some geometrical characteristic of inversion, in Inversion tectonics: Geological Society (London) Special Publication Classics, edited by M. A. Cooper and G. D. Williams,17-39.

Homza, T. X., and W. K. Wallace (1994), Geometric and kinematic models for detachment folds with fixed and variable detachment depths, J. Struct. Geol., 17, 4, 575-588, doi: 10.1016/0191-8141(94)00077-D.

Hovorka, D., S. Meres, and P. Ivan (1994), Pre-Alpine Western Carpathians Basement Complexes: Lithology and Geodynamic Setting, *Mitt. Österr. Geol. Ges.* 86, 33-44.

Hrušecký, I., D. Plašienka, and L. Pospíšil (2006), Identification of the North European platform below the eastern part of the Western Carpathian Flysch belt, in *The Carpathians and their foreland: Geology and hydrocarbon resources*, AAPG Mem. 84, edited by J. Golonka and F. J. Picha, pp. 717-727.

Hrušecký, I., L. Pospíšil, and M. Kohút (2002), Geological interpretation of the reflection seismic profile 753/92, in *Hydrocarbon potential of the Eastern Slovakian Basin and adjacent areas*, Open File Report, edited by I. Hrušecký, Geol. Surv. Slovak Republic, Bratislava (in Slovakian).

Huerta, A.D., and D.W. Rodgers (2006), Constraining rates of thrusting and erosion: Insights from kinematic thermal modeling, *Geology*, 34, 7, 541-544.

Hurai, V., F. Marko, A.K. Tokarski, A. Świerczewska, J. Kotulová, A. Biroň, (2006), Fluid inclusion evidence for deep burial of the Tertiary accretionary wedge of the Carpathians, *Terra Nova* 18, 440-446.

Hurford A.J. (1990a), International Union of Geological Sciences Subcommittee on Geochronology recommendation for the standardization of fission track dating calibration and data reporting, *Nucl Tracks*, 17, 233-36.

Hurford AJ, Green PF. (1982), A users' guide to fission track dating. *Earth Planet. Sci. Lett.*,59:343-54.

Hurford A.J., P.F. Green (1983), The zeta age calibration of fission-track dating. *Chem. Geol.*, 1, 285-317

Ionesi, L. (1971), *Flisul paleogen din bazinul vaili Moldovei*, edited by Acad. RSR, 200 pp. (in Romanian).

Jaglarz, P., and J. Szulc (2003), Middle Triassic evolution of the Tatricum sedimentary basin: an attempt of sequence stratigraphy to the Wierchowa Unit in the Polish Tatra Mountains, *Ann. Soc. Geol. Polon.*, 73, 169-182.

Jankowski, L. (2007), Chaotic complexes in Gorlice region, *Biul. Państw. Inst. Geol.*, 426, 27-52(in Polish, English abstract).

Jankowski, L., R. Kopciowski, W. Ryłko (2004), Geological Map of the Outer Carpathians: borderlands of Poland, Ukraine and Slovakia, *Pol. Geol. Inst.*, Warszawa.

Jankowski, L., R. Kopciowski, W. Ryłko (2004), Geological Map of the Outer Carpathians: borderlands of Ukraine and Romania, *Pol. Geol. Inst.*, Warszawa.

Jankowski, L., R. Kopciowski, W. Ryłko (2012), The state of knowledge of geological structures of the Carpathians between Biała and Rysa River-Discussion, *Biul. Państw. Inst. Geol.* 449, 203-216. (In Polish with English summary).

Janočko, J., M. Pereszlényi, D. Vass, V. Bezák, S. Jacko Jr., S. Jacko, M. Kohút, M. Polák , and J. Mello (2006), Geology and hydrocarbon resources of the Inner Western Carpathians, Slovakia, and Poland, in *The Carpathian and their foreland: Geology and hydrocarbon resources*, AAPG Mem. 84, edited by J. Golonka and F. J. Picha, 569-603.

Johnston, S.T., and S. Mazzoli (2009), The Calabrian Orocline: buckling of a previously more linear orogeny, in *Ancient Orogens and Modern Analogues*, *Geol. Soc., Lond., Sp. Publ.*, edited by J.B. Murphy, J.D. Keppie and A.J. Hynes, 327, 113-125.

Joja, T., V. Mutihac, M. Muresan (1968), Crystalline–Mesozoic and Flysch Complexes of the East Carpathians (Northern Sector), in *Guide to Excursion 46 AC, Romania*, *Int. Geol. Congr., XXIII Session, Prague*, 5-63.

Jurewicz, E. (1994), Structural analysis of the Pieniny Klippen Belt at Jeworki, Carpathians, Poland, *Stud. Geol. Pol.*, 106, 7-87. (In Polish, English summary).

Jurewicz, E. (2000a), Tentative reconstructions of the stress axes from the thrust-folding stage in the Tatra Mts. on the basis of slickensides in the granitoid core, southern Poland. *Prz. Geol.*, 48, 239-246. [In Polish with English summary].

Jurewicz, E. (2000b), Tentative correlation of the results of structural analysis in the granitoid core and nappe units of the Tatra Mts., southern Poland. *Prz. Geol.*, 48, 1014-1018. [In Polish with English summary].

Jurewicz, E. (2005), Geodynamic evolution of the Tatra Mts. and the Pieniny Klippen Belt (Western Carpathians): problems and comments, *Acta Geologica Polonica*, 55 ,3, 295-338.

Jurewicz, E., and B. Bagiński (2005), Deformation phases in the selected shear zones within the Tatra Mts granitoid core. *Geol. Carpath.*, 56, 17-28.

Kaličiak, M., and L. Pospisil (1990), Neogene magmatism in Transcarpathian depression: geological and geophysical evaluation, *Miner. Slovaca* 22, 481-498, (in Slovakian).

Kastens, K.A., et al. (1988), ODP Leg 107 in the Tyrrhenian Sea: Insight into passive margin and backarc basin evolution, *GSA Bull.*, 100, 1140-1156.

Kázmér, M., S. Kovács (1985), Permian– Palaeogene paleogeography along the Eastern part of the Insubric – Periadriatic Lineament system: evidence for continental escape of the Bakony – Drauzug Unit. *Acta Geol. Hung.*, 28 (1–2), 71– 84.

Keetley, J.T., Hill, K.C. (2000), 3D structural modeling of the Kutubu oil fields, PNG, presented at AAPG International Conference and Exhibition; Abstracts 84, AAPG, 1446

Ketcham, R.A. (2005), Forward and inverse modelling of low-temperature thermochronology data. *Rev, Mineral. and Geochem.*, 58, 275-314.

Ketcham, R.A., R. A. Donelick, W. D. Carlson (1999), Variability of apatite fission-track annealing kinetics: III. Extrapolation to geological time scales, *Am. Mineral.*, 84, 1235-1255, doi: 10.2138/am.2006.464.

Kohút, M. and S.C., Sherlock (2003), Laser microprobe Ar⁴⁰- Ar³⁹ analysis of pseudotachylyte and host-rocks from the Tatra Mountains, Slovakia: evidence for late Palaeogene seismic/tectonic activity, *Terra Nova*, 15, 417-424, doi: 10.1046/j.1365-3121.2003.00514.x.

Korab, T., and T. Durkovic (1978), Geology of the Dukla unit (east Slovakian flysch) (in Slovakian with English summary), Bratislava, Geologický Ústav D. Stura, pp. 194.

Koszarski, L., and A. Ślącza (1976), The Outer (Flysch) Carpathians: The Cretaceous, in *Geology of Poland*, vol I, Stratigraphy part 2, edited by S. Cieslinski, pp. 495-498, 657-679, 740-748, Inst. Geol., Warszawa.

Kotański, Z., (1961), Tectogénèse et reconstitution de la paléogéographie de la zone haut-tatarique dans les Tatras, *Acta Geol. Polon.*, 11, 187-467. [In Polish with French summary]

Kotański, Z., (1963a), On the character of the Western Carpathian Mesozoic geosyncline and the Podhale epimiogeosyncline, *Acta Geol. Polon.*, 13, 13-25. [In Polish with English summary]

Kotarba, M. J., Y. V. Koltun (2006), The origin and habitat of hydrocarbons of the Polish and Ukrainian parts of the Carpathian Province, in *The Carpathians and their foreland: Geology and hydrocarbon resources*, edited by Golonka J. and F. J. Picha, AAPG Mem., 84, 395-442.

Kotlarczyk, J. (1978), Stratigraphy of the Ropianka Formation in the Skole unit of the Flysch Carpathians (in Polish with the English summary). *Polska Akademia Nauk Oddział w Krakowie, Komisja Nauk Geologicznych Prace Geologiczne*, 108, 1-82.

Kotlarczyk, J., 1985, An outline of the stratigraphy of marginal tectonic units of the Carpathian orogen in the Krakow-Przemysl area: Guide to Excursion 4. Carpatho-Balkan Geological Association-XIII Congress, Krakow, Poland, 171 p.

Kotlarczyk, J. (1985), An outline of the stratigraphy of marginal tectonic units of the Carpathian orogen in the Krakow-Przemysl area. Guide to Excursion 4, paper presented at the 13th Congress of Carpatho-Balkan Geological Association, Krakow, Poland, 171.

Králiková, S., R. Vojtko, P. Andriessen, M. Kováč, B. Fügenschuh, J. Hók and J. Minár (2014 a), Late Cretaceous-Cenozoic thermal evolution of the northern part of the Central Western Carpathians (Slovakia): revealed by zircon and apatite fission track thermochronology, *Tectonophysics*, 615-616, 142-153, doi: 10.1016/j.tecto.2014.01.002.

Králiková, S., R. Vojtko, L' Sliva, J. Minár, B Fügenschuh, M. Kováč and J. Hók (2014 b), Cretaceous-Quaternary tectonic evolution of the Tatra Mts. (Western Carpathians): constraints from structural, sedimentary, geomorphological, and fission track data, *Geologica Carpathica*, 65, 4, 307-326, doi: 10.2478/geoca-2014-0021.

Král', J. (1977), Fission track ages of apatites from some granitoid rocks in West Carpathians, *Geol. Zbor. Geol. Carpath.*, 28, 269-276.

Kropotkin, P. N., (1991), Nappes of the Maramures zone of the Eastern Carpathians, *Geotectonics*, 25, 46-52.

Krzywiec, P. (2001), Contrasting tectonic and sedimentary history of the central and eastern parts of the Polish Carpathian foredeep basin-results of seismic data interpretation, *Mar. and Petrol. Geol.*, 18, 13-38, doi: 10.1016/S0264-8172(00)00037-4.

Krzywiec, P., & P. Jochym (1997), Characteristics of the Miocene subduction zone of the Polish Carpathians: results of flexural modelling, *Przegląd Geologiczny*, 45 (8), 785-792 (in Polish with English summary).

Kruglov, S. S., (1965), O prirode marmaroshskikh utiosov Sovetskikh Karpat (About the nature of the Marmarosh Klippens of the Soviet Carpathians) (in Russian): Geologicheskii Sbornik Lvovskogo Geologicheskogo Obsestva, 9, 41-54.

Kruglov, S. S., (1969), Pro stratygrafichne polozhennya pudynhovych piskovykiv i havelitiv v zoni peninskykh skel (Zakarpattia) (About stratigraphical position of pudding sandstones and gritstones within the Pieniny Klippen zone (Zakarpattia) (in Ukrainian): Proceedings of the Academy of Sciences of the Ukrainian SSR, 10, 874-877.

Kruglov, S. S., (2001), The problems of tectonics and paleogeodynamics of western Ukraine (a critical survey of the new publications) (in Ukrainian), Ukrainian Interdisciplinary Committee for Tectonics, 83 p.

Książkiewicz, M. (1957), Geology of the Northern Carpathians, Geol. Rdsch., 45, 369-411.

Książkiewicz, M. (1960), Palaeogeographic outline of the Polish Flysch Carpathians, Prace Inst. Geol., 33, 209-231.

Książkiewicz, M. (1962), Geological atlas of Poland: Stratigraphic and facial problems, Inst. Geol., Wyd. Geol., Warsaw, Poland, 16 maps.

Książkiewicz, M. (1965), Les Cordillères dans les mers crétacées et paleogenes des Carpathes du Nord, Bull. Soc. Géol. France, 7, 443-455.

Książkiewicz, M. (1977), Tectonics of the Carpathians, in Geology of Poland, Tectonics, Wyd. Geol., vol. 4, edited by W. Pozaryski, pp. 476-604, Warsaw, Poland.

Książkiewicz, M. (1977), Plate movement hypothesis and Carpathian development, Ann. Soc. Géol. Pol., 47, 321-353 (in Polish).

Laslett G.M., P.F. Green, I.R. Duddy, A.J.W. Gleadow (1987), Thermal annealing of fission tracks in apatite, 2. A quantitative analysis, Chem. Geol., 65,1-13.

Leško, B., and O. Samuel (1968), *Geology of the Eastern Slovakian Flysch* (in Slovakian with English summary), Bratislava, Slovenska Akademia ved., 256.

Lewandowski, M., M. Krobicki, B.A. Matyja, and A. Wierzbowski (2005), Palaeogeographic evolution of the Pieniny Klippen Basin using stratigraphic and palaeomagnetic data from the Veliky Kamenets section (Carpathians, Ukraine), *Palaeogeogr. Palaeocl.*, 216, 53-72.

Lexa, J., V. Bezák, M. Elečo, J. Mello, M. Polák, M. Potfaj, J. Vazár, (2000), *Geological map of Western Carpathians and adjacent areas 1:500000*, Geological Survey of Slovak Republic, Bratislava.

Lock, J., and S. Willet (2008), Low-temperature thermochronometric ages in fold-and-thrust belts, *Tectonophysics*, 456, 3-4, 147-162.

Lomize, M.G., 1968. Late Jurassic volcanism in the Eastern Carpathians. *Vest. Mord. Univ.* 6, 42- 58. (in Russian only).

Ludwiniak, M. (2010), Multi-stage development of the joint network in the flysch rocks of western Podhale (InnerWestern Carpathians, Poland), *Acta Geol. Polon.*, 60 (2), 283-316.

Mahel', M. (1981), Island character of Klippen Belt; Vahicum - continuation of Southern Penninicum in West Carpathians, *Geol. Zbor. - Geol. Carpath.*, 32, 293-305.

Mahel', M. (1986), Geological structure of the Czechoslovakian Carpathians. Palealpine units I. *Veda*, Bratislava, pp. 503 (in Slovak).

Mahel', M, and T. Buday (1968), *Regional geology of Czechoslovakie: Part 2, The West Carpathians*: Praha, Geol. Survey of Czechoslovakia, 723.

Malata, T. and K. Żytko (2006), *Kuźmina-1* (in Polish). Profile Głębokich Otworów Wiertniczych, Państwowego Instytutu Geologicznego, 110, pp. 68.

Malinowski, M., A. Guterch, M. Narkiewicz, J. Probulski, A. Maksym, M. Majdański, P. Środa, W. Czuba, E. Gaczyński, M. Grad, T. Janik, L. Jankowski, and A. Adamczyk (2013), Deep seismic reflection profile in Central Europe reveals complex pattern of Paleozoic and Alpine accretion at the East European Craton margin, *Geophys. Res. Lett.*, 40, 1-6, doi: 10.1002/grl.50746.

Malinverno, A., and W.B.F. Ryan (1986), Extension in the Tyrrhenian Sea and shortening in the Apennines as a result of arc migration driven by sinking of the lithosphere, *Tectonics*, 5, 227–245.

Maluski, H., P. Rajlich, and P. Matte, (1993), ^{40}Ar - ^{39}Ar dating of the Inner Carpathians Variscan basement and Alpine mylonitic overprinting, *Tectonophysics* 22(3), 313-337.

Mancktelow N.S., B. Grasemann (1997), Time-dependent effects of heat advection and topography on cooling histories during erosion, *Tectonophysics*, 270, 167-195.

Marchegiani, L., Bertotti, G., Cello, G., Deiana, G, Mazzoli, S., Tondi, E. (1999), Pre-orogenic tectonics in the Umbria-Marche sector of the Afro-Adriatic continental margin, *Tectonophysics*, 315, 123-143, doi: 10.1016/S0040-1951(99)00277-2.

Marciniec, P., and Z. Zimnal (2006), Borzęta IG-1 (in Polish), Profile Głębokich Otworów Wiertniczych, Państwowego Instytutu Geologicznego, 109, pp. 66.

Márton, E., P. Pagác, I. Túnyi (1992), Paleomagnetic investigations on Late Cretaceous - Cenozoic sediments from the NW part of the Pannonian Basin, *Geol. Carpath.* 43, 363–369.

Márton, E., L. Fodor (1995), Combination of palaeomagnetic and stress data-a case study from North Hungary., *Tectonophysics*, 242, 99–114.

Márton, E., P. Márton (1999), Tectonic aspects of a palaeomagnetic study on the Neogene of the Mecsek Mountains, *Geophys. Trans*, 42 (3– 4), 159–180.

Matějka, A., (1929), Quelques remarques sur la zone des Klippes internes des environs de Novoselica en Russie subcarpathique. Věstn. Státného Geol. Úst. Úst. Českoslov. Repub. 5, 359- 363.

Matenco, L., and G. Bertotti (2000), Tertiary tectonic evolution of the external East Carpathians (Romania), Tectonophysics, 316, 255-286.

Matyszkiewicz, J., and T. Słomka (1994), Organodetrital conglomerates with ooids in the Cieszyn Limestone (Tithonian-Berriasian) of the Polish Flysch Carpathians and their paleogeographic significance, Ann. Soc. Geol. Polon., 63, 211-248.

Mazzoli, S., and A.M. Algarra (2011), Deformation partitioning during transpressional emplacement of a 'mantle extrusion wedge': the Ronda peridotites, western Betic Cordillera, Spain, J. Geol. Soc., 168, 2, 373-382, doi: 10.1144/0016-76492010-126.

Mazzoli, S., L. Jankowski, R. Szaniawski and M. Zattin (2010), Low-T thermochronometric evidence for post-thrusting (<11 Ma) exhumation in the Western Outer Carpathians, Poland., Comptes Rendues Geosci., 342, 162-169, doi: 10.1016/j.crte.2009.11.001.

Meesters A. G. C. A., and T. J. Dunai (2002b), Solving the production-diffusion equation for finite diffusion domains of various shapes Part II. Application to cases with a-ejection and nonhomogeneous distribution of the source, Chem. Geol.,186, 347-363.

Milička, J., M. Pereszlényi and A. Nagy (2011), Hydrocarbon potential of Northern promontories of the Pannonian Basin System in Slovakia, Mineralia Slovaca, 43, 351-364.

Mora, A., W. Casallas, R. A. Ketcham, D. Gomez, M. Parra, J. Namson, D. Stockli, A. Almendral, W. Robles and B. Ghorbal (2014), Kinematic restoration of contractional basement structures using thermokinematic models: A key tool for petroleum system modeling, *AAPG Bull.*, in press, doi:10.1306/04281411108.

Morley, C.K. (1996), Models for relative motion of crustal blocks within the Carpathian region, based on restorations of the Outer Carpathian thrust sheets, *Tectonics*, 15, 885-904, doi: 10.1029/95TC03681.

Mount, V. S., J. Suppe and S.C. Hook (1990), A forward modeling strategy of cross section, *Am. Assoc. Pet. Geol. Bull.*, 74, 521-531.

Myśliwiec, M., Z. Borys, B. Bosak, B. Liszka, K. Madej, A. Maksym, K. Oleszkiewicz, M. Pietrusiak, B. Plezia, G. Staryszak, G. Świętnicka, C. Zielińska, K. Zychowicz, P. Gliniak, R. Florek, J. Zacharski, A. Urbaniec, A. Górka, P. Karnkowski and P. H. Karnkowski (2006), Hydrocarbon resources of the Polish Carpathian Foredeep: Reservoirs, traps, and selected hydrocarbon fields, in *The Carpathians and their foreland: Geology and hydrocarbon resources*, AAPG Mem. 84, edited by J. Golonka and F. J. Picha, 351-393, doi: 10.1306/985613M843073.

Nemcok, M. (1993), Transition from convergence to escape: field evidence from the West Carpathians. *Tectonophysics*, 217, 117-142.

Nemčok, J.,(ed.), V. Bezák, A. Biely, A. Gorek, P. Gross, R. Halouzka, M. Janák, Š. Kahan, Z. Kotański, , J. Lefeld, J. Mello, P. Reichwalder, W. Rackowski, P. Roniewicz, W. Ryka, J. Wieczorek, and J. Zelman (1994), *Geologická mapa Tatier 1: 50 000*. MŽP SR-GÚDŠ, MOSZNL, PIG, Bratislava.

Nemčok, M., M.P. Coward, W.J. Sercombe, R.A. Klecker (1999), Structure of the West Carpathian accretionary wedge: Insights from cross-section construction and sandbox validation, *Phys. Chem. Earth*, 24, 659-665, doi:10.1016/S1464-1895(99)00096-4.

Nemčok, M., P. Krzywiec, M. Wojtaszek, L. Ludhová, R. A. Klecker, W. J. Sercombe and M. P. Coward (2006a), Tertiary development of the Polish and eastern Slovak parts of the Carpathian accretionary wedge: insights from balanced cross sections, *Geol. Carpath.*, 57, 355-370.

Nemčok, M., J. Nemčok, M. Wojtaszek, L. Ludhová, R.A. Klecker, W.J. Sercombe, M.P. Coward, J. Franklin, J. Keith (2000), Results of 2D balancing along 20° and 21°30' longitude and pseudo-3D in the Smilno Tectonic Window: implications for shortening mechanisms of the West Carpathian accretionary wedge, *Geol. Carpath.*, 51, 281-300.

Nemčok, M., J. Nemčok, M. Wojtaszek, L. Ludhová, N. Oszczypko, W.J. Sercombe, M. Cieszkowski, Z. Paul, M.P. Coward and A. Ślącza (2001), Reconstruction of Cretaceous rifts incorporated in the Outer West Carpathian wedge by balancing, *Mar. Petrol. Geol.*, 18, 39-64, doi: 10.1016/S0264-8172(00)00045-3.

Nemčok, J., and D. Poprawa, coord., (1988-1989), *Geological Atlas of Western Outer Carpathian and their Foreland*. Państwowy Instytut Geologiczny. Warszawa.

Nemčok, M., L. Pospíšil, I. Hrušecký, and T. Zsíros (2006), Subduction in the remnant Carpathian Flysch Basin, in *The Carpathians and their foreland: Geology and hydrocarbon resources, AAPG Mem., 84*, edited by J. Golonka and F. J. Picha, pp. 767-785, doi: 10.1306/985628M843083.

Olszewska, B. W., and J. Wieczorek (1998), The Paleogene of the Podhale Basin (Polish Inner Carpathians)-micropaleontological perspective, *Przeg. Geol.*, 46 (8/2), 721-728.

Oszczypko, N. (1991), Stratigraphy of the Palaeogene deposits of the Bystrica subunit (Magura nappe, Polish Outer Carpathians), *Bull. Pol. Acad. Sci. Earth Sci.*, 39, 415-431.

Oszczypko, N. (2004), The structural position and tectonosedimentary evolution of the Polish Outer Carpathians, *Przeg. Geol.*, 52, 8-2.

Oszczypko, N. (2006), Late Jurassic-Miocene evolution of the Outer Carpathian fold-and-thrust belt and its foredeep basin (Western Carpathians, Poland), *Geol. Quart.*, 50 (1), 169–194.

Oszczypko, N., J. Dudziak, and E. Malata (1990), Stratygrafia osadów płaszczowiny magurskiej (kreda-paleogen) w Beskidzie Sądeckim, Karpaty, Stud. Geol. Polon., 97, 109-181.

Oszczypko, N., M. Oszczypko-Clowes, J. Golonka, and F. Marko (2005c), Oligocene-Lower Miocene sequences of the Pieniny Klippen Belt and adjacent Magura Nappe between Jarabina and Poprad River (East Slovakia and South Poland): their tectonic position and paleogeographic implications, Geol. Quart., 49 (4), 379-402.

Oszczypko, N., P. Krzywiec, I. Popadyuk, and T. Peryt (2006), Carpathian foredeep basin (Poland and Ukraine): its sedimentary, structural, and geodynamic evolution, in The Carpathians and their foreland: Geology and hydrocarbon resources, AAPG Mem., 84, edited by J. Golonka and F. J. Picha, pp. 293-350, doi: 10.1306/985612M843072.

Panaiotu, C. (1998), Paleomagnetic constraints on the geodynamic history of Romania. Rep. Geod. 7 (37), 205– 216.

Parrish, R. R. (1983), Cenozoic thermal evolution and tectonics of the Coast Mountains of British Columbia 1. Fission-track dating, apparent uplift rates, and patterns of uplift, Tectonics, 2, 601-631.

Paul, Z., and D. Poprawa (1992), Budowa geologiczna płaszczowiny magurskiej w strefie przypienińskiej w świetle badań uzyskanych z wiercenia Nowy Targ PIG 1, Przeg. Geol., 7, 404-409.

Peszat, C. (1967), The lithological development and condition of sedimentation of the Cieszyn Limestones (with English summery), Prace Geol. Odd. Pan w Krakowie, 44, 1-111.

Petrik, I., P. Nabelek, M. Janák, and D. Plašienka (2003), Condition of formation and crystallization kinetics of highly oxidized pseudotachylytes from the High Tatras (Slovakia), J. Petrol., 44, 901-927.

Picha, F., J. S. Zdeněk, and O. Kreci (2006), Geology and hydrocarbon resources of the Outer Western Carpathians and their foreland, Czech Republic, in *The Carpathians and their foreland: Geology and hydrocarbon resources*, AAPG Mem., 84, edited by J. Golonka and F. J. Picha, pp. 49-175, doi: 10.1306/985607M843067.

Plašienka, D. (1995a), Passive and active margin history of the northern Tatricum (Western Carpathians, Slovakia), *Geol. Rundsch.*, 84, 748-760, doi:10.1007/BF00240565.

Plašienka, D. (1995 b), Mesozoic evolution of Tatric units in the Malé Karpati and Považský Inovec Mts.: Implications for the position of the Klape and related units in western Slovakia, *Geol. Carpath.*, 46,101-112.

Plašienka, D. (1998), Geodynamic development of Central Western Carpathians during Jurassic and Cretaceous, in *Geodynamic Development of the Western Carpathians*, edited by M. Rakúš, Geol. Surv. Slovak Republic D. Stur Publ., Bratislava, pp. 107-130.

Plašienka, D. (2003), Dynamics of Mesozoic pre-orogenic rifting in the Western Carpathians. *Mitt. Österr. Geol. G.*, 94, 79-98.

Plašienka, D., and M. Mikuš (2010), Geological structure of the Pieniny and Šariš sections of the Klippen Belt between the Litmanová and Drienica villages in Eastern Slovakia. Bratislava, *Miner. Slov.*, 42 (2), 155-178. (In Slovak, English summary).

Plašienka, D. (2012), Early stage of structural evolution of the Carpathian Klippen Belt (Slovakian Pieniny sector), *Miner. Slov.*, 44, 1-16.

Polák, M. (2008), General geological map of the Slovak Republic. Map sheet 27 - Poprad. Štátny Geologický ústav Dionýza Štúra.

Prokešová, R., D. Plašienka, and R. Milovský (2012), Structural pattern and emplacement mechanisms of the Krížna cover nappe (Central Western Carpathians), *Geol. Carpath.* 63 (1), 13-32, doi: 10.2478/v10096-012-0001-y.

Popadyuk, I., M. Vul, G. Ladyzhensky, and P. Shpak (2006), Petroleum geology of the Boryslav-Pokuttya zone, the Ukrainian Carpathians, in *The Carpathians and their foreland: Geology and hydrocarbon resources*, edited by J. Golonka and F. J. Picha, AAPG Mem. 84, 455-466.

Rahn, M. K., & Grasemann, B. (1999). Fission track and numerical thermal modeling of differential exhumation of the Glarus thrust plane (Switzerland). *Earth and Planetary Science Letters*, 169(3), 245-259.

Rakús, M., M. Misík, J. Michalík, R. Mock, T. Durkovic, T. Koráb, R. Marschalko, J. Mello, M. Polák, and J. Jablonsky (1990), Paleogeographic development of the West Carpathians: Anisian to Oligocene, in *Evolution of the Northern Margin of Tethys*, vol. 3, edited by M. Rakús et al., *Mém. Soc. Géol. Fr.*, 154, 39-62.

Ratschbacher, L., W. Frisch, H.G. Linzer, O. Merle (1991 a), Lateral extrusion in the Eastern Alps, part 2: structural analysis, *Tectonics*, 10, 257-271.

Ratschbacher, L., O. Merle, P. Davy, and P. Cobbold (1991 b), Lateral extrusion in the eastern Alps, part 1, Boundary conditions and experiments scaled for gravity, *Tectonics*, 10, 245-256.

Reiners, P. W., K. A. Farley and H. J. Hickes (2002a), He diffusion and (U-Th)/He thermochronometry of zircon: Initial results from Fish Canyon Tuff and Gold Butte. *Tectonophysics*, 249, 247-308.

Reiners P. W., T. A. Ehlers, J. I. Garver, S. G. Mitchell, D. R. Montgomery, J. A. Vance, and S. Nicolescu (2002b), Late Miocene exhumation and uplift of the Washington Cascades, *Geology*, 30, 767-770

Reiners, P. W. (2005), Zircon (U-Th)/He Thermochronometry: Reviews in *Mineralogy and Geochemistry*, 58, 1, 151-179.

Reiners P.W. and M. T. Brandon (2006), Using Thermochronology to Understand Orographic Erosion, *Annu. Rev. Earth Planet. Sci.*, 34, 419-66,

Reiners, P.W., T.L. Spell, S. Nicolescu, K.A. Zanetti (2004), Zircon (U-Th)/He thermochronometry: He diffusion and comparisons with $^{40}\text{Ar}/^{39}\text{Ar}$ dating. *Geochim. Cosmochim. Ac.*, 68, 1857-1887, doi: 10.1016/j.gca.2003.10.021.

Roca, E., G. Bessereau, E. Jawor, M. Kotarba, and F. Roure (1995), Pre-Neogene evolution of the Western Carpathians: Constraints from the Bochnia-Tatra Mountains section (Polish Western Carpathians), *Tectonics*, 14(4), 855-873, doi: 10.1029/95TC00828.

Roniewicz, P. (1959), Sedimentary characteristics in the High-Tatra Series. (In Polish, English summary), *Acta Geol. Polon.*, 9, 301-317.

Rossetti, F., B. Goffé, P. Monié, C. Faccenna, and G. Vignaroli (2004), Alpine orogenic PTt deformation history of the Catena Costiera area and surrounding regions (Calabrian Arc, southern Italy): the nappe edifice of Northern Calabria revised with insights on the Tyrrhenian-Appennine system formation, *Tectonics*, 23, 1, TC 6011, doi:10.1029/2003TC001560.

Roure, F., E. Roca, and W. Sassi (1993), The Neogene evolution of the Outer Carpathian flysch units (Poland, Ukraine and Romania): Kinematics of a foreland / fold-and-thrust belt system, *Sediment. Geol.*, 86, 177-201, doi: 10.1016/0037-0738(93)90139-V.

Royden, L.H. (1988), Late Cenozoic Tectonics of the Pannonian Basin System, in *The Pannonian Basin, a Study in Basin Evolution*, edited by L.H. Royden, and F. Horvath, AAPG Mem. 45, 27-48.

Royden, L., & B. C. Burchfiel (1989), Are systematic variations in thrust belt style related to plate-boundary processes? (The Western Alps versus the Carpathians). *Tectonics*, 8 (1), 51-61.

Royden, L., & G. Karner (1984), Flexure of lithosphere beneath Apennine and Carpathian foredeep basins: evidence for insufficient topographic load, *AAPG Bull.*, 68, 704-712.

- Rutherford E. (1905), Present problems in radioactivity, *Popular Science* (May), 1-34.
- Rudinec, R. (1978), Paleogeographical, lithofacial and tectonic development of the Neogene in eastern Slovakia and its relation to volcanism and deep tectonic. *Geol. Zbor. (Bratislava), Geol. Carpath.*, 29, 2, 225-240.
- Safran, E. B. (2003), Geomorphic interpretation of low-temperature thermochronologic data: Insights from two-dimensional thermal modelling, *J Geophys. Res.-Sol. Ea.*, 1978–2012, 108,B4.
- Sanderson, D.J. (1982), Models of strain variation in nappes and thrust sheets; a review, *Tectonophysics*, 88 (3-4), 201-233.
- Samuel, O., and O. Fusan (1992), Reconstruction of subsidence and sedimentation of Central Carpathian Paleogene. *Zapadne Karpaty, Ser. Geol.*, 16, 7-46.
- Sandulescu, M. (1984), *Geotectonica României*, edited by Technica, Bucharest, 450 pp. (in Romanian).
- Săndulescu, M. (1988), Cenozoic tectonic history of the Carpathians, in *The Pannonian Basin: A Study in Basin Evolution*, edited by L. Royden and F. Horvath, *AAPG Mem.*, 35, 17-25.
- Sandulescu, M., H.G. Krautner, I. Balintoni, D. Russo-Sandulescu, M. Micu (1981°), The structure of the East Carpathians (Moldavia–Maramures area), *Carp.-Balc. Assoc., XII Congr.*
- Sandulescu, M., M. Stefanescu, A. Butac, I. Patrut, P. Zaharescu, (1981b), Genetical and structural relations between flysch and molasse (The East Carpathians), *Carp.-Balc. Assoc., XII Congr.*
- Santantonio, M. (1993), Facies associations and evolution of pelagic carbonate platform/basin systems: examples from the Italian Jurassic, *Sedimentology*, 40, 1039–1067, doi: 10.1111/j.1365-3091.1993.tb01379.x.

Santantonio, M. (1994), Pelagic carbonate platform in the Geologic Record: their Classification, and Sedimentary and Paleotectonic evolution, *Am Assoc Petr Geol Bull*, 78, 122–141.

Sartori, R. (2003), The Thyrrhenian backarc basin and subduction of the Ionian lithosphere, *Episodes*, 26, 217-221.

Semyrka, G. (2009), Vitrinite reflectance and types of kerogen in well sections in the eastern part of the Polish Carpathians, *Geologia*, 35(2/1), 49-59.

Schmid, S. M., D. Bernoulli, B. Fügenschuh, L. Matenco, S. Schefer, R. Schuster, M. Tischler and K. Ustaszewski (2008), The Alpine-Carpathian-Dinaridic orogenic system: correlation and evolution of tectonic units, *Swiss J. Geosci.*, 101, 139-183, doi: 10.1007/s00015-008-1247-3.

Schmid, S.M., B. Fügenschuh, E. Kissling, and R. Schuster (2004 b), TRANSMED Transects IV, V and VI: Three lithospheric transects across the Alps and their forelands, in, *The TRANSMED Atlas: The Mediterranean Region from Crust to Mantle*, edited by Cavazza W., F.M. Roure, W. Spakman, G.M. Stampfli and P.A. Ziegler Springer, Berlin and Heidelberg, attached CD (version of the explanatory text available from the first author as pdf-file upon request).

Ślaczka, A. (1971), Geology of the Dukla unit (in Polish with English summary): *Prace Inst. Geol.*, 1, 1-63.

Ślaczka, A., and R. Unrug, (1976), Trends of textural and structural variations in turbidite sandstone (Oligocene, Outer Carpathians): *Rocznik Polskiego Towarzystwa Geologicznego*, 46, 55-75.

Ślaczka, A., S. Kruglov, J. Golonka, N. Oszczypko, and I. Popadyuk (2006), *Geology and Hydrocarbon Resources of the Outer Carpathians, Poland, Slovakia, and Ukraine: General Geology*,

in The Carpathians and their foreland: Geology and hydrocarbon resources: *AAPG Mem. 84*, edited by J. Golonka and F. J. Picha, pp. 221-258, doi: 10.1306/985610M843070.

Slavin, W.J. (1963), Triasovye i jurskie otloženija Vostočnych Karpat i pannonskogo sredinnogo massiva, Gosgeoltechizdat, Moskva.

Slavin, W.J. (1966), Yurskaya Sistema, in *Geologiya SSSR, Karpaty*, edited by Siemienienko, N.P., et al., vol 48, 77-92.

Śmigielski, M., F.M. Stuart, P. Krzywiec, C. Persano, H.D. Sinclair, K. Pisaniec and K. Sobien (2012), Neogene exhumation of the Northern Carpathians revealed by low temperature thermochronology, *Geophys. Res. Abstr.*, 14, EGU 2012-12063.

Sokołowski, S. (1973), Geology of Palaeogene and Mesozoic basement of the Podhale Trough southern limb in then column of the Zakopane deep borehole (in Polish with English summary), *Biul. Inst. Geol.*, 265, 5-103.

Soták, J. (1998a), Sequence stratigraphy approach to the Central Carpathian Paleogene (Eastern Slovakia): eustasy and tectonics as controls of deep sea fan deposition, *Slovak Geological Magazine*, 4 (3), 185-190 (Bratislava).

Soták, J. (1998b), Central Carpathian Paleogene and its constrains, *Slovak Geological Magazine*, 4 (3), 203-211.

Soták J., M. Pereszlenyi, R. Marschalko, J. Milicka and D. Starek (2001), Sedimentology and hydrocarbon habitat of the submarine-fan deposits of the Central Carpathian Paleogene Basin (NE Slovakia), *Mar. Petrol. Geol.*, 18, 87-114.

Soták, J., D. Plašenka, J. Spišiak and P. Uher, (1993), Neptunian carbonate dykes hosted by basic volcanic rocks in the Považsky Inovec Mts. – Western Carpathians, *Mineralia Slovaca*, 25, 193-201. [In Slovak with English summary].

Soták, J., R. Rudinec, and J. Spišiak, (1993), The Peninic “pull-apart” dome in the pre-Neogene basement of the Transcarpathian Depression (Eastern Slovakia), *Geol. Carpath.*, 44, 1, 11-16.

Soták, J., J. Spisiak, I. Barath, J. Bebej, A. Biron, B. Hamrsmid, M. Hrnčarova, N. Hudackova, V. Hurai, J. Kotulova, M. Kovac, F. Marko, R. Marschalko, J. Michalik, J. Milicka, M. Misik, A. Nagymarosy, P. Pitonak, M. Pereszlenyi, D. Plasienska, R. Prokesova, D. Rehakova, and L. Svabenicka (1996), Geological assessment of the Levocské vrchy Mts.-research report, pp.1193, Geofond Bratislava.

Sperner, B. (1996), Computer programs for the kinematic analysis of brittle deformation structures and the Tertiary evolution of the Western Carpathians (Slovakia), Tübingen Geowissenschaftliche Arbeiten, Reihe A, 27, 1-81.

Sperner, B., L. Ratschbacher, and M. Nemčok (2002), Interplay between subduction retreat and lateral extrusion: tectonics of the Western Carpathians, *Tectonics*, 21(6), 1051, doi: 10.1029/2001TC901028.

Spiegel C., B. Kohn, D. Belton, Z. Berner, A. Gleadow (2009), Apatite (U–Th–Sm)/He thermochronology of rapidly cooled samples: The effect of He implantation, *Earth and Planetary Sc. Lett.*, 285, 105-114, doi: 10.1016/j.epsl.2009.05.045.

Šrodoň, J., M. Kotarba, A. Biroň, P. Such, N. Clauer and A. Wójtowicz (2006), Diagenetic history of the Podhale-Orava Basin and the underlying Tatra sedimentary structural units (Western Carpathians): evidence from XRD and K-Ar of illite-smectite, *Clay Miner.*, 41, 751-774.

Stefaniuk, M. (2006), Some results of a new magnetotelluric survey in the area of the Polish Outer Carpathians, in *The Carpathians and their foreland: Geology and hydrocarbon resources: AAPG Mem.*, 84, edited by J. Golonka and F. J. Picha, pp. 707-716, doi: 10.1306/985624M843081.

Steiger, R. H. and E. Jäger, (1977), Subcommittee on geochronology: Convention on the use of decay constants in geo- and cosmochronology, *Earth. Planet. Sc. Lett.*, 36, 359-362.

Strutt, R.J. (1905), On the radio-active minerals, *Proceedings of the Royal Society of London*.

Struzik, A.A., M. Zattin, and R. Anczkiewicz (2002), Apatite fission track analyses from the Polish Western Carpathians, *Geolines*, 14, 87-89.

Stüwe, K., L. White, and R. Brown (1994), The influence of eroding topography on steady-state isotherms. Application to fission track analysis. *Earth and Planetary Science Letters*, 124(1), 63-74.

Suppe, J. (1983), Geometry and kinematics of fault-bend folding, *Am. J. Sci.*, 283, 684-721.

Sviridenko, V.G., (1976), Geological structure of the PreNeogene substratum of the Transcarpathian Depression. *Miner. Slovaca (Kosice)*, 8, 5, 395-406 (English summary).

Świdziński, H. (1948), Stratigraphical index of the Northern Flysch Carpathians, *Bull. Panst. Inst. Geol.*, 37, 1-128.

Świerczewska, A. (2005), The interplay of the thermal and structural histories of the Magura Nappe (Outer Carpathians) in Poland and Slovakia, *Miner. Polon.*, 36(2), 91-144.

Szaniawski, R., M. Ludwiniak, and J. Rubinkiewicz (2012), Minor counterclockwise rotation of the Tatra Mountains (Central Western Carpathians) as derived from paleomagnetic results achieved in hematite-bearing Lower Triassic sandstones, *Tectonophysics*, 560-561, 51-61, doi:10.1016/j.tecto.2012.06.027.

Tözsér, J., and R. Rudinec (1975), Geological structures and mineral resources of the Neogene in Eastern Slovakia and Its Substratum. *Miner. Slovaca (Kosice)*, 7, 3, 81-104, (English summary).

Tomek, Č. (1993), Deep crustal structure beneath the central and inner West Carpathians. *Tectonophysics*, 226, 417-431.

Tomek, Č., and J. Hall (1993), Subducted continental margin in the Carpathians of Czechoslovakia: *Geology*, 21, 535-538.

Uchman, A. (2004), Tatry, ich skały osadowe i badania sedymentologiczne in *Geologia Tatr: Ponadregionalny Kontekst Sedymentologiczny*, edited by W: Kędzierski, M., Leszczyński, S. and A. Uchman, pp. 5-21.

Uhlig, V. (1890), *Ergebnisse geologischer Aufnahmen in den westgalizischen Karpathen. II. Th. Der pieninische Klippenzug*, *Jb. geol. B.-A.*, Bd. 40, H. 3-4.

Unrug, R. (1968), *Kordyliera śląska jako obszar źródłowy materiału klastycznego piaskowców fliszowych Beskidu Śląskiego i Beskidu Wysokiego (Polskie Karpaty zachodnie)*, *Rocz. Pol. Tow. Geol.*, 38 (1), 81-164.

Vass, D., and J. Čverčko (1985), *Neogene lithostratigraphic units in Eastern Slovakian Lowland*, *Geol. Práce, Správy*, 82, 111-126, (English summary).

Vermeesch, P., D. Seward, C. Latkoczy, M. Wipf, D. Guenther and H. Baur (2007), *Alpha-emitting mineral inclusions in apatite, their effect on (U-Th)/He ages, and how to reduce it*. *Geochim. Cosmochim. Ac.* 71, 1737-1746, doi: 10.1016/j.gca.2006.09.020.

Vermeesch, P. (2009), *RadialPlotter: a Java application for fission track, luminescence and other radial plots*, *Radiat. Meas.* 44, 409-410, doi: 10.1016/j.radmeas.2009.05.003.

Verrall, P. (1981), *Structural interpretation with application to North Sea problems*. Course note no. 3, join. Association for Petroleum Exploration courses (UK).

Vitale, S., S. Ciarcia, S. Mazzoli, M. N. Zaghoul (2011), *Tectonic evolution of the 'Liguride' accretionary wedge in the Cilento area, southern Italy: a record of early Apennine geodynamics*, *J. Geodynam.*, 51, 25-36.

Vitale, S., L. Fedele, F. d. A. Tramparulo, S. Ciarcia, S. Mazzoli, and A. Novellino (2013), *Structural and petrological analyses of the Frido Unit (southern Italy): New insights into the early tectonic evolution of the southern Apennines–Calabrian Arc system*, *Lithos*, 168-169, 219-235, doi: 10.1016/j.lithos.2013.02.006.

Voigt, S., and M. Wagneich (co-ord.), F. Surlyk, I. Walaszczyk, D. Uličný, S. Čech, T. Voigt, F. Wiese, M., Wilmsen, B. Niebuhr, M. Reich, H. Funk, J. Michelín, J. W. M. Jagt., P. J. Felder and A. S. Schulp (2008) Cretaceous, in *The Geology of the Central Europe II: Mesozoic and Cenozoic*, edited by McCann T., pp. 923-998.

Vörös, A. (2001), Paleobiogeographical analysis: a tool for the reconstruction of Mesozoic Tethyan and Penninic basins, *Acta Geol. Hung.*, 44 (2-3), 145-158.

Wagner, M. (2011), Petrologic studies and diagenetic history of coaly matter in the Podhale flysch sediments, Southern Poland, *Ann. Soc. Geol. Pol.*, 81, 173-183.

Wessely, G. (1988), Structure and development of the Vienna Basin in Austria, in *The Pannonian Basin, A study in Basin Evolution*, edited by L. Royden, F. Horvath, AAPG Mem., 45, 333-346.

Wójcik, A., P. Marciniak, P. Nescieruk (2006), Tokarnia IG-1 (in Polish). Profile Głębokich Otworów Wiertniczych, Państwowego Instytutu Geologicznego, 108, pp.58.

Wójcik-Tabol, P. (2003), Reflectance of dispersed organic matter particles in shales of the Magierowa Member in the Pieniny Klippen Belt compared with clay crystallinity and isotopical data, *Miner. Soc. Pol.- Special Papers*, 22, 236-239.

Wolf R.A. , K.A. Farley, D.M. Kass (1998), Modeling of the temperature sensitivity of the apatite (U–Th)/He thermochronometer, *Chemical Geology*, 148, 105-114.

Zattin, M., B. Andreucci, L. Jankowski, S. Mazzoli and R. Szaniawski (2011), Neogene exhumation in the Outer Western Carpathians, *Terra Nova*, 00, 1-9, doi:10.1111/j.1365-3121.2011.01011.x.

Ziegler, P.A., and S. Cloetingh (2004), Dynamic processes controlling evolution of rifted basins, *Earth Sci. Reviews*, 64, 1-50, doi: 10.1016/S0012-8252(03)00041-2.

Zlínska, A. (1992), Zur Biostratigraphischen Gliederung des neogens des Ostslowakischen Beckens, *Geol. Práce, Spr.*, 96, 51-57.

Zoetemeijer, R., C. Tomek, & S. Cloetingh (1999), Flexural expression of European continental lithosphere under the Western Outer Carpathians, *Tectonics*, 18, 843-861.

Zoetemeijer, R., and W. Sassi (1992) 2D reconstruction of thrust evolution using the fault-bend fold method, in *Thrust tectonics*, edited by Mc Clay, 133-140.

Zuchiewicz, W., N. Oszczypko (2008), Topography of the Magura floor thrust and morphotectonics of the Outer West Carpathians, Poland. *Ann. Soc. Geol. Pol.*, 78, 135-149.

